DOE/ET/27111--T6

DE85 009787

REPORT OF INVESTIGATIONS NO. 134

DEPOSITIONAL SETTING, STRUCTURAL STYLE, AND SANDSTONE DISTRIBUTION IN THREE GEOPRESSURED GEOTHERMAL AREAS, TEXAS GULF COAST

C.D. WINKER, R.A. MORTON,
T.E. EWING, and D.D. GARCIA

assisted by
L. P. Chong, J. H. Han,
J. L. Lawton, R. J. Padilla y Sanchez,
J. J. Palmer, and R. D. Rasco

OST-8514

950 1193

Funded by the U.S. Department of Energy, Division of Geothermal Energy, Under Contract Nos. DE-AS05-76ET28461 and DE-AC08-79ET27111

BUREAU OF ECONOMIC GEOLOGY
W.L. FISHER, DIRECTOR
THE UNIVERSITY OF TEXAS AT AUSTIN
AUSTIN, TEXAS 78712

1983

DISCLAIMER

CONTENTS

Figures

Tables

ABSTRACT

Three areas in the Texas Gulf Coastal Plain were studied using electric logs and seismic-reflection data to interpret their depositional and structural history and to compare their potential as geopressured-geothermal reservoirs. The Cuero study area, on the lower Wilcox (upper Paleocene) growth-fault trend, is characterized by closely and evenly spaced, subparallel, down-to-the-basin growth faults, relatively small expansion ratios, and minor block rotation. Distributary-channel sandstones in the geopressured lower Wilcox Group of the South Cook fault block appear to be the best geothermal aquifers in the Cuero area. The Blessing study area, on the lower Frio (Oligocene) growth-fault trend, shows wider and more variable fault spacing and much greater expansion ratios and block rotation, particularly during early Frio time. Thick geopressured sandstone aquifers are laterally more extensive in the Blessing area than in the Cuero area. The Pleasant Bayou study area, like the Blessing area, is on the Frio growth-fault trend, and its early structural development was similar; rapid movement of widely spaced faults resulted in large expansion ratios and major block rotation. However, a late-stage pattern of salt uplift and withdrawal complicated the structural style. Thick geopressured lower Frio sandstone aquifers are highly permeable and laterally extensive, as in the Blessing area.

In all three areas, geopressured aquifers were created where early, rapid movement along down-to-the-basin growth faults juxtaposed shallow-water sands against older shales, probably deposited in slope environments. Major transgressions followed the deposition of reservoir sands and probably also influenced the hydraulic isolation that allowed the buildup of abnormal pressures. Of the three areas, the Pleasant Bayou area has the best potential for geothermal energy production because of larger fault block area, greater thickness and lateral continuity of individual sandstones, and higher formation temperatures and pressures.

Keywords: geopressure, geothermal energy, Gulf Coastal Plain, Texas, seismic surveys, structural geology, Tertiary, clastic sediments.

INTRODUCTION

As part of a regional assessment of the feasibility of producing geothermal energy and dissolved methane from deep, geopressured Tertiary sandstone aquifers beneath the Texas Gulf Coastal Plain, three areas were selected for detailed, site-specific investigation (fig. 1). These areas were chosen on the basis of thickness, continuity, and permeability of sandstones, structural continuity, high formation temperatures, and high pressure gradients, as determined from regional studies of the Paleocene-Eocene Wilcox Group (Bebout and others, 1982) and the Oligocene Frio Formation (Bebout and others, 1978; Weise and others, 1981). Detailed investigations of sandstone geometry were necessarily limited to areas with relatively dense and evenly distributed deep well control.

The specific purpose of this study was to integrate seismic reflection data and well data to predict reservoir size and continuity. These detailed studies led to analyses of the genesis and continuity of geopressured sandstone reservoirs and to a good regional model of the structure and deposition of Cenozoic shelf margins (Winker, 1982; Winker and Edwards, 1983). Although production of geothermal energy and dissolved methane are not economic under market conditions of the 1980's (Wrighton, 1981), these studies may prove relevant to future assessments of potential geothermal energy production in Texas.

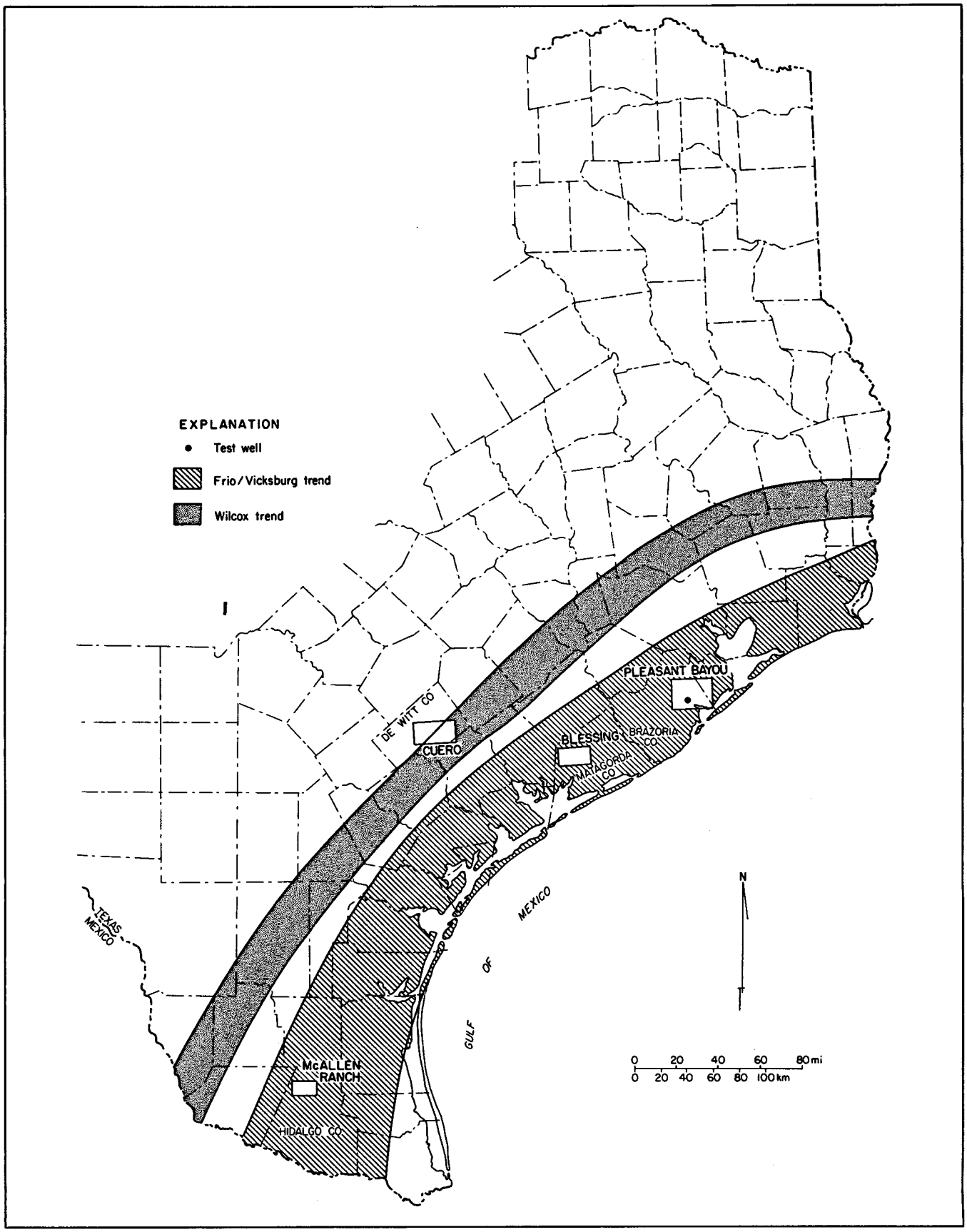

Figure 1. Location of areas studied for this report in relation to geothermal exploration trends, Texas Gulf Coast. McAllen Ranch included for comparison of structural style (fig. 48).

REGIONAL SETTING

Geopressured sandstone reservoirs occur in the basinward parts of large Tertiary deltaic complexes. The Cuero study area (fig. 2) is on the southwestern margin of the lower Wilcox (upper Paleocene) Rockdale delta system (Fisher and McGowen, 1967) in a transitional area between the dip-fed deltaic systems to the northeast and the strike-fed barrier-strandplain systems to the southwest. Lower Wilcox sandstones attain a maximum net thickness farther to the northeast in the Rockdale depocenter, but that area is too sparsely drilled on its downdip geopressured fringe for adequate assessment of geothermal resources.

The Pleasant Bayou study area (fig. 3) lies on the southeastern margin of the Houston delta complex of the Frio Formation (Galloway and others, 1982); the Blessing study area is transitional between the Houston delta system and the Greta-Carancahua strandplain to the southwest. The Norias delta complex in South Texas is a larger deltaic system within the Frio Formation (Galloway and others, 1982), but its high percentage of chemically unstable volcanogenic sandstones has led to extensive cementation and reduced porosity and permeability (Loucks and others, 1981), rendering the Norias complex less attractive for geothermal exploration (Bebout and others, 1978). The downdip geopressured Vicksburg Formation (Oligocene) in South Texas is similarly limited in geothermal potential (Loucks and others, 1981).

Geothermal trends (Bebout and others, 1978, 1982) correspond to zones of syndepositional down-to-the-basin normal faults, or growth faults. Rapid movement along these faults helped create the hydraulic isolation of sandstone beds necessary for the buildup of excess fluid pressure (Fowler, 1970; Harkins and Baugher, 1969). By analogy with Quaternary structures in the Gulf Coast Basin, these growth-fault trends can be interpreted as ancient continental-shelf margins. According to this model, faulting was caused primarily by large-scale, deep-seated gravity sliding of the continental slope (Rettger, 1935; Cloos, 1968; Bruce, 1973; Crans and others, 1980; Winker, 1982). Geopressured sandstone aquifers were created where large influxes of sand prograded the shoreline close to the contemporaneous shelf edge (fig. 4), and shallow-water sand deposits were hydraulically isolated by rapid subsidence along large regional faults (fig. 5).

An alternative model of similar deposits by Berg (1981) suggests that major sand deposition took place basinward of the contemporaneous shelf edge. However, regional studies show that geopressured sandstones are integral parts of prograding deltaic systems. Furthermore, detailed sedimentological descriptions of geopressured reservoirs (Morton and others, 1983) are similar to descriptions of sandstones deposited in shallow water (Bebout and others, 1978, 1982; Han, 1981; Loucks and others, 1981; Tyler and Han, 1982; W. E. Galloway, personal communication, 1982).

METHODS OF INVESTIGATION

Stratigraphic Correlation

Cenozoic stratigraphic units in the subsurface of the Texas Gulf Coast (table 1) consist primarily of interbedded sandstone and shale. Most subsurface units are informally defined, lithostratigraphic rather than chronostratigraphic units, and contacts are therefore generally transitional and time-transgressive along both regional strike and dip. Subsurface units are further constrained regionally by foraminiferal zones, defined mainly by the uppermost occurrences of diagnostic species of benthic foraminifers. Distribution of these foraminifers is to some extent environmentally controlled, so that in a regressive depositional sequence, the uppermost foraminifers tend to occur higher in the stratigraphic section toward the basin. Because of this facies control, the tops of foraminiferal zones used for correlation may be considerably diachronous.

For these reasons, stratigraphic correlation within each study area was based primarily on distinctive marker horizons (table 1) recognizable on spontaneous potential (SP) and resistivity (R) logs. In most cases, these log markers were picked at major changes in the sandstone/shale ratio or at the tops of major upward-coarsening cycles characterized by funnel-shaped patterns on electric logs and

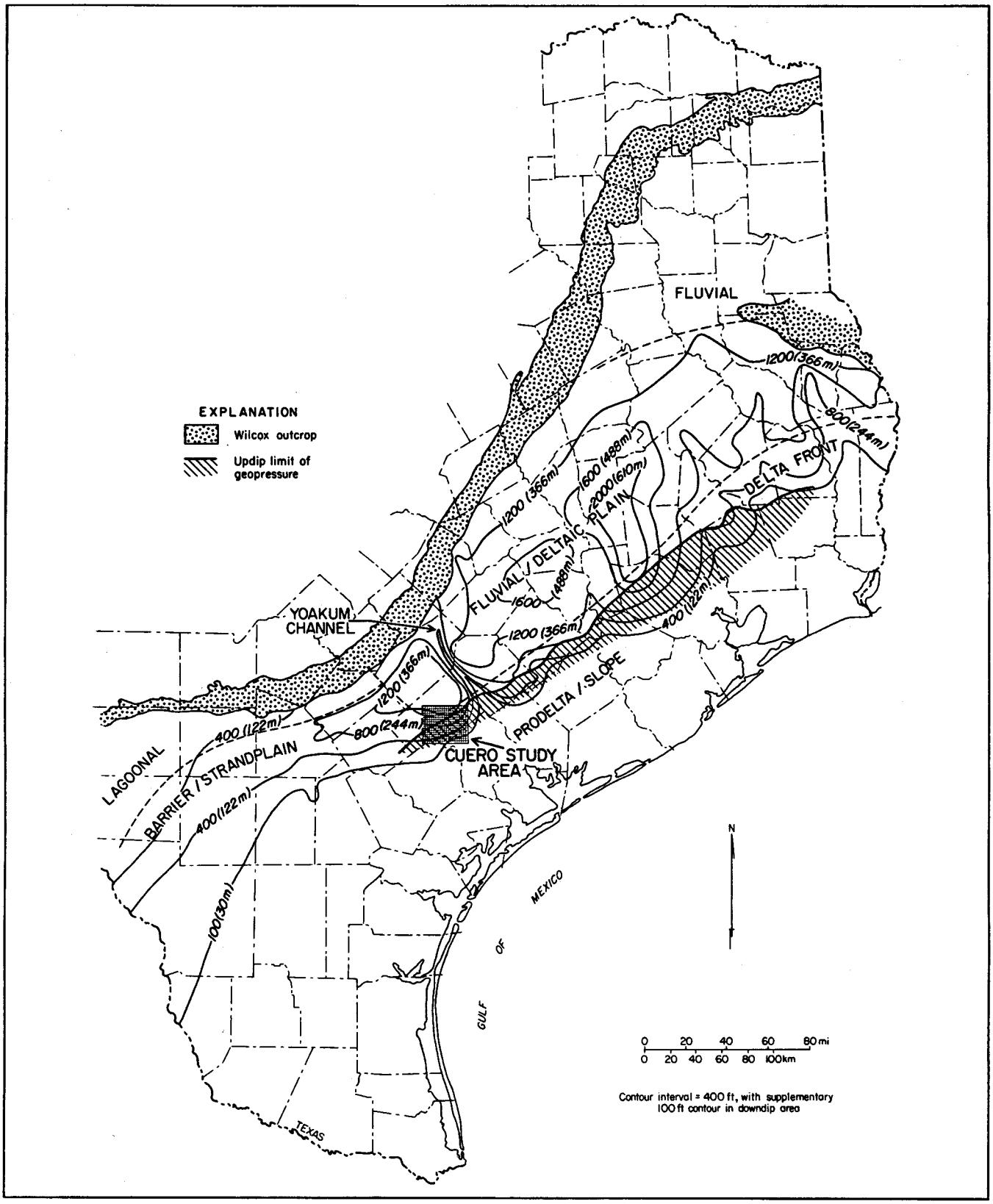

Figure 2. Location of Cuero study area in relation to regional facies (after Fisher and McGowen, 1967), net-sandstone distribution (after Bebout and others, 1982), and geopressure (defined by 13 lb/gal drilling mud density) in the lower Wilcox Group (upper Paleocene) in Texas. Downdip wells do not penetrate the entire Wilcox section; closure of contours is therefore speculative.

interpreted as progradational deltaic cycles (Fisher and others, 1969; Asquith, 1970). Such log markers are not regionally persistent, but most can be correlated throughout individual study areas. As a point of reference for all correlations, one well in each study area was designated a type well (table 1). In the Pleasant Bayou area, a geothermal test well (General Crude Oil/Department of Energy Pleasant Bayou No. 2) that was drilled before this study began was used as the type well. Accuracy was maintained by correlating in closed loops where possible; correlations across growth faults were made where expansion of the section is least. Typical correlation problems encountered near ancient shelf margins in the Gulf Basin include (1) missing section caused by normal faulting; (2) expansion of section (as much as 10:1) across growth faults; (3) rapid basinward changes in lithofacies and log character; and (4) substantial deviations from extrapolated regional dips (Winker, 1982). Shallower and farther updip, the major correlation problems are caused by lateral discontinuity of individual sandstone beds. To minimize such correlation problems, all available well control was used.

Sandstone Facies and Continuity

Sandstone facies were interpreted primarily from electric-log patterns (from gamma-ray logs in a few wells). Cores from a few wells were also available for examination. Log facies were interpreted both from vertical log patterns for individual wells and from lateral persistence of individual sandstones from one well to another. Principles of paleo-

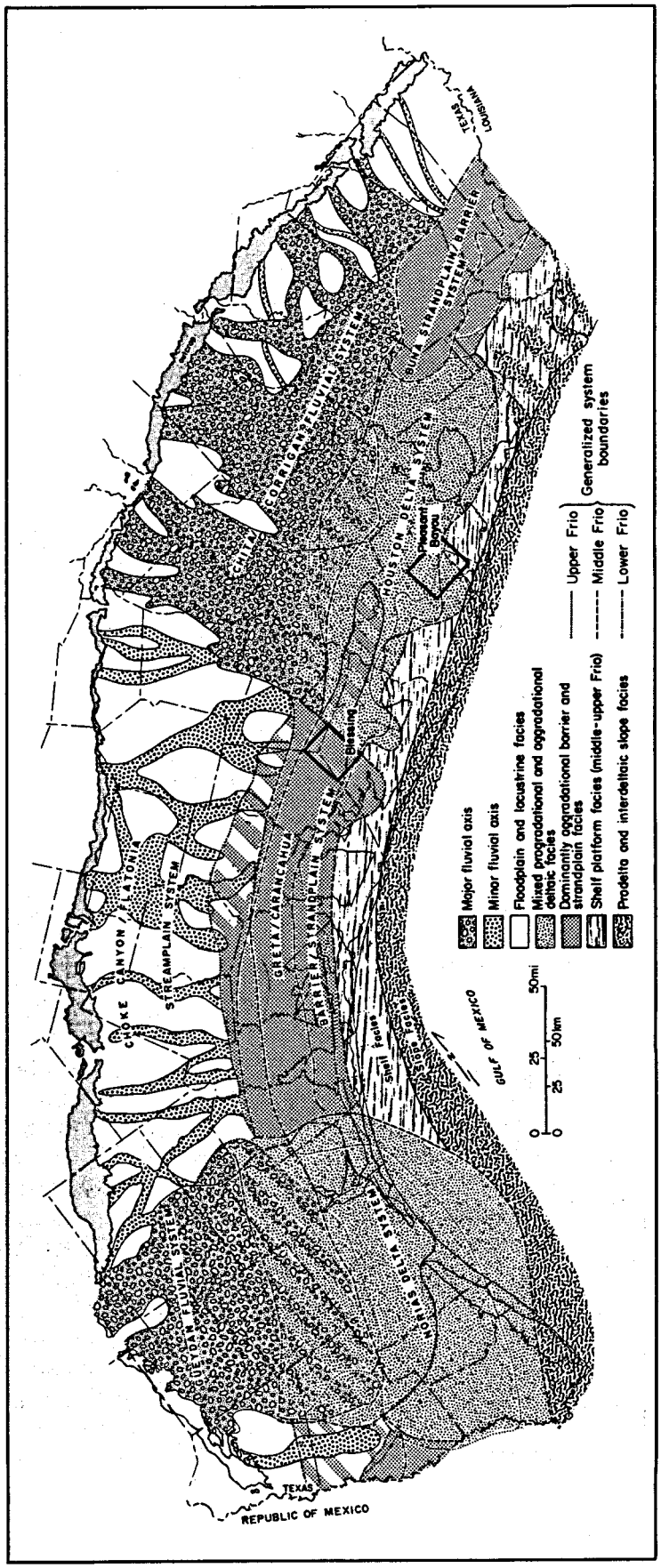

Figure 3. Location of Blessing and Pleasant Bayou study areas in relation to regional depositional systems of the Oligocene Frio Formation in Texas (after Galloway and others, 1982).

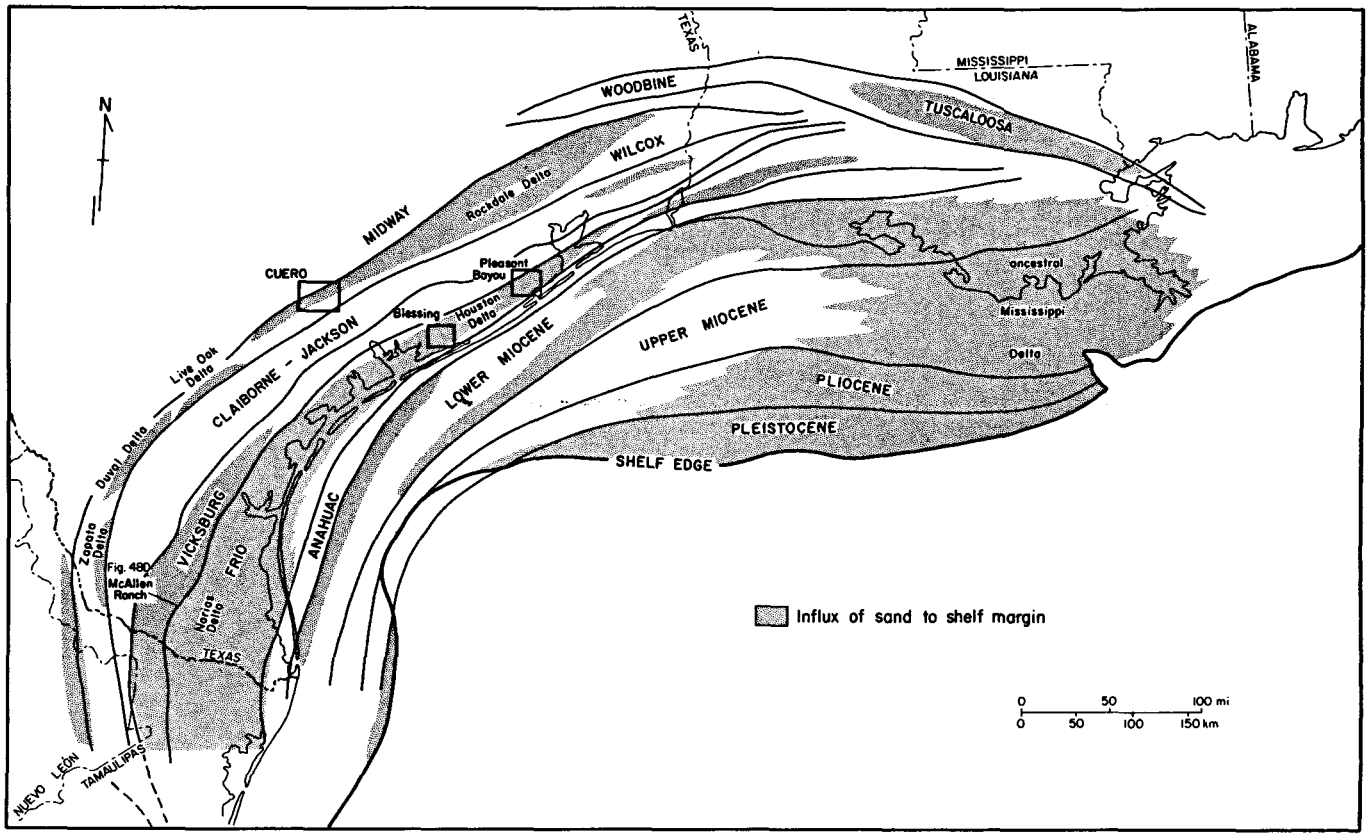

Figure 4. Location of the three study areas in relation to regional post-Edwards shelf-margin trends and shelf-margin delta complexes (major influxes of sand) in the northwestern Gulf of Mexico Basin (after Winker, 1982).

Table 1. Approximate stratigraphic correlation of electric-log and seismic correlation markers (TW, D1, TA, B1, etc.) and informal stratigraphic units (1, 2, 3, etc.) in four geothermal study areas. McAllen Ranch is included for comparison of structural style (fig. 48). Type wells are listed for each study area.

APPROX. AGE (MY.)	EPOCH	REGIONAL STRATIGRAPHIC UNITS, TEXAS GULF COAST	STUDY AREAS: THIS STUDY — PLEASANT BAYOU (#2 Pleasant Bayou)	THIS STUDY — BLESSING (Texaco #16 Thomas)	THIS STUDY — CUERO (Atlantic #1 Schorre)	HAN, 1982 — McALLEN RANCH (Shell #10 McAllen)
—20—	MIOCENE		1	1		
		ANAHUAC FM	TA	B1		1
			2	B2		
		FRIO FM	T2	2		
			T3	3		
—30—	OLIGOCENE		T4	B3	1	
			T5	B4		2
			6	B5		3
		VICKSBURG GROUP	7	6		4
				7		5
		JACKSON GROUP				6
—40—		YEGUA FM			C1	
	EOCENE	CLAIBORNE GROUP			2	
—50—					TW	
		WILCOX GROUP			D1	
					D3	
					D4	
—60—	PALEOCENE	MIDWAY GROUP			7	

▨ Interval of optimum geopressured sandstone aquifers

environmental interpretation from log patterns are discussed in greater detail by Fisher and others (1969).

Sandstone characteristics considered favorable for reservoir quality are (1) lateral persistence of sandstones; (2) vertical continuity, as evidenced by the absence of shale breaks and quantified by maximum sandstone thickness; and (3) net sandstone greater than 50 ft thick. Upward-fining sandstones with sharp bases are interpreted to represent channel deposits and are thought to have average permeabilities equal to or higher than laterally equivalent sandstones with upward-coarsening log patterns. These criteria provided the basis for mapping the optimum geopressured reservoir facies in each fault block of interest.

Interval Velocities and Seismic Interpretation

Accurate control of subsurface P-wave velocities was essential for interpreting the

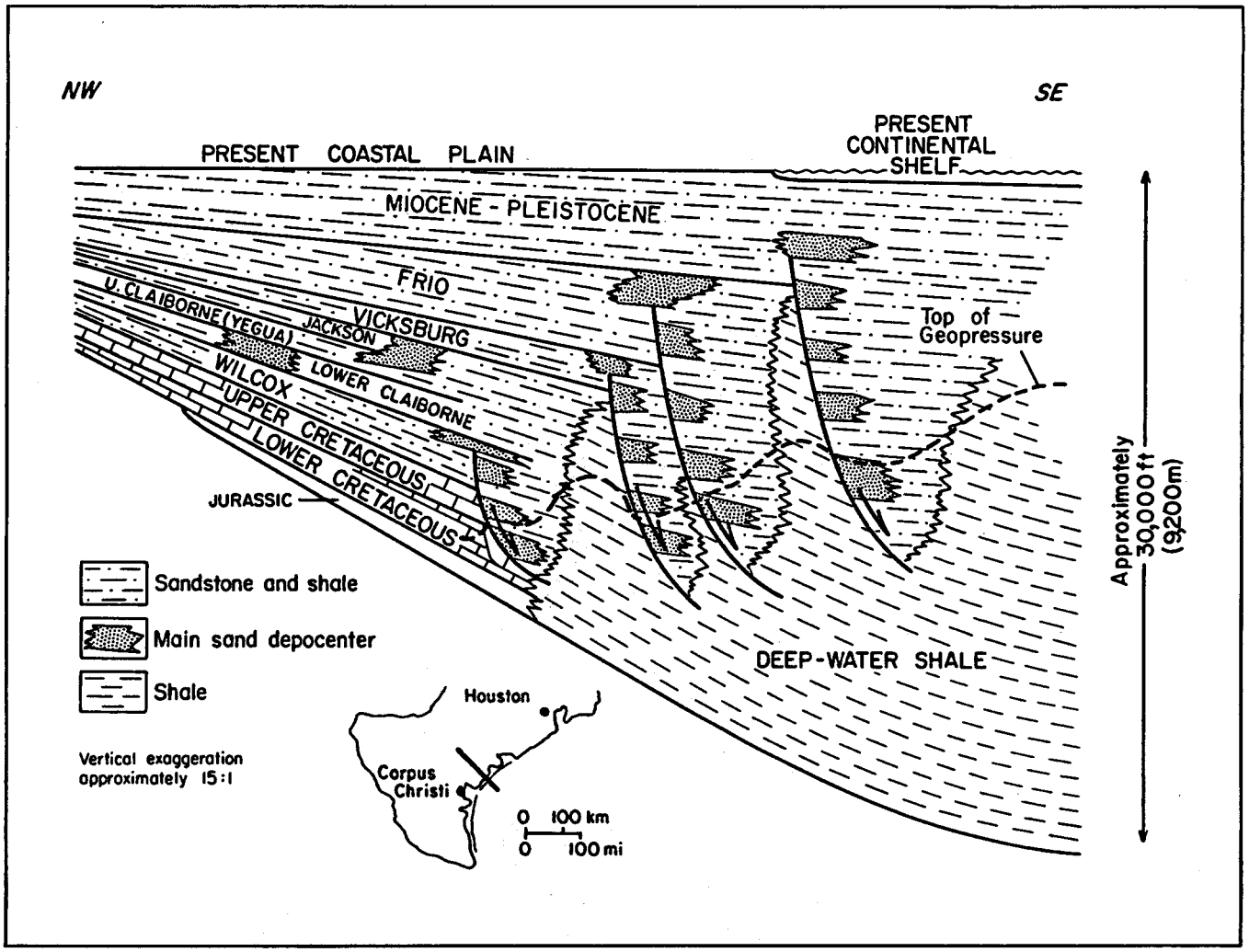

Figure 5. Schematic cross section, central Texas Gulf Coast, showing relationship among major growth faults, expansion of section, sand depocenters, and top of geopressure (after Bebout and others, 1982).

seismic-reflection sections, both for tying wells to sections and for estimating dips of fault and bedding planes. An additional objective was to test the possibility of mapping the top of geopressure from an inversion of interval velocity. Velocity information is available from three sources. (1) Acoustic logs indicate the fine-scale velocity structure and can be integrated to give a time-to-depth conversion. They can also be processed to generate synthetic seismograms, which can be used to tie wells to seismic sections. (2) Root-mean-square (RMS) velocities can be estimated from applied stacking velocities or power-spectrum displays and can be inverted using the Dix equation to give interval velocities (Dobrin, 1976, p. 230). (3) Velocity surveys of wells provide estimates of interval velocities by measuring the downhole travel time from surface shots near the well.

A preliminary study of velocity distribution in the Cuero study area indicated that velocity surveys provide the most reliable source of interval velocities and time-to-depth conversion (fig. 6). Some acoustic logs contained systematic errors (underestimation of velocity, particularly in shale) that became apparent upon integration. Synthetic seismograms were generated for some wells but were of insufficient quality to assist in tying wells to seismic sections. Stacking velocities exhibited lateral incoherence, which limited their value for time-to-depth conversion. At the depth of geopressure, the quality of power-spectrum displays (velocity analyses) was seldom good enough to pick velocity

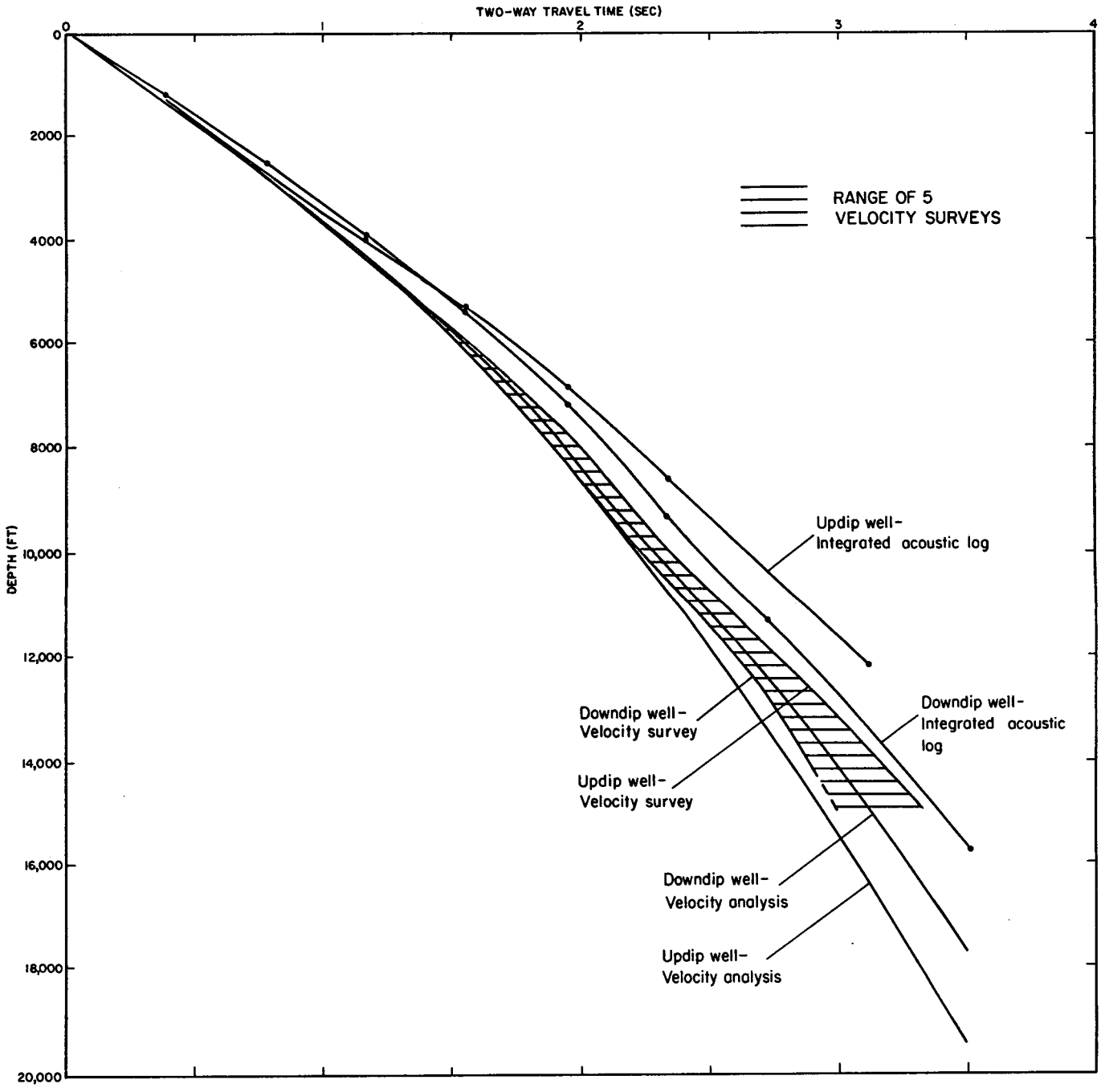

Figure 6. Time-depth curves for wells in the Cuero study area, comparing results from velocity surveys with velocity analyses and acoustic logs.

inversions reliably. Velocity surveys are subject to errors in picking the first breaks because of attenuation and changes of waveform at depth, but they were ultimately given the most weight as a source of velocity information.

In all three areas, velocities were found to vary primarily as a function of stratigraphy. In general, velocities decrease with formation pressure and increase with depth of burial and with sandstone percentage. However, no clear-cut relationship between the top of geopressure and interval-velocity inversions was observed in any of the three areas.

Structural Interpretation

Faults were recognized from (1) missing stratigraphic section on individual well logs, (2) characteristic appearance on seismic sections (as discussed by Dobrin, 1976, p. 264), and (3) discontinuities encountered when contouring structure and isopach maps. In many areas, well density and seismic coverage were sufficient to allow contouring of fault planes. Such maps and depth-converted seismic sections showed that most faults near the depth of interest dip at approximately 45°. Therefore, in areas of sparse well control, particularly in downdip areas, faults picked in a few isolated wells were projected at a 45° dip to the mapping horizon.

In each study area, structure maps were constructed on five or six log-derived marker horizons (table 1), and isopach maps were constructed for the corresponding intervals, using all available deep well control except for the few deviated wells. Seismic sections were used primarily to verify the direction and magnitude of dips. Time-structure and isochron maps were constructed to guide the contouring of well data and to extend the mapping into areas of sparse or absent well control. Structure and isopach maps were then cross-checked for internal consistency. In the Pleasant Bayou area, the area of greatest structural complexity, isopach maps proved to be invaluable for recognizing and mapping deep faults. Isopach maps were also a significant aid in structural mapping in the Blessing area.

Isopach maps can be regarded, to a first approximation, as paleostructure maps. However, isopach maps differ from true paleostructure maps because of (1) paleotopographic or paleobathymetric relief, (2) subsequent compaction of the interval, and (3) subsequent extension, as indicated by post-depositional normal faulting. To correct for this last effect, fault blocks were graphically restored to their original relative position on isopach maps by removing the horizontal component of post-depositional faulting. In this way, the isopach maps were made approximately palinspastic, resulting in some distortion of the base maps and grids.

Fault movement cannot be quantified by displacement rates because the absolute duration of the shorter depositional intervals is poorly known (table 1). It is more meaningful to quantify the timing of fault movement by the expansion index (or growth ratio), defined as the downthrown thickness divided by the upthrown thickness of a stratigraphic interval (Thorsen, 1964). For most faults mapped in this study, the expansion indices are largest for the deepest intervals and decline steadily upward, although there are some notable exceptions. This upward decline indicates a gradual weakening of the extensional regime with time, interpreted by Winker and Edwards (1983) to result from migration of the shelf margin basinward of the area. The extensional regime presumably began when the area was still in an upper-slope environment. However, the slope facies is seldom penetrated by the drill, and on seismic sections it normally appears noisy, transparent, or chaotic; it is therefore not mapped.

CUERO AREA

The Cuero study was based on analysis of electric logs from approximately 100 wells and 36 mi (55 km) of proprietary seismic data (fig. 7). In addition, 25 mi (40 km) of new seismic data were shot specifically for this project. Cores from the type well (Atlantic No. 1 Schorre) were logged by J. H. Han to enhance the paleoenvironmental interpretation. Velocity surveys from five wells and numerous velocity analyses provided the basis for time-to-depth conversion of seismic sections.

Stratigraphy

In the Cuero area, three major regressive-transgressive cycles—lower Wilcox, upper Wilcox, and Yegua—occurred before the final Oligocene regression (fig. 8, table 2). These cycles provided the primary basis for stratigraphic subdivision in the study area. Geopressured sandstones are limited to the downdip lower Wilcox (upper Paleocene), which represents the first of these regressive cycles.

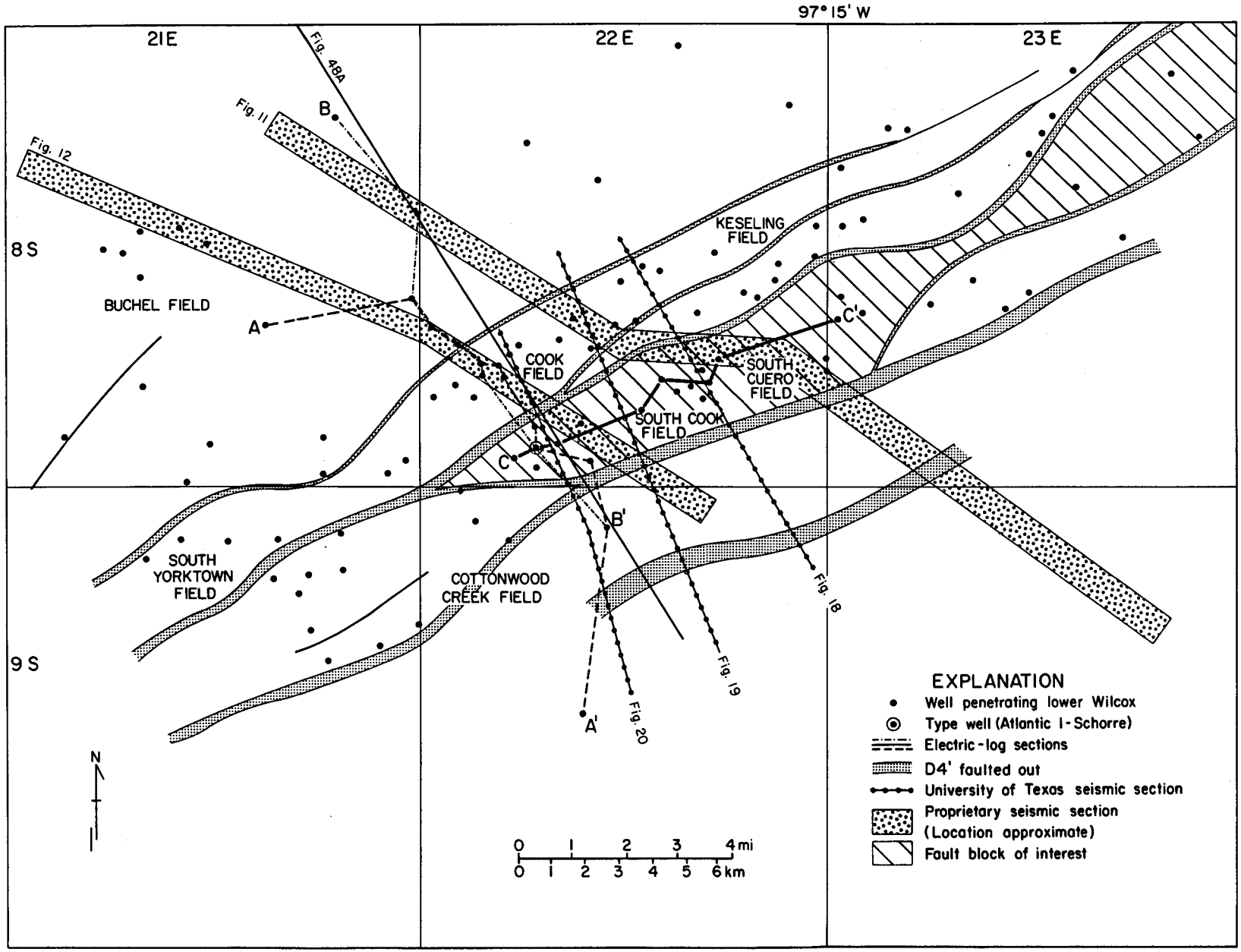

Figure 7. Data base map, Cuero study area. Grid is numbered according to the GeoMap system, which corresponds to USGS 7.5-minute quadrangles. Exact locations of two seismic sections are not shown because of proprietary restrictions.

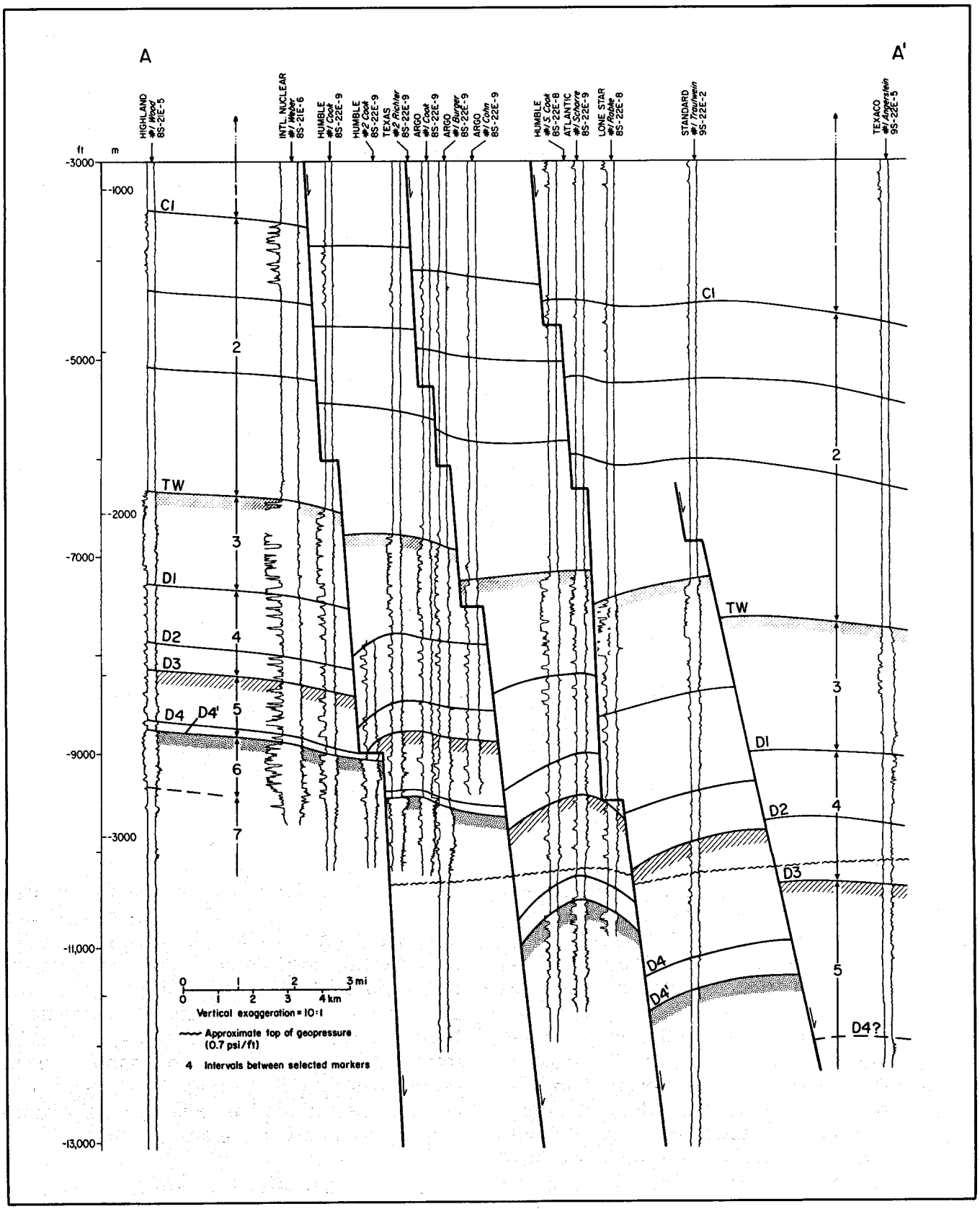

Figure 8. Structural dip section of the Cuero study area. Location of section is shown in figure 7. Stratigraphic positions of correlation markers and informal stratigraphic units are given in tables 1 and 2. All well logs in this report are electric logs; spontaneous potential (SP) is on the left and resistivity (R) is on the right. Determination of the top of geopressure is discussed in Bebout and others (1982).

Table 2. Characteristics of informal stratigraphic units in the Cuero area.

Unit numbers for isopach maps and structural sections	Log-correlation marker	Stratigraphic unit	Lithology	Relative velocity	Seismic signature	Overall transgressive/ regressive character
1						
	C1					
2		Claiborne Group	Mostly shale; thin sandstones (Yegua) near top	Low; approximately linear increase with depth	Moderate amplitude, high continuity	Transgressive (regressive in Yegua)
	TW					
3		Upper Wilcox Group	High sandstone	High, with large discontinuity at top	Strong reflector at top dominates signature	Regressive
	D1					
4		Middle Wilcox Group	Shale, with sandstone decreasing upward; shales out downdip within study area	Lower than upper Wilcox	Low amplitude, low continuity updip. High frequency, high continuity downdip	Transgressive
	D3					
5						
	D4'					
6		Lower Wilcox Group	High sandstone, shales out downdip within study area	High updip; declines substantially downdip due to lithofacies change and geopressure	Low amplitude, low continuity updip. Some increase in amplitude and continuity downdip, but data quality deteriorates in growth-fault zone	Regressive
	(boundary transitional)					
7		Midway Group	Virtually all shale (progradational prodelta/slope sequence)	Low	Moderate amplitude; well-developed oblique clinoforms. Poor data quality in growth-fault zone	Regressive

Subdivision of the Wilcox into upper, middle, and lower is informal. In this report, the local top of lower Wilcox (D4') is defined as the beginning of the middle Wilcox transgression, marked by an upward decrease in sandstone percentage (fig. 8). The beginning of the middle Wilcox transgression is diachronous along regional strike; the D4' marker is therefore stratigraphically lower than the top of lower Wilcox used in earlier regional studies (Fisher and McGowen, 1967; Bebout and others, 1982). Updip of the study area, the entire Wilcox section becomes uniform, making subdivision into upper, middle, and lower difficult. Of the five electric-log correlation markers (table 2), TW, D1, and D3 were used in an earlier report on the Cuero area (Bebout and others, 1982). Correlation was mostly straightforward; the only serious difficulties were encountered at D3 and D4' downdip of the South Cook fault block (fig. 7). The base of Wilcox, which is transitional and time-transgressive, represents a change in facies from delta-plain and delta-front sandstones to prodelta (slope) shales (fig. 9). Therefore, no correlatable log marker exists for the Wilcox-Midway boundary in the study area.

Interval Velocities

In general, interval velocities in the Cuero area (fig. 10) are a function of stratigraphy

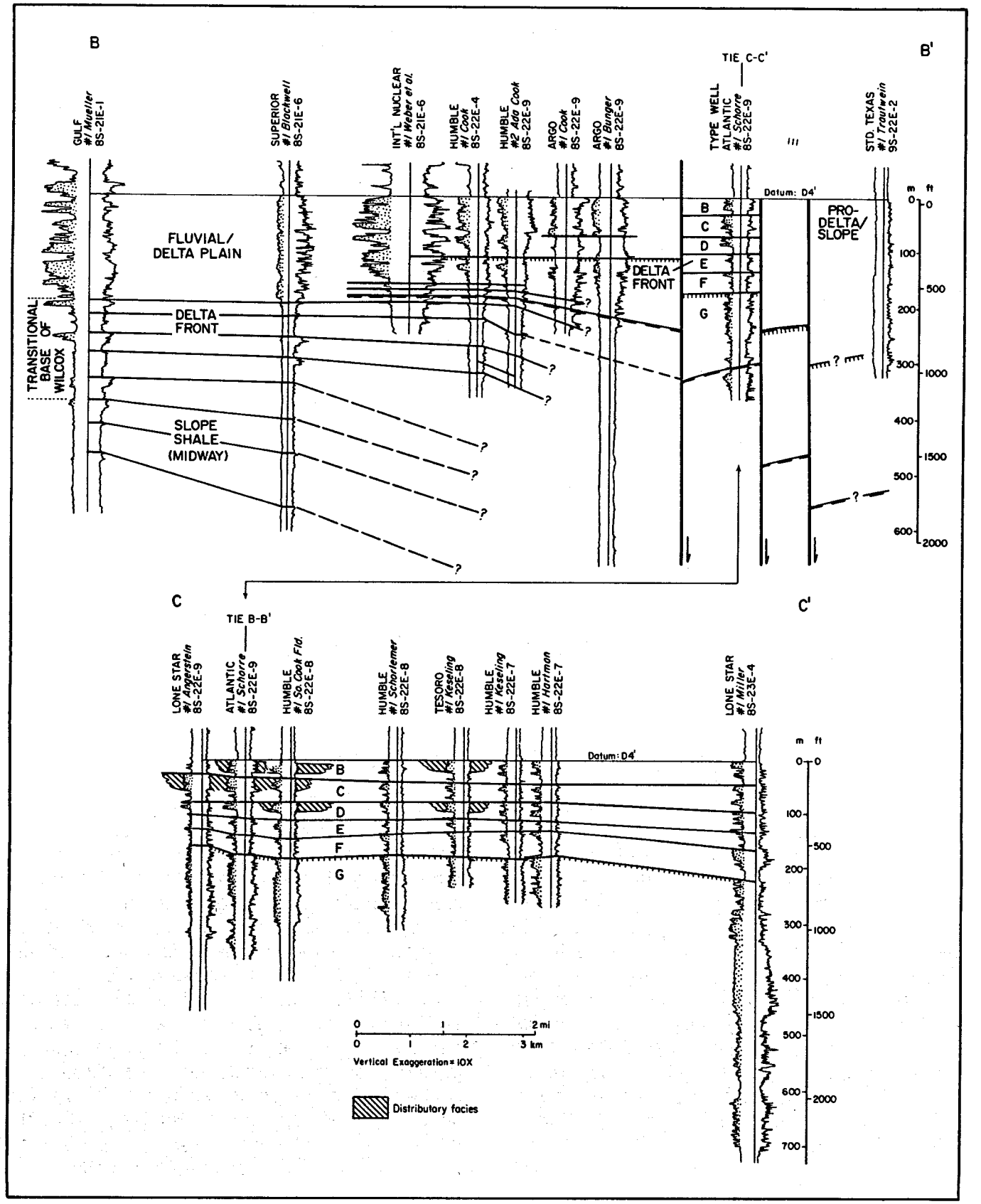

Figure 9. Stratigraphic dip section (B-B') and strike section (C-C') of the lower Wilcox Group illustrating typical log facies in the Cuero area. Locations are shown in figure 7.

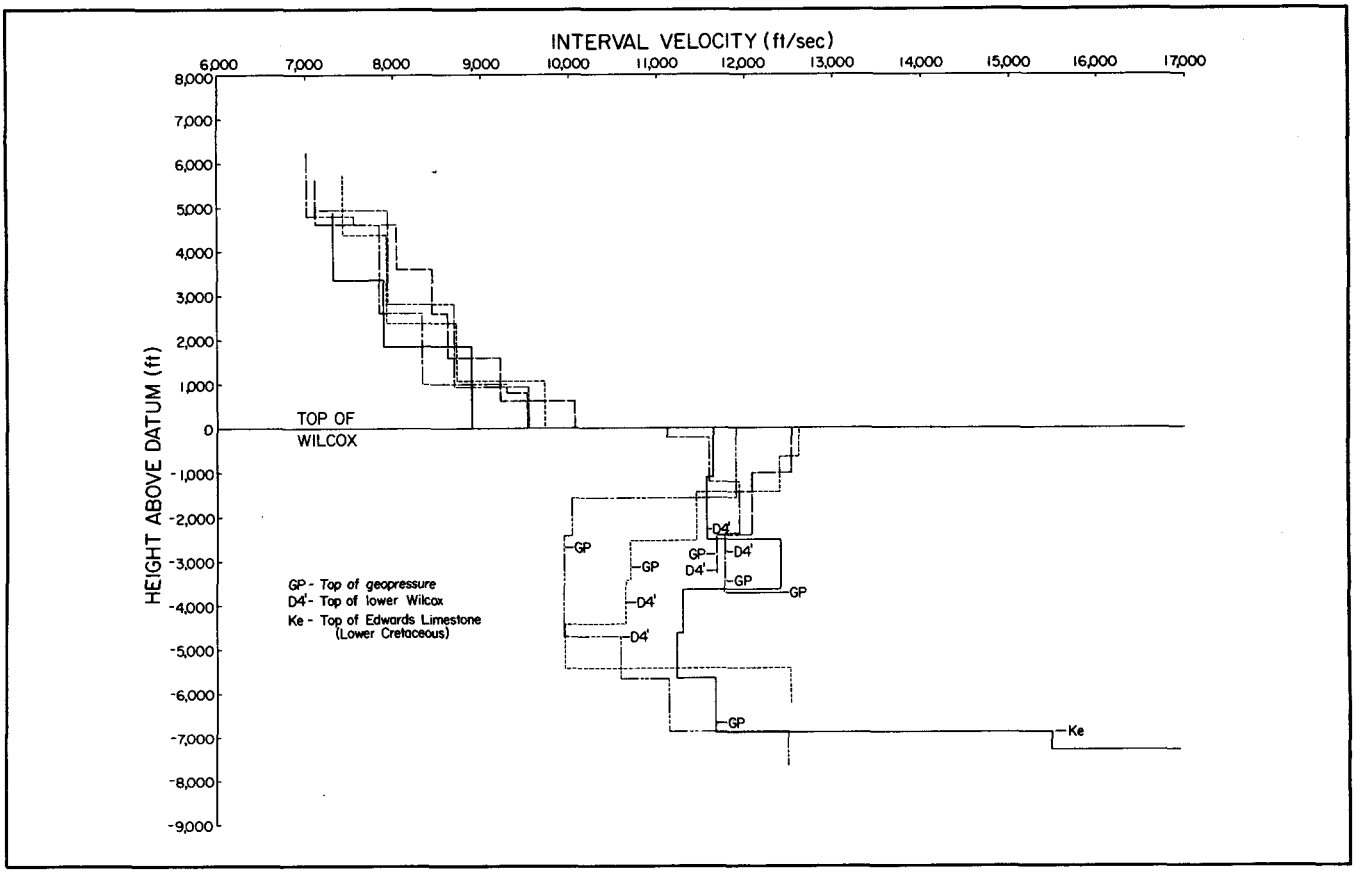

Figure 10. Interval velocities based on velocity surveys from five wells that are distributed widely enough to bracket velocities in the study area. Note large velocity discontinuity at the top of the Wilcox strata. Velocity inversions do not show a clear relationship to the top of geopressure.

(table 2). The most consistent feature of the velocity data in this area is a large discontinuity at the top of the Wilcox, which results in a high-amplitude reflector (figs. 11 and 12). Major velocity inversions result from (1) a transition from Wilcox sandstone to Midway shale (in the updip area); (2) a transition from a more sandy upper Wilcox to a more shaly middle Wilcox; and (3) a low-velocity lower Wilcox downdip, in the growth-fault zone. Only the last inversion is likely to be related to a transition from normal pressure (normal consolidation of shale) to overpressure (underconsolidation of shale). Consequently, it would be unreasonable to map the top of geopressure in this area from the first major velocity inversion.

Lower Wilcox Sandstone Facies

The lower Wilcox regressive sequence comprises a series of stacked, upward-coarsening cycles that increase upward in sandstone percentage (fig. 13). Spatial relationships among sandstone facies (table 3) are summarized by two stratigraphic sections (fig. 9) and a paleogeographic map (fig. 14). The stratigraphic dip section shows the basic vertical progression of facies associated with progradation: (1) prodelta/slope shales (characterized by clinoform reflectors on seismic sections), overlain by (2) delta-front sandstones, overlain by (3) the fluvial/delta-plain facies of sandstones and shales. A similar basinward progression can be seen on the same section, although the pattern is complicated somewhat by expansion of the section across growth faults. On a strike section within the main fault block (fig. 9), delta-front sandstones grade laterally into thick, massive or upward-fining sandstones, interpreted as distributary channel fill or channel-mouth bars on the basis of core descriptions (fig. 13). These channel-fill sandstones exhibit high (>100 md)

permeabilities in the Atlantic No. 1 Schorre well.

The distribution of sandstone facies reflects the paleogeographic relationships of the Rockdale delta system as a whole (figs. 2 and 14). The Cuero area lies in a transition from predominantly deltaic systems, with fluvial/deltaic-plain facies grading basinward into distributary and delta-front facies, to predominantly strike-fed barrier-strandplain facies characterized by high continuity along strike.

Within the geopressured part of the lower Wilcox, distributary channel-fill sandstones exhibit the best potential as geothermal reservoirs. However, the small areal extent of these sandstones (figs. 14 and 15) places severe constraints on the possible location and producing volume of a geothermal well. Ideally, a well site should be chosen to intersect two or more overlapping sandstones of high potential. In the Cuero area, there is insufficient latitude in well-site location to fulfill these criteria while avoiding interference with existing conventional gas production from the South Cook field (fig. 15).

Structure

The structural style in the Cuero area (figs. 16 through 21) is typical of the lower Wilcox trend (Bebout and others, 1982). Major growth faults are all down-to-the-basin, having a relatively small throw (1,000 ft) and minor rollover, which is nonetheless sufficient to create anticlinal closures within fault blocks. Fault traces are subparallel and fairly evenly and closely spaced. This results in long, narrow fault blocks with low structural relief; the style changes little from one mapping horizon to the next (figs. 16 and 17). The small amount of rollover (figs. 18 through 20) indicates that the faults probably flatten into a décollement only at

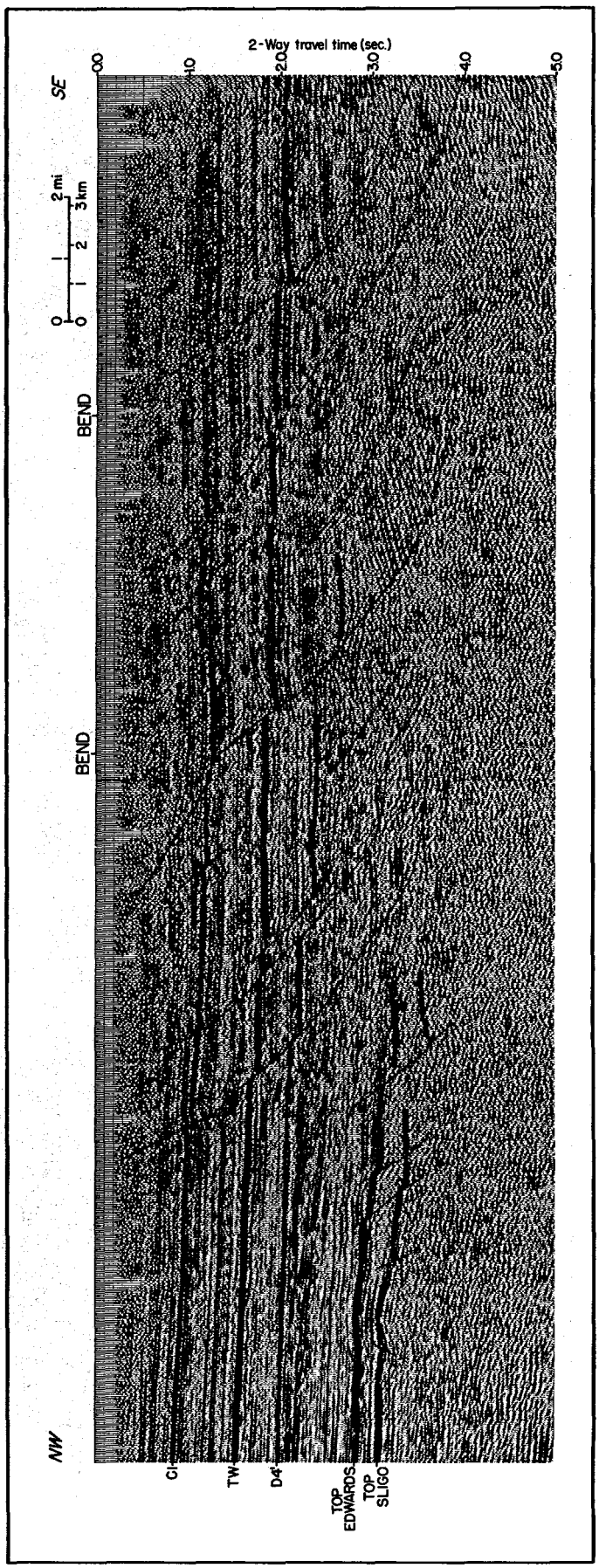

Figure 11. Seismic section (migrated) illustrating overall structural style of the study area. Location is shown in figure 7. Stratigraphic positions of correlation markers are shown in table 1. Unusual fault patterns are caused by a bend in the line. Also note Sligo and Edwards carbonate shelf margins and clinoform reflectors in the Midway Group (below D4', northwest part of section).

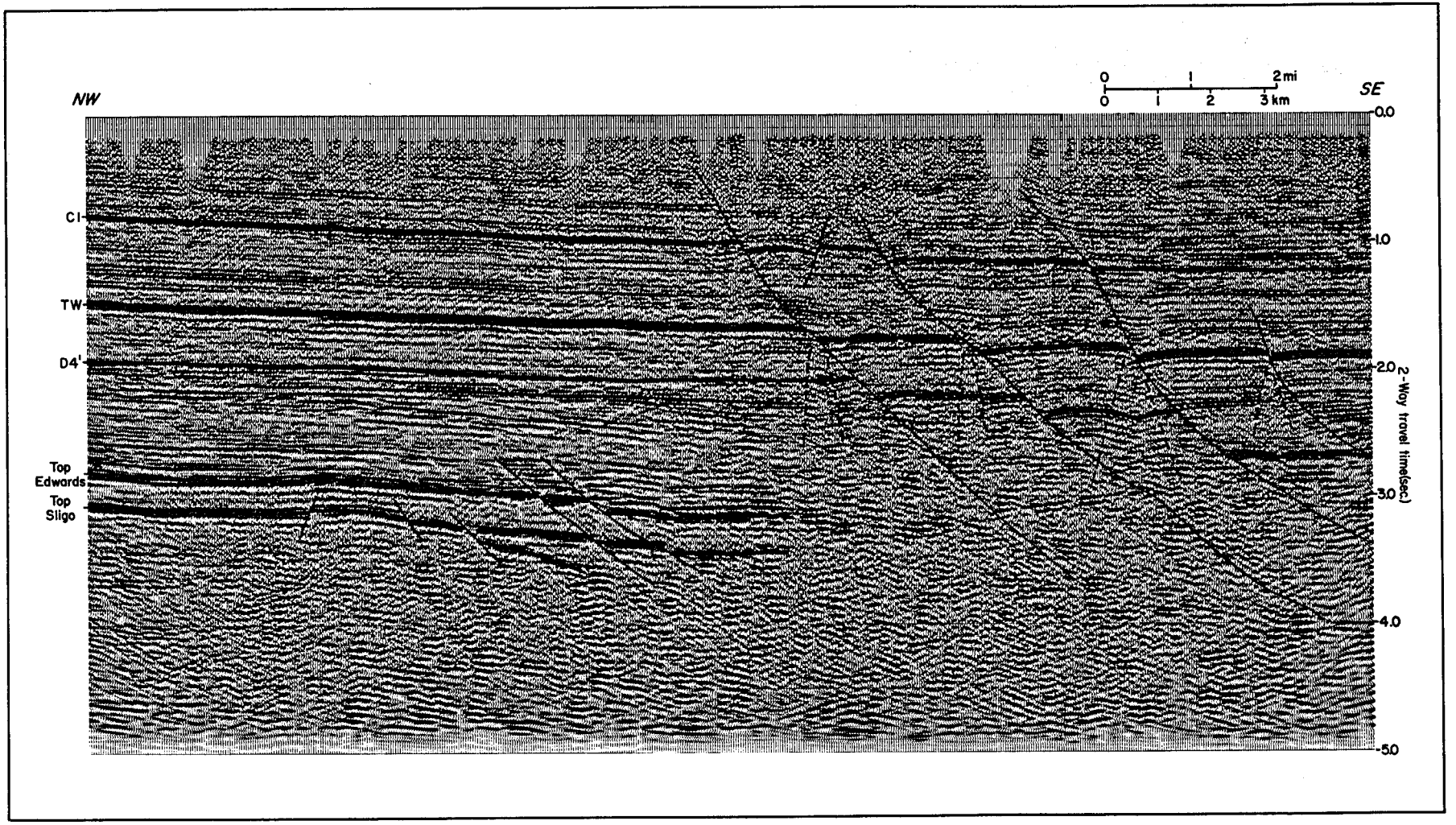

Figure 12. Seismic section (migrated) with orientation nearer to true structural dip than in figure 11. Location is shown in figure 7. Faults cutting TW appear to cause a "wipe-out" zone below, with apparent velocity pulldown. This section also shows carbonate shelf margins and Midway Group clinoforms.

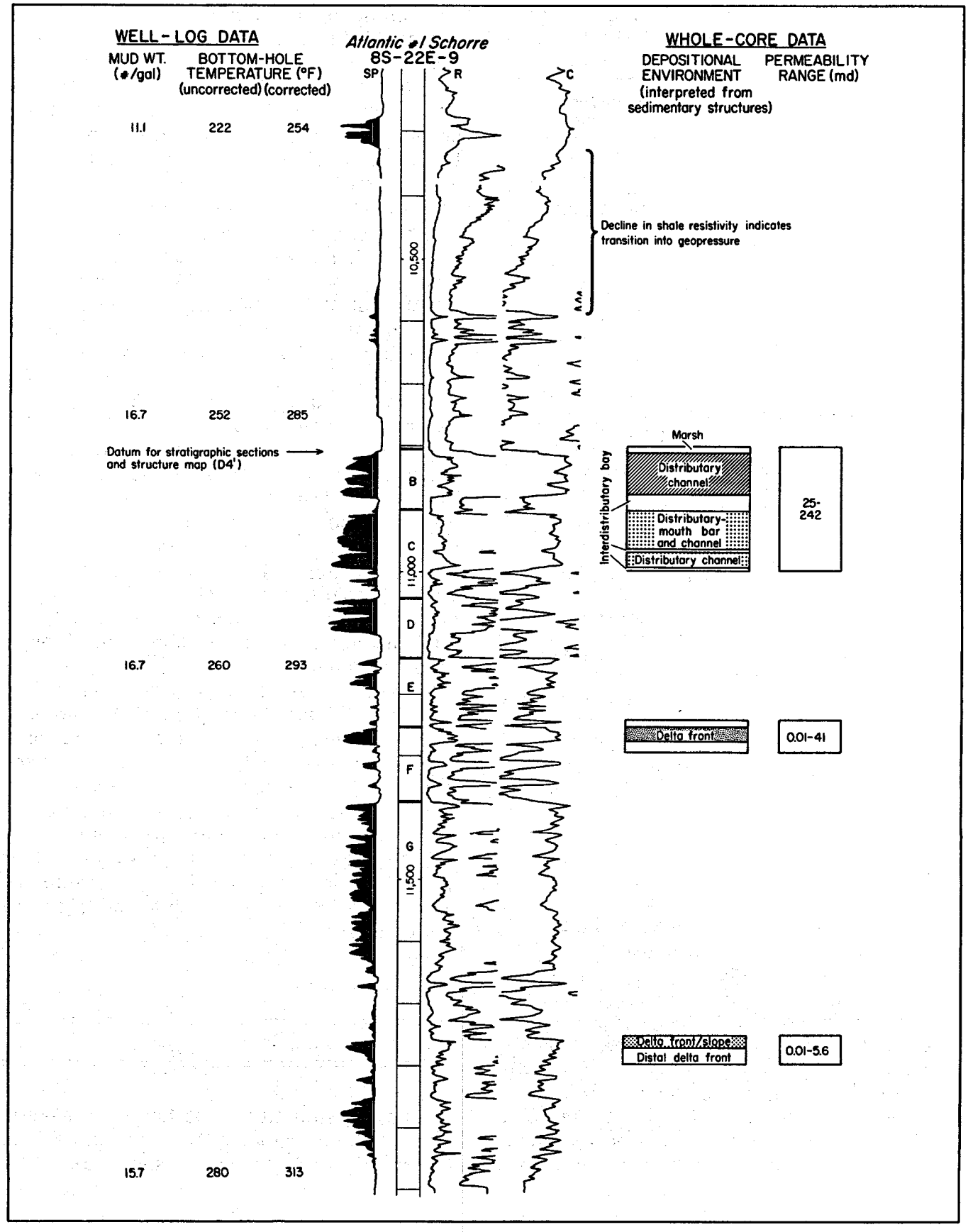

Figure 13. Lower Wilcox section in the type well, with supplementary data. Environmental interpretations are based on core analysis.

Table 3. Electric-log analysis of facies in the lower Wilcox (unit 6), used for paleogeographic mapping in the Cuero area.

Environmental interpretation	Log characteristics	Geographic distribution
Fluvial/deltaic plain	High sandstone, blocky patterns; laterally discontinuous (individual sands cannot be correlated)	Updip of growth faults; to northeast; toward Rockdale delta
Strandplain	Thin sandstones, mostly upward-coarsening, high lateral continuity in strike and dip directions	Mostly updip of growth faults; to southwest of fluvial/deltaic-plain facies
Delta front	Similar to strandplain facies*; high lateral continuity in strike direction	Along growth-fault trend, basinward of fluvial/deltaic-plain facies
Distributary channel	Thick sandstones, blocky to upward-fining, few shale breaks	Within growth-fault trend, laterally continuous with delta-front sandstones
Prodelta/slope	Low sandstone; greatly expanded section; correlation virtually impossible	Downdip of main fault block

*Similar pattern was also observed below fluvial/deltaic-plain facies in Midway-Wilcox transition.

considerable depth, which may be below the Lower Cretaceous Edwards Limestone in thin, non-diapiric Jurassic salt.

Initiation of growth faulting corresponds approximately to the Midway-Wilcox stratigraphic boundary. There are three possible explanations of this timing: (1) Growth faulting began once the shelf margin prograded beyond the buried Lower Cretaceous shelf edge; this may have allowed the shale section to attain the critical thickness (Crans and Mandl, 1981) required for gravity sliding. (2) Growth faulting began with a major influx of sand; therefore, growth faulting could have been caused by loading of sand on top of mud (Bruce, 1973). (3) If décollement took place in non-diapiric salt, growth faulting may have begun once the shelf margin reached the updip limit of salt, which permitted large-scale gravity sliding. It should be noted that the presence of salt has not been documented in this part of the Gulf Basin and is not apparent from available seismic-reflection data.

Reconstruction of the earliest structural growth is hampered by the difficulty in correlating any marker below D4' because of the transitional Wilcox-Midway boundary. From stratigraphic dip sections with a datum of D4', it appears that faults bounding the South Cook field were active during early Wilcox time and had growth ratios of 1.5 to 2 (fig. 9). During deposition of interval 5 (middle Wilcox strata), these same faults continued to move, and growth ratios were below 2 (fig. 21). This early, relatively rapid growth isolated lower Wilcox sandstones and permitted pressure to build up in the South Cook fault block (fig. 17). The fault farthest updip did not begin to move until the time of deposition of interval 4 (upper-middle Wilcox); this fault did not create a pressure trap. Growth ratios of other faults declined with time; by the time of deposition of interval 2 (Claiborne), growth ratios had dropped below 1.1 (fig. 21). By this time, the shelf margin had prograded approximately 20 to 30 mi basinward of its position in early Wilcox time (fig. 4). In post-Claiborne time (approximately 40 m.y. duration), the main structural activity was regional southeastward tilting (fig. 21). In spite of tilting, closure of rollover anticlines was maintained (figs. 18 through 20).

BLESSING AREA

The Blessing study was based on electric logs from approximately 120 wells and 150 mi (95 km) of proprietary seismic sections (fig. 22). Velocity surveys from six wells facilitated time-to-depth conversion of seismic sections. Only sidewall cores were available from this area.

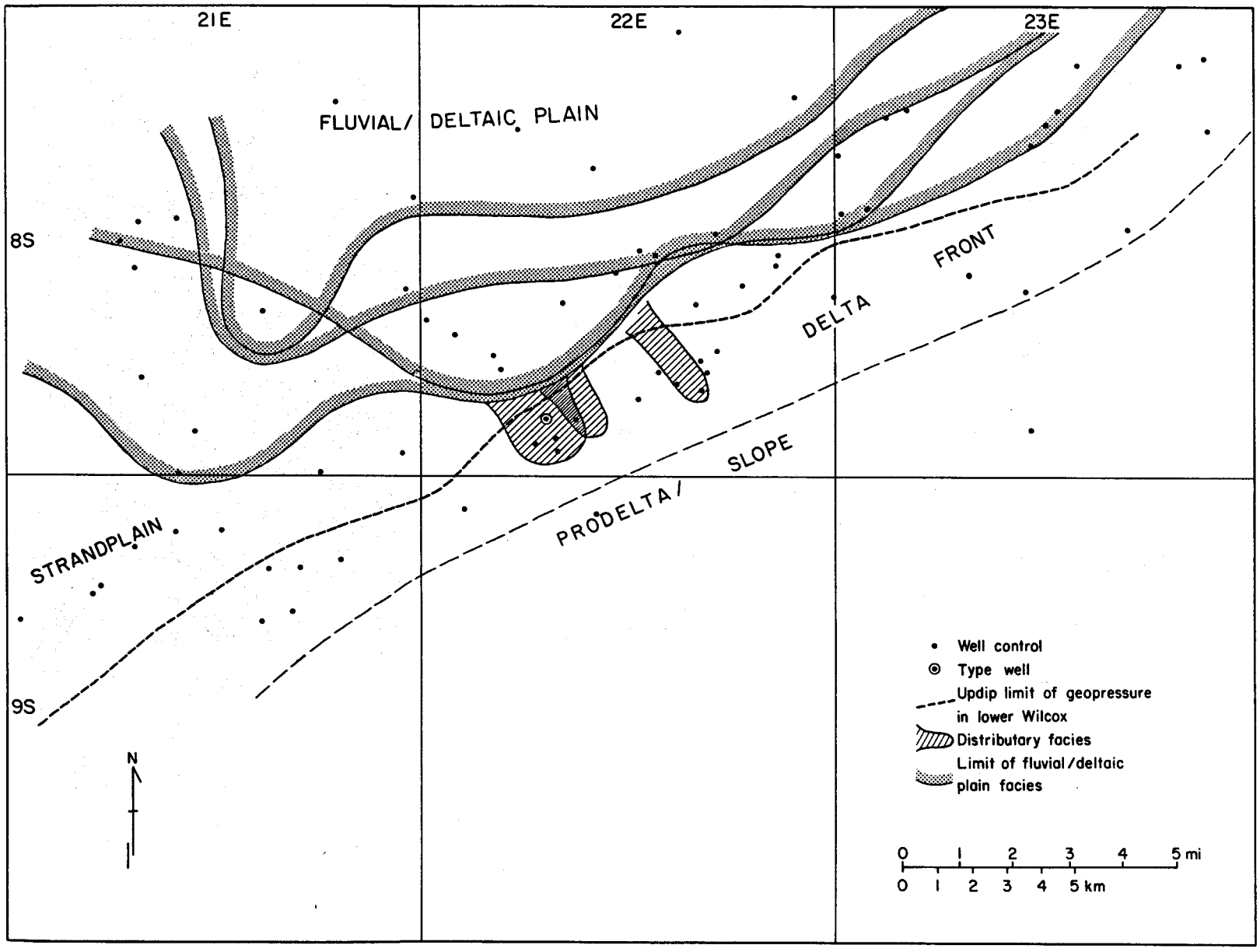

Figure 14. Lower Wilcox paleogeography of the Cuero study area, derived from electric-log analysis of facies. Extent of the fluvial/deltaic-plain facies shifted during early Wilcox time.

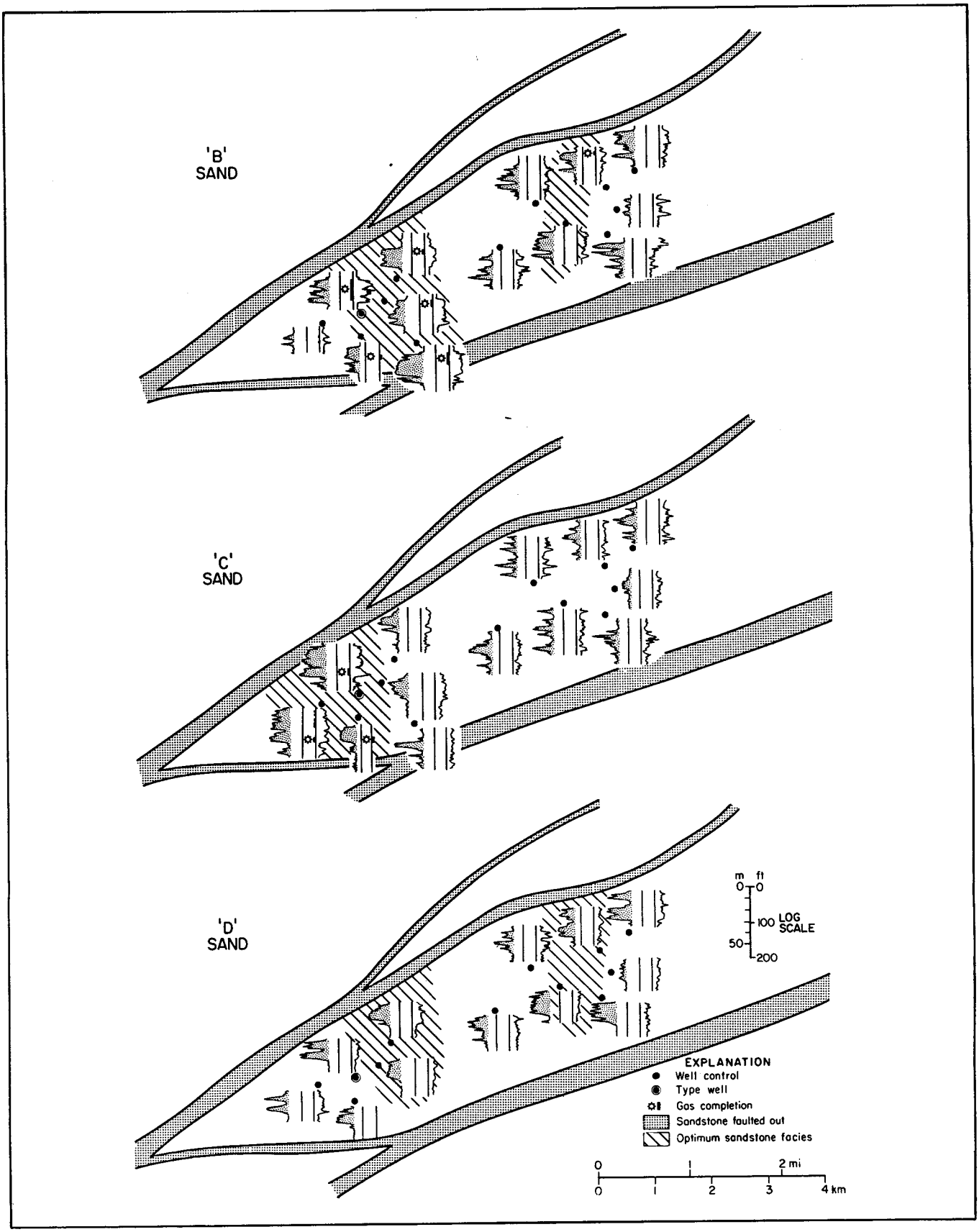

Figure 15. Geographic distribution of log patterns of three geopressured lower Wilcox sandstone aquifers in the South Cook fault block (fig. 7). Optimum sandstone facies are interpreted as distributary-mouth bars (figs. 13 and 14). 'B,' 'C,' and 'D' sands are identified in figures 9 and 13.

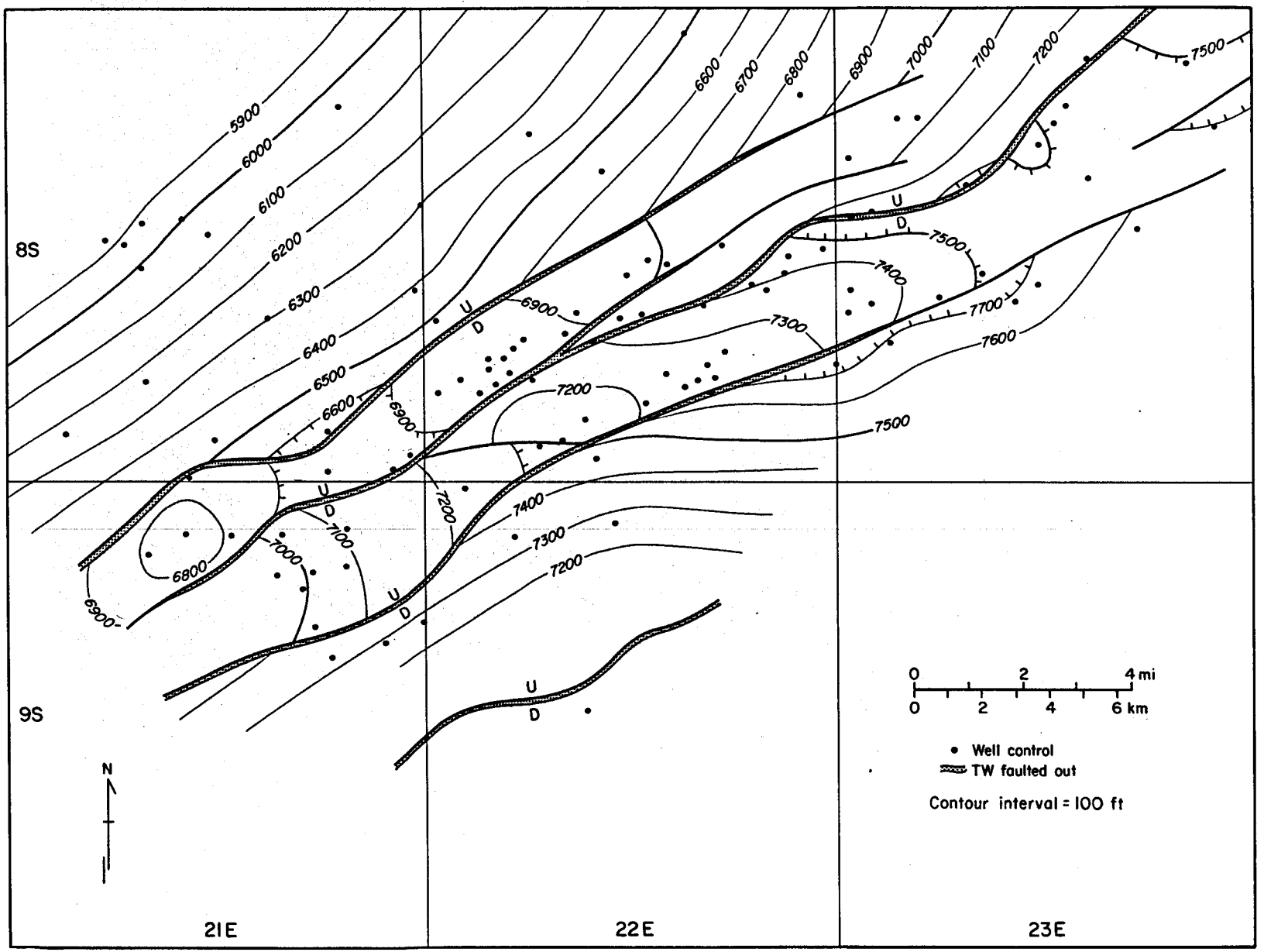

Figure 16. Structure map of top of Wilcox Group (TW marker). Note low structural relief and nearly parallel fault orientations.

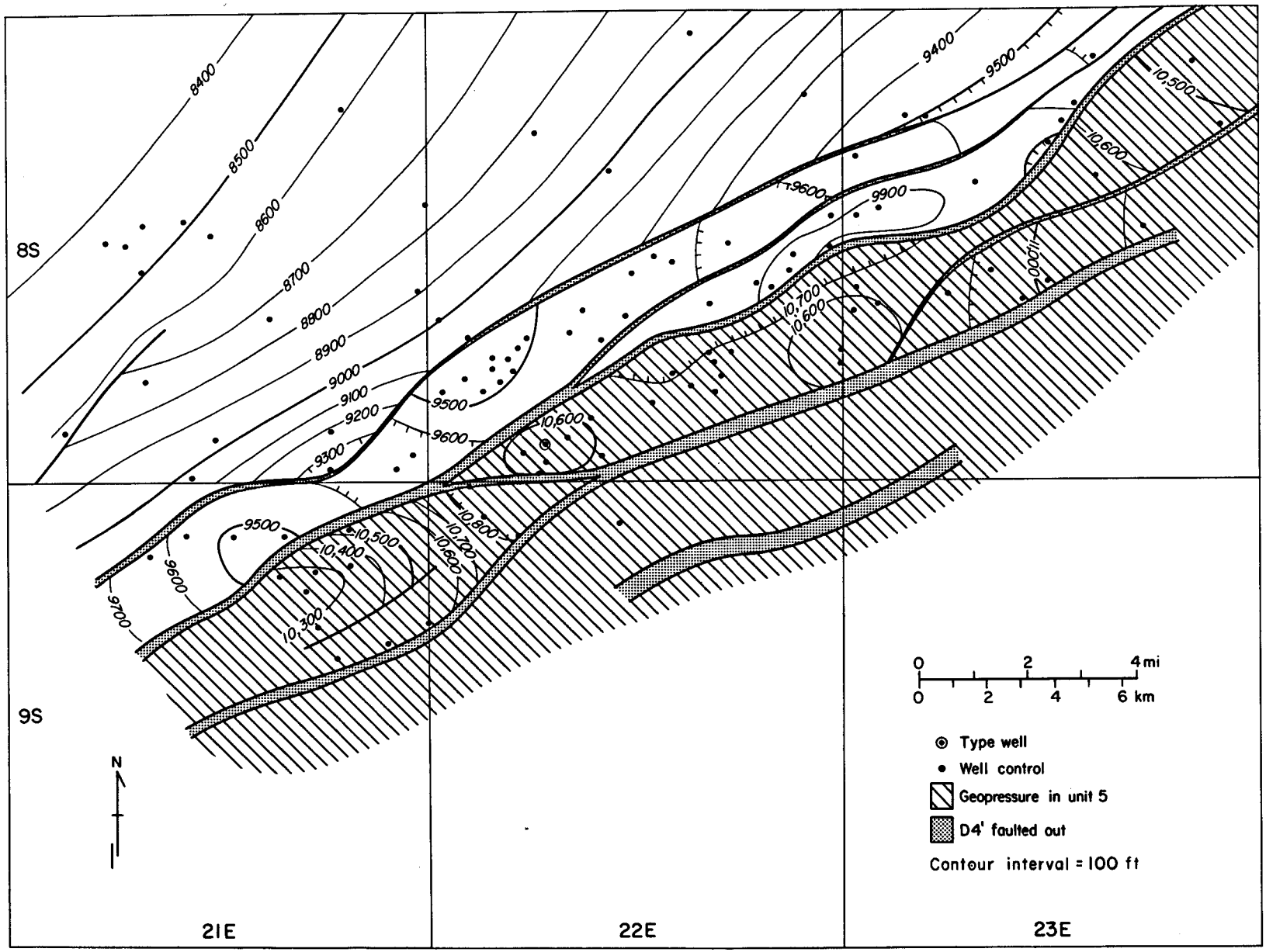

Figure 17. Structure map of top of lower Wilcox Group (D4' marker). Note similarity to structure on TW (fig. 16). Geopressure is limited to the South Cook fault block and farther downdip.

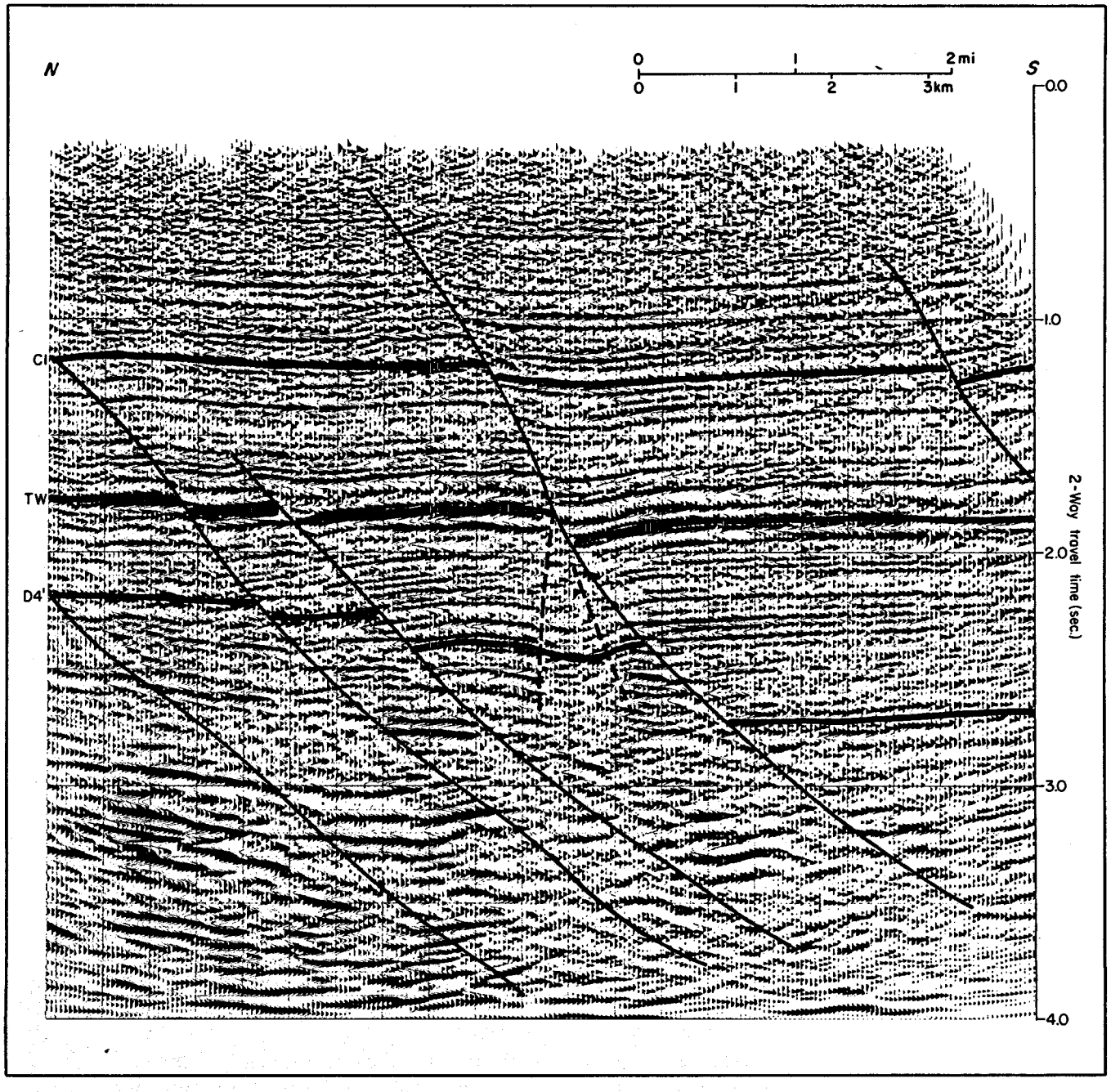

Figure 18. Seismic section UT-2 (migrated) crossing the South Cook fault block. Location is shown in figure 7. Stratigraphic position of correlation markers is shown in table 1. Note low structural relief and minimal rollover, suggesting deep décollement, possibly below the Cretaceous section. Also note "wipe-out" zone and pulldown below fault displacement of top of Wilcox (velocity discontinuity), similar to that in figure 12.

Stratigraphy

The maximum pre-Miocene regression in this area occurred in early Frio time (*Anomalina bilateralis* zone); thus, lower Frio sandstones have the greatest potential as geothermal reservoirs in the Blessing area. During the rest of Frio time, the area underwent a net transgression, which reached its maximum extent in Anahuac time (fig. 23; table 4). A second major regression occurred in the early Miocene.

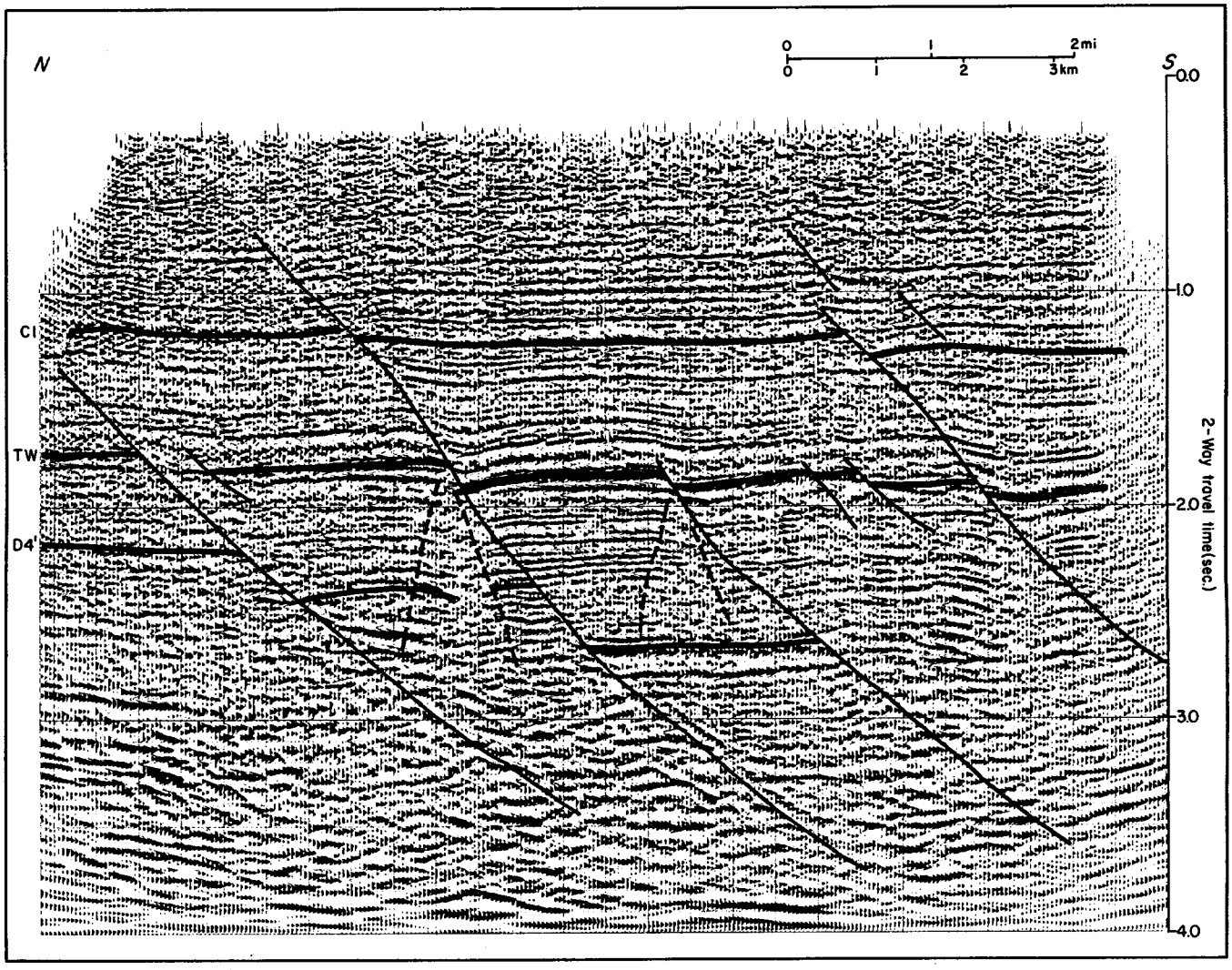

Figure 19. Seismic section UT-3 (migrated). Location is shown in figure 7. Stratigraphic position of correlation markers is shown in tables 1 and 2.

Correlation markers are the same as those used by Weise and others (1981) in a preliminary study of the Blessing area; only minor changes in correlations were made from the earlier study. Precise correlations of the lower Frio markers across major growth faults are difficult because of very large growth ratios. However, the sandy section of the lower Frio is reasonably well defined on both sides of most growth faults, so that an approximate base of the sandy Frio can be recognized across the study area (fig. 24).

Interval Velocities

As determined from six velocity surveys in the area, velocity distribution in the Blessing area is controlled primarily by stratigraphy (fig. 25), as it is in the Cuero area. In the Miocene section above the Anahuac Shale, interval velocities increase steadily with depth, reaching a maximum of about 8,000 ft/sec near the base of the sandy Miocene section. The top of the Anahuac is marked by a moderate velocity inversion in four of the six surveys. Within the Frio, velocities vary from 8,000 ft/sec to more than 10,000 ft/sec; velocities generally increase downward, but the trend is irregular. Local velocity inversions exist but do not correlate well with the top of geopressure. Local zones of high velocities noted in one velocity survey are probably artifacts of the data.

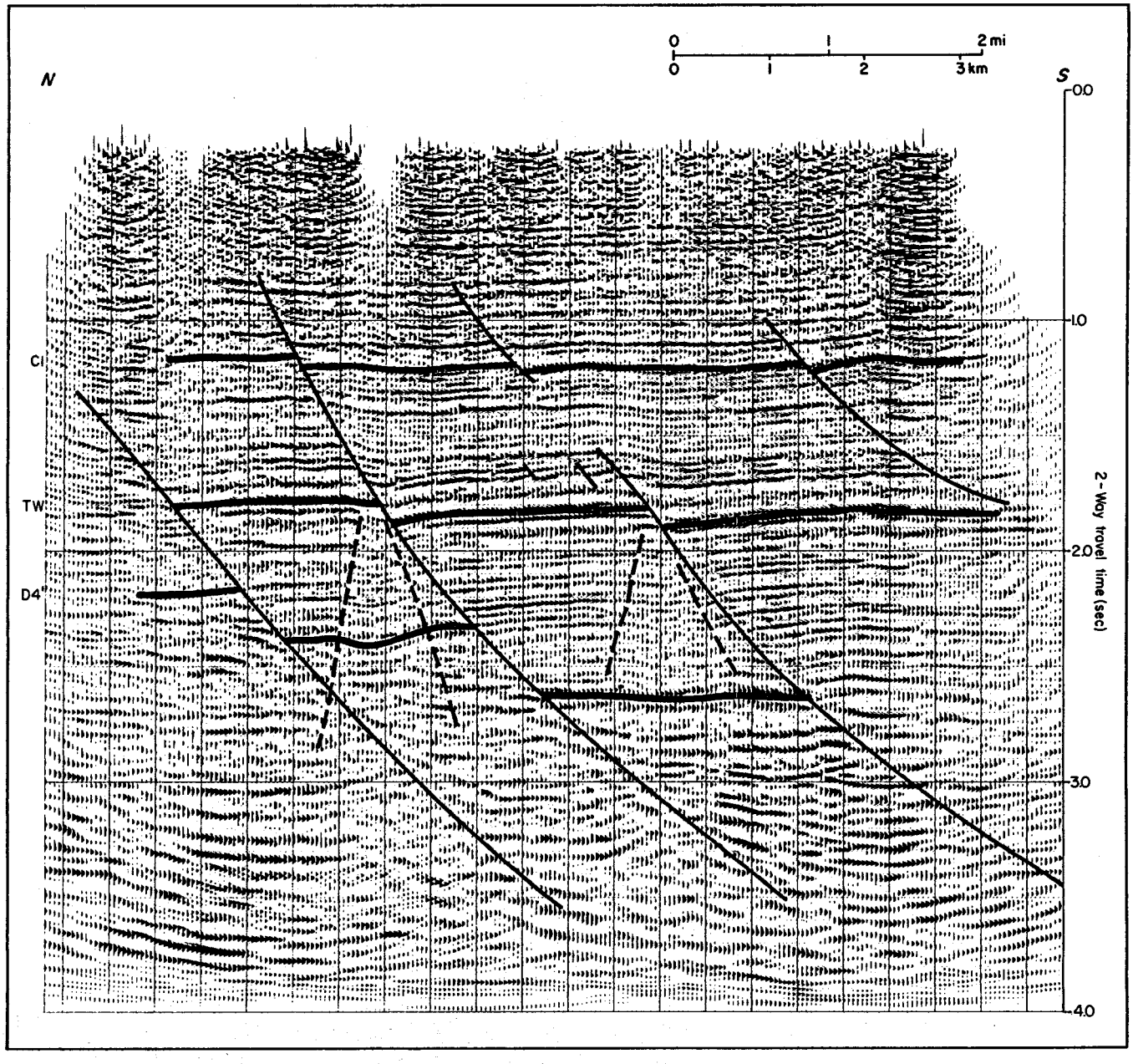

Figure 20. Seismic section UT-4 (migrated). Location is shown in figure 7. Stratigraphic position of correlation markers is shown in tables 1 and 2.

Lower Frio Sandstone Facies

The lower Frio (unit 6) facies in the Blessing area exhibits distinctive electric log patterns (table 5) that appear to be more closely related to differences in subsidence rate than to depositional environment. The facies updip of the major growth faults is characterized by low lateral continuity (fig. 24, A-A') and probably represents primarily channel deposits, perhaps of small-scale fluvial systems. The other facies show predominantly upward-coarsening log patterns and probably represent marginal-marine environments. Optimum reservoir sandstones are limited to strike-oriented trends within the Blessing field fault block (fig. 26) where individual sandstones without shale breaks attain thicknesses greater than 100 ft.

In areas of extremely low or high subsidence rates, individual sandstones are

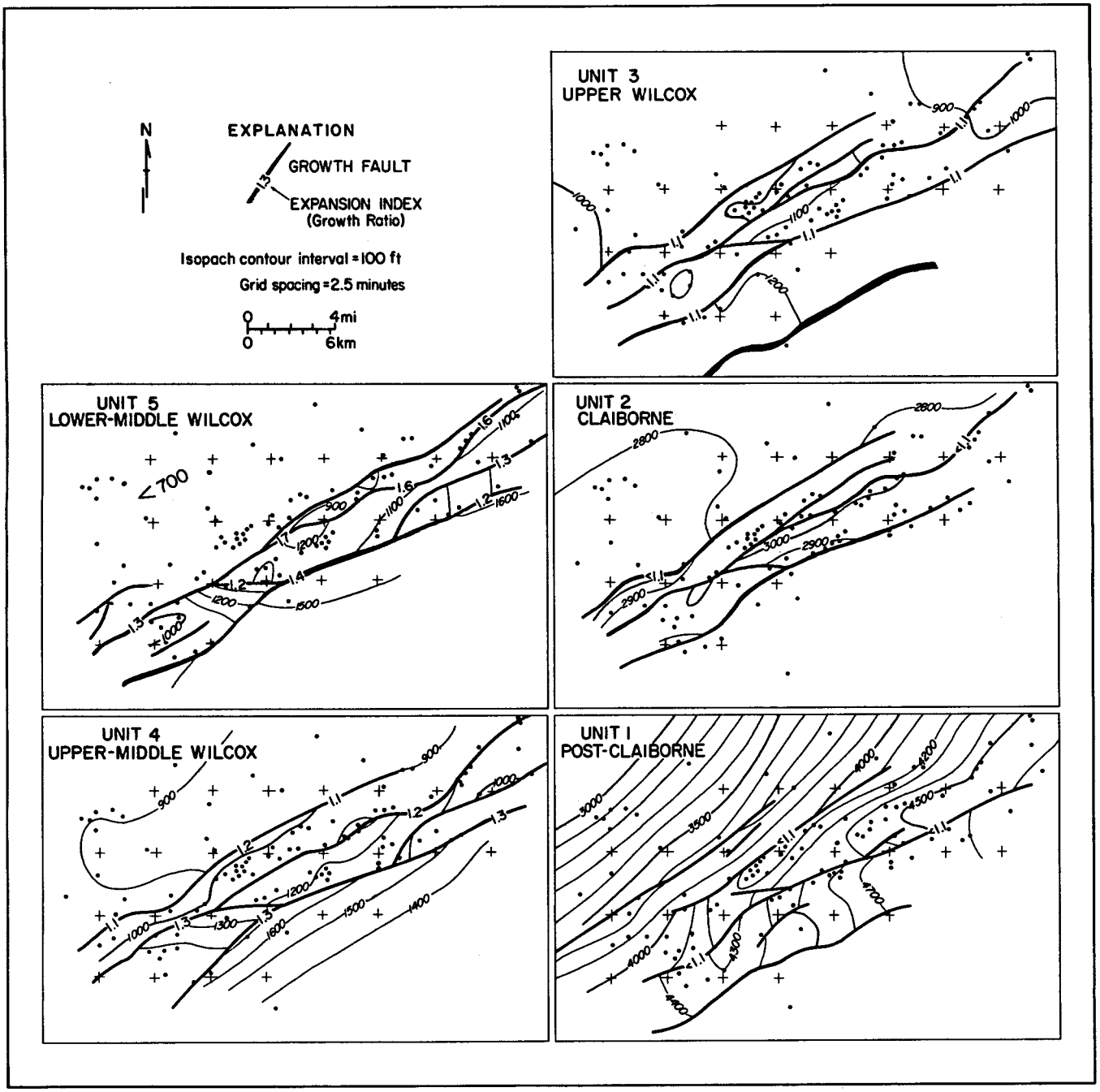

Figure 21. Sequential isopach maps illustrating post-D4' structural evolution of the Cuero study area. Slight distortion of the grid is caused by palinspastic restoration. The major change through time is a gradual weakening of the regional extensional regime, as evidenced by steadily declining expansion indices. Regional basinward tilting was primarily post-Claiborne. Movement of the updip fault is not apparent until unit 4.

generally thinner. To the north, against the main geopressure-sealing growth fault where subsidence rates are highest, the thick sandstones appear to break up into several thinner sandstones and intercalated shales. To the south, the reservoir sandstones thin because of both lower subsidence rates and a basinward decrease in sandstone percentage.

Permeabilities of the sand bodies are low (sidewall cores show about 25 md) but do show some increase upward within the

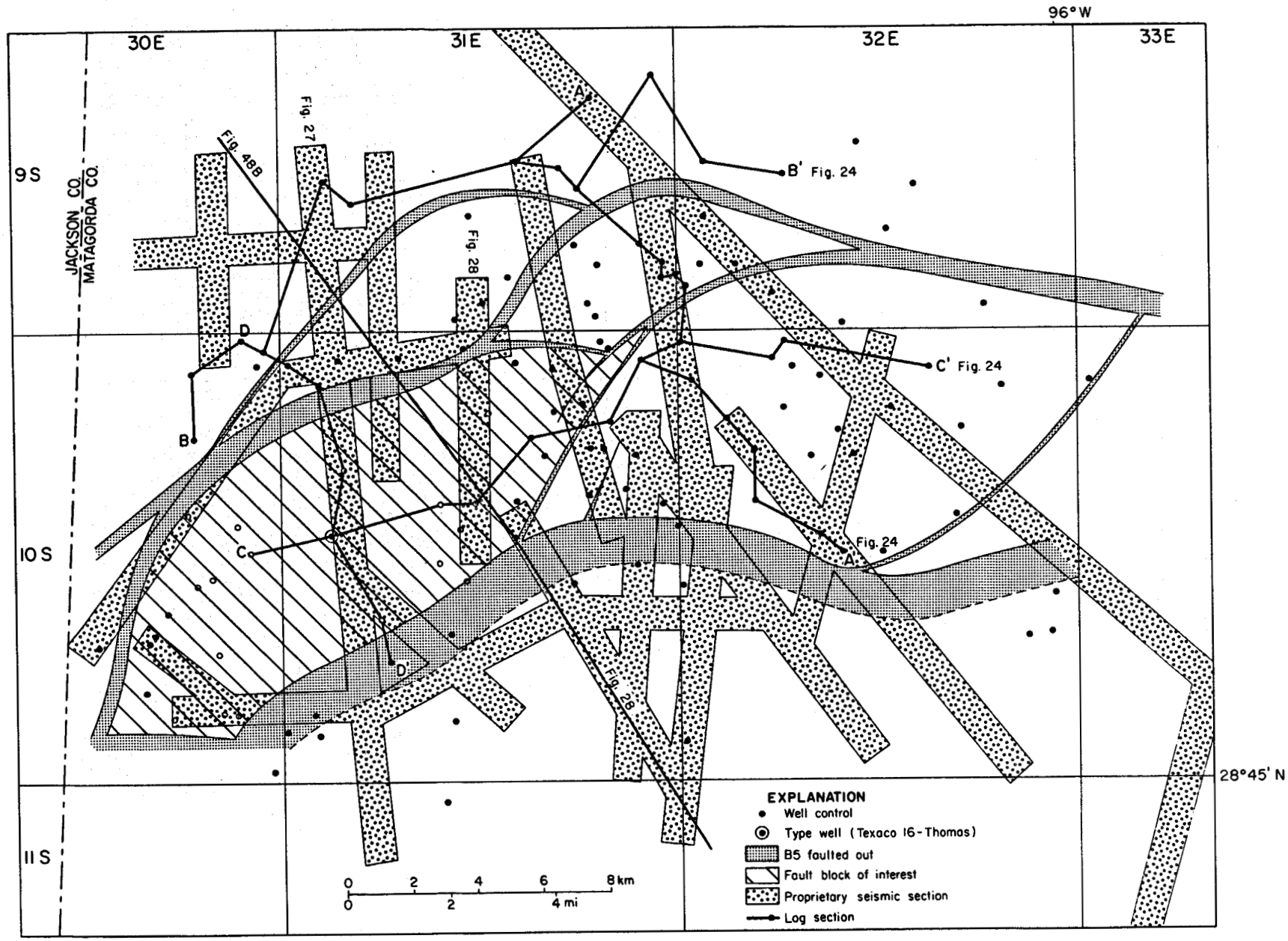

Figure 22. Data base map, Blessing study area.

Table 4. Characteristics of informal stratigraphic units in the Blessing area.

Unit numbers for isopach maps and structural sections	Log-correlation marker	Benthic foraminiferal zone	Stratigraphic unit	Lithology	Relative velocity	Seismic signature	Overall transgressive/ regressive character
1			Undifferentiated Miocene and younger	Thin sandstones, in shale; net thickness increases downdip	Fairly high; approximately linear increase with depth	Moderate to high amplitude and continuity (highest at base of unit)	Regressive
2	B1	*Discorbis*	Anahuac	Shale	Low to moderate, no increase with depth	Virtually transparent	Transgressive
3	B2	*Het.-Marg. and Cibicides hazzardi*		Shale; thin sandstones near base	Moderate, increasing with depth	Transparent at top, high amplitude at base	Transgressive (stacked regressive cycles)
4	B3	*Nodosaria blanpiedi*	Upper Frio	Sandstone and shale, mostly thin sandstone	Moderate to high, increasing with depth	Moderate to high amplitude and continuity	
5	B4	*Textularia seligi/Text. mississippiensis*	Middle Frio	Sandstone and shale, moderate amounts of sandstone	Fairly high, slight increase with depth	Moderate to high amplitude and continuity	
6	B5	*Anomalina bilateralis*	Lower Frio	Sandstone and shale, moderate amounts of sandstone	Fairly high, slight increase with depth	Low to moderate amplitude and continuity	Regressive
7	B6	*Textularia warreni*	Vicksburg	Shale	Probably low	Generally low to moderate amplitude	

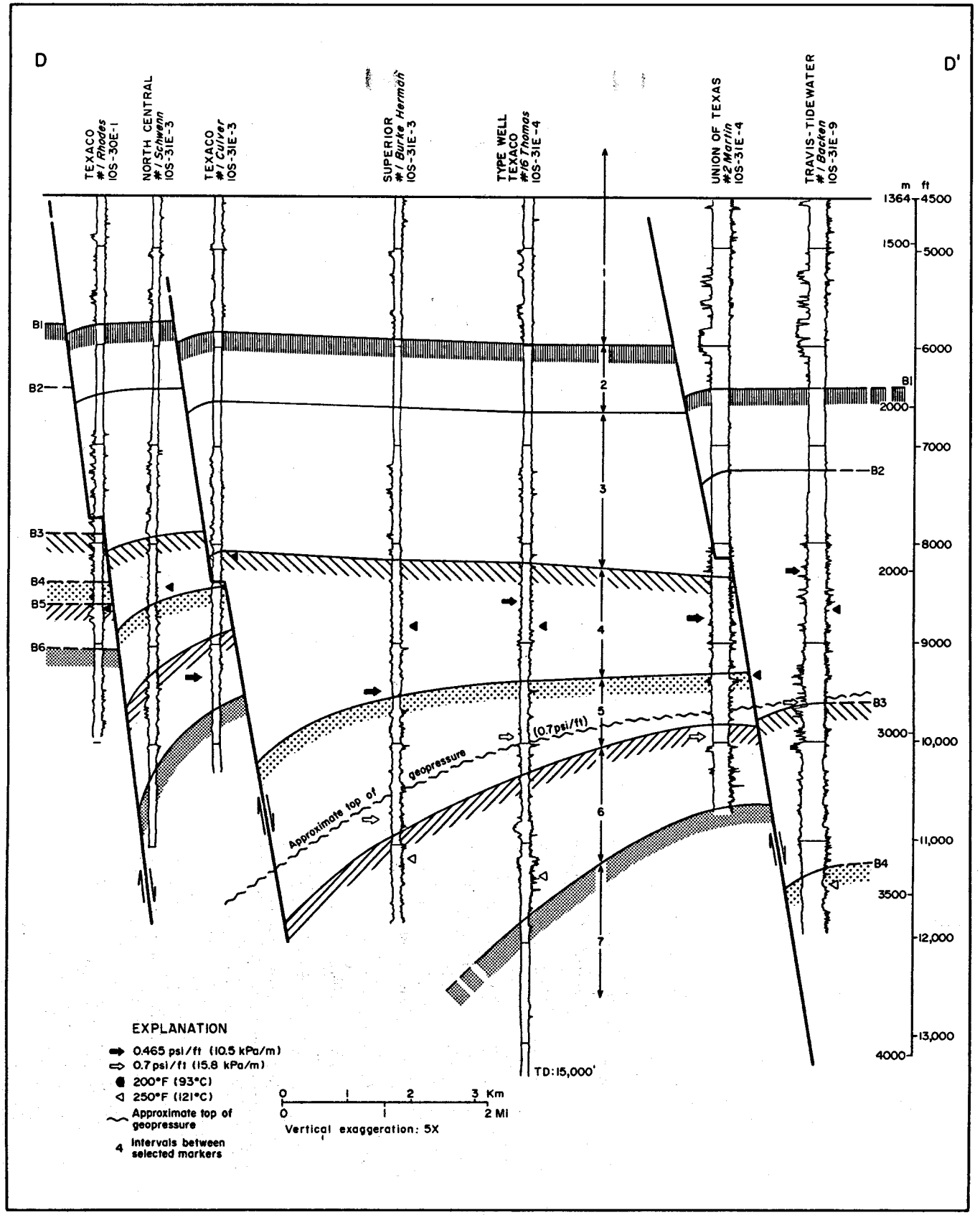

Figure 23. Structural dip section, Blessing area. Location is shown in figure 22. Stratigraphic position of correlation markers is shown in table 1. Equilibrium formation temperatures derived from log-header data; formation pressure gradients derived from shale resistivity plots. After Weise and others, 1981.

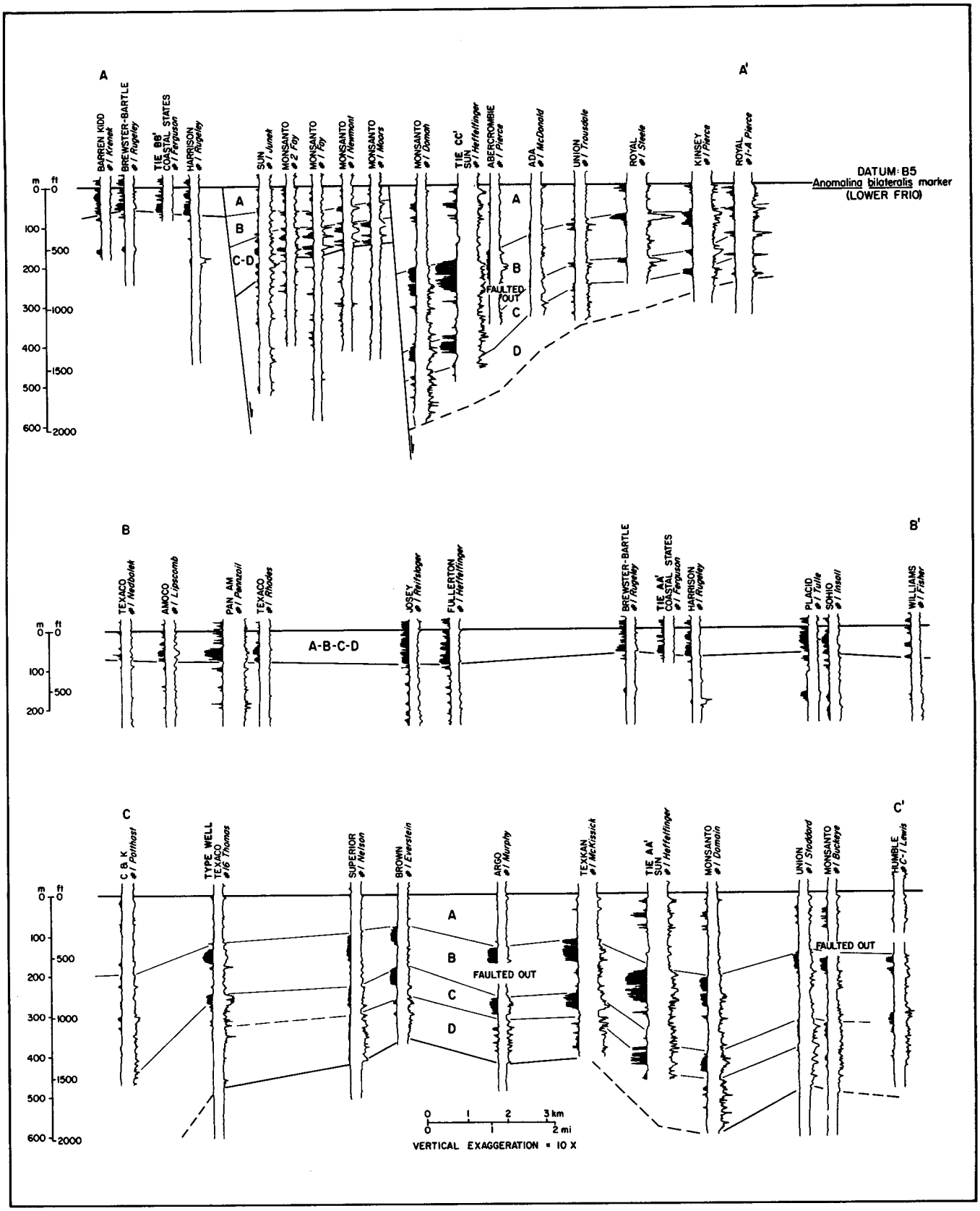

Figure 24. Stratigraphic sections of the lower Frio *Anomalina bilateralis* zone in the Blessing area. Locations are shown in figure 22. Spacing of adjacent logs has been modified somewhat to avoid crowding. Note that vertical sequences, sandstone geometry, and differentiation of cycles are strongly influenced by subsidence rate.

individual sand bodies. The area of optimum sandstone is extensive and is favorably aligned with the elongation of the Blessing fault block (fig. 16). These factors indicate considerable geothermal aquifer volume.

Structure

The structural style in the Blessing area (figs. 27 through 30) is typical of the Frio trend in the central Texas Gulf Coast, having highly sinuous, predominantly down-to-the-basin growth faults of variable spacing, thousands of feet of displacement at depth, growth ratios as high as 10:1, and extensive rollover on the downthrown sides. Displacements and growth ratios typically vary greatly along the major faults. Faults flatten somewhat with depth, but the décollement has not been seen on seismic sections. However, the listric nature of these faults can be inferred from the substantial amount of rollover.

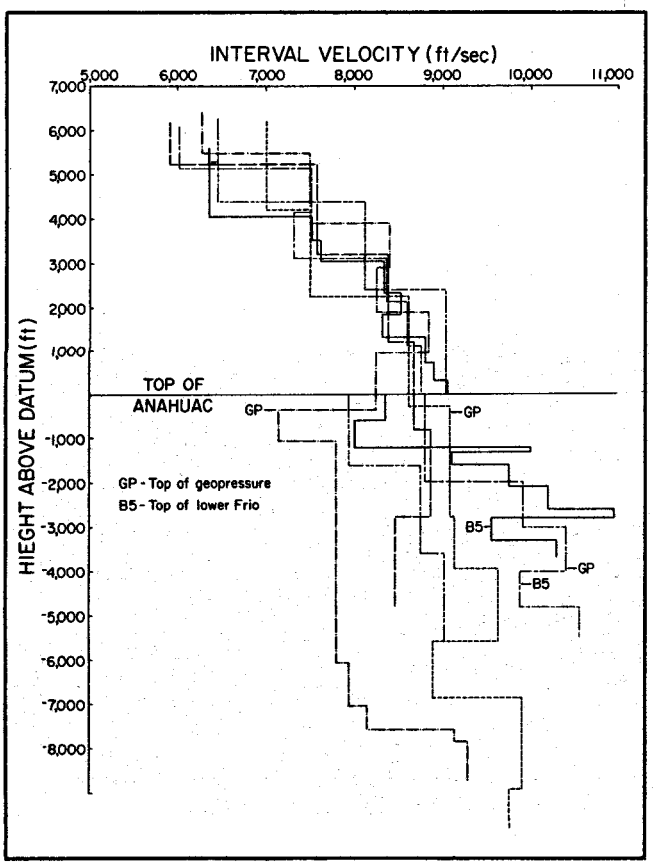

Figure 25. Interval velocities based on velocity surveys of six wells in the Blessing area.

Table 5. Electric-log analysis of facies in the *Anomalina bilateralis* zone (unit 6), lower Frio Formation, Blessing area.

Environmental interpretation		Log characteristics	Geographic distribution
Fluvial/ deltaic plain and channels	low subsidence rate	Thin, laterally discontinuous sandstones	Updip of growth faults
Coastal barrier/ strandplain, possibly some channels	moderate subsidence rate	Thin, laterally persistent sandstones, mostly upward coarsening	Fault block north of Blessing; southern part of Blessing fault block
	high subsidence rate	Thick, laterally persistent sandstones, few shale breaks, log pattern variable	Center of Blessing fault block
	very high subsidence rate	Numerous thin sandstones, abundant shale breaks, laterally continuous with thick sandstone facies	Northern part of Blessing fault block, near major growth fault

In the Blessing area, two major sets of growth faults cut the lower Frio Formation (fig. 30). The updip set consists of several arcuate faults enclosing lesser fault blocks and bounding the Blessing block on the north, separating it from the Tidehaven and Francitas fields (fig. 22). Downdip of the Blessing block is a single large growth fault separating the Blessing block from the Trull field to the south. Both sets of faults have relatively minor displacement in the Miocene strata.

In addition to these faults, smaller faults cut across the Blessing fault block (fig. 30). A zone of small faults bisects the Blessing block east of the Blessing field, where geopressured sandstone aquifers are best developed. These small faults were inferred from electric-log correlation, but were not apparent on seismic sections. A small cross fault is inferred to bound the Blessing block on the southwest.

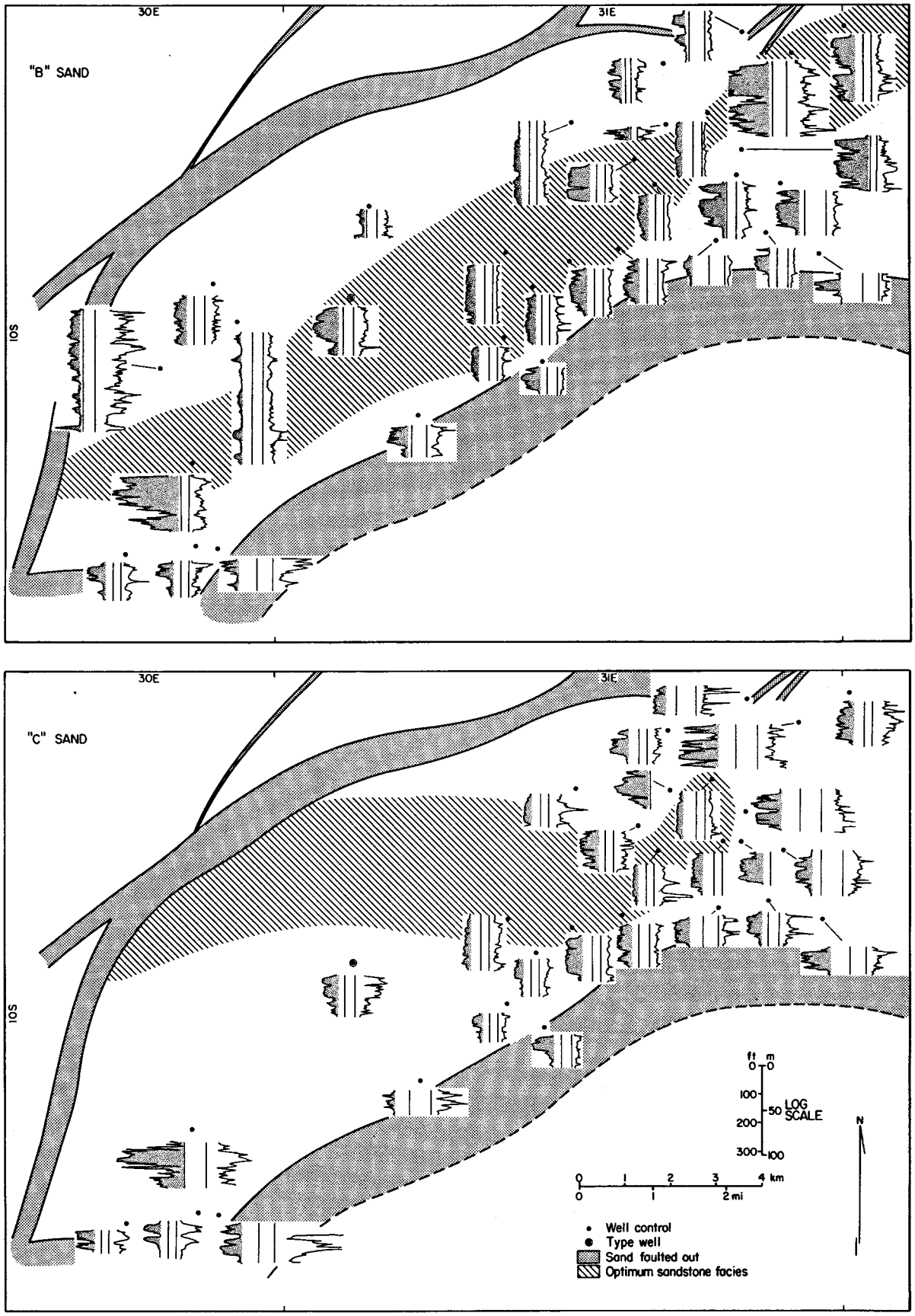

Figure 26. Geographic distribution of electric-log patterns in two lower Frio geopressured sandstone aquifers in the western part of the Blessing fault block. 'B' and 'C' sands are identified in figure 26.

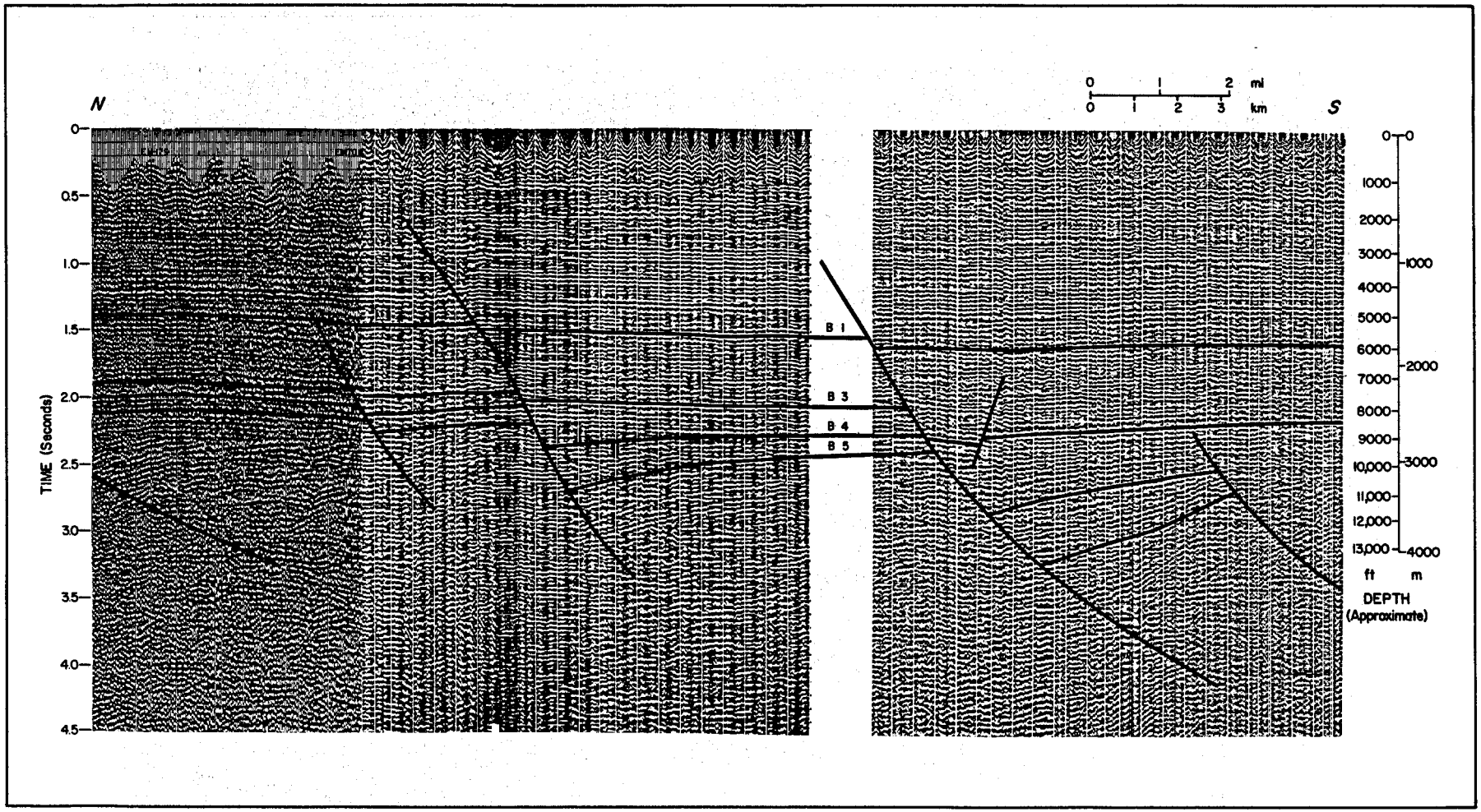

Figure 27. Single-fold seismic section illustrating typical structural style of the Blessing area: down-to-the-basin listric normal faults with considerable expansion and rollover of the deeper units. Location is shown in figure 22. Stratigraphic position of correlation markers is shown in table 1.

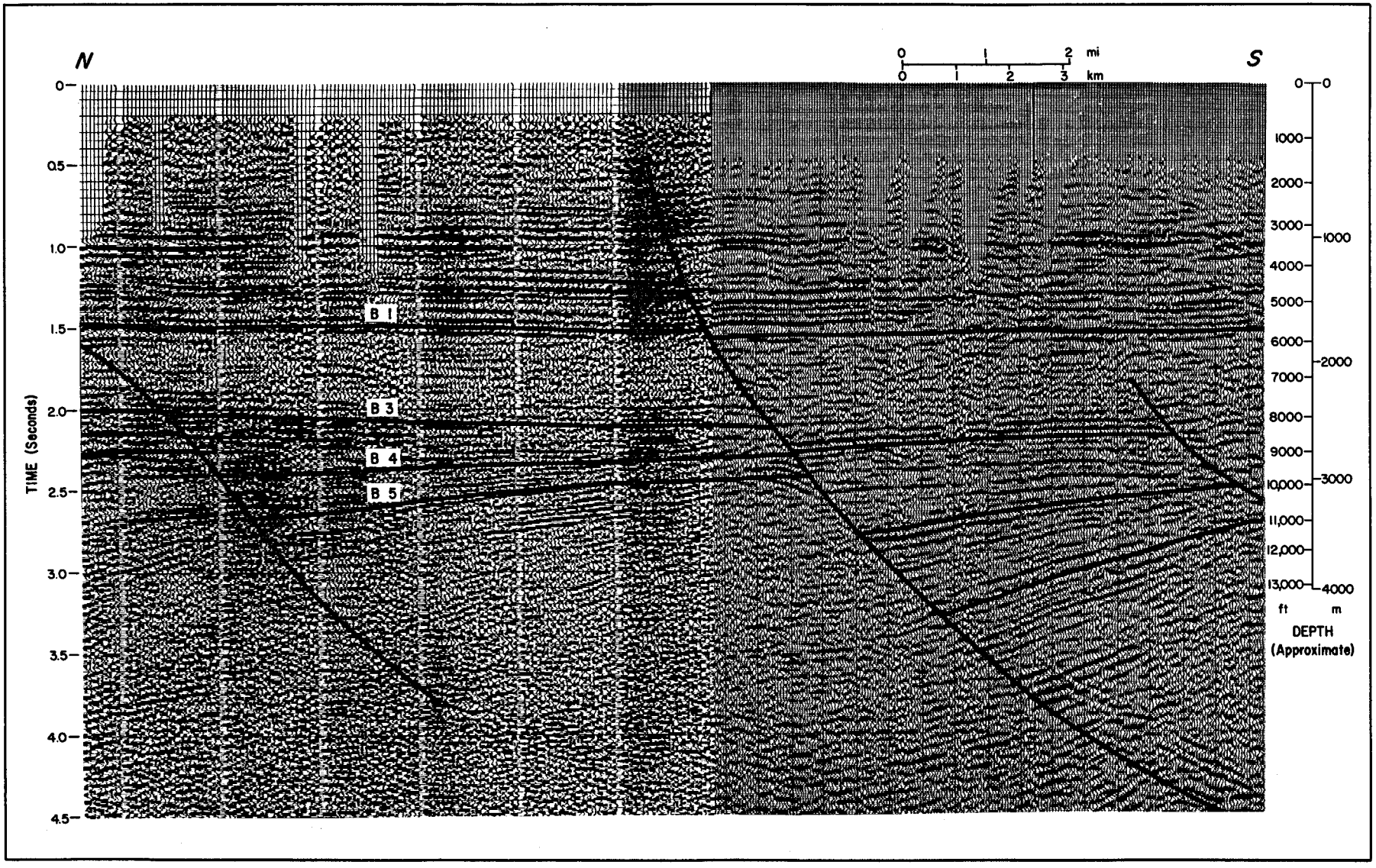

Figure 28. Twelve-fold seismic section (unmigrated) illustrating structural style. Small cross-faults in the Blessing fault block (fig. 30) are not apparent on this section and were recognized only from well data. Location is shown in figure 22.

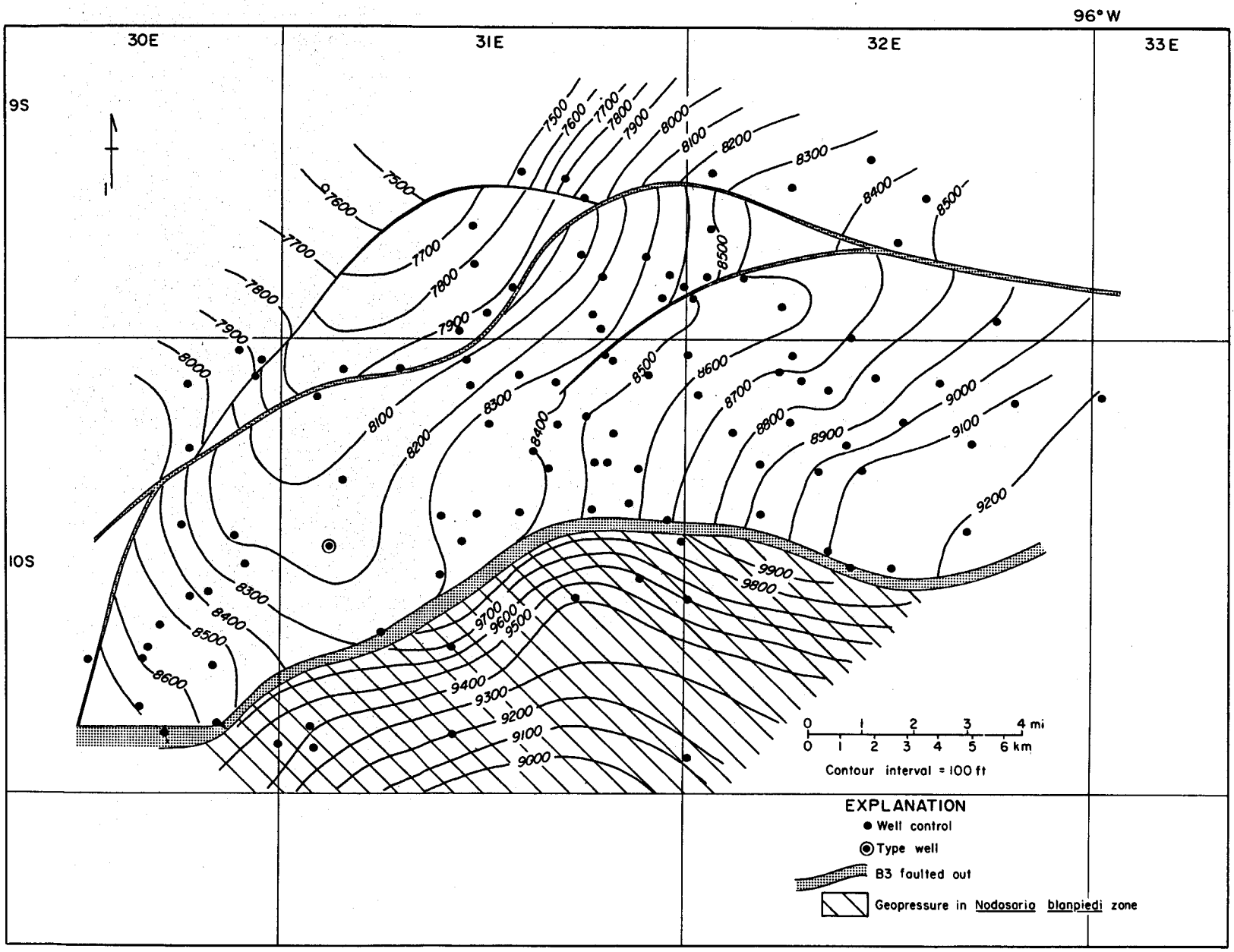

Figure 29. Structure map on B3 marker (upper Frio Formation), Blessing area. Faults in this area are much more sinuous than faults in the Cuero study area, and fault blocks are wider.

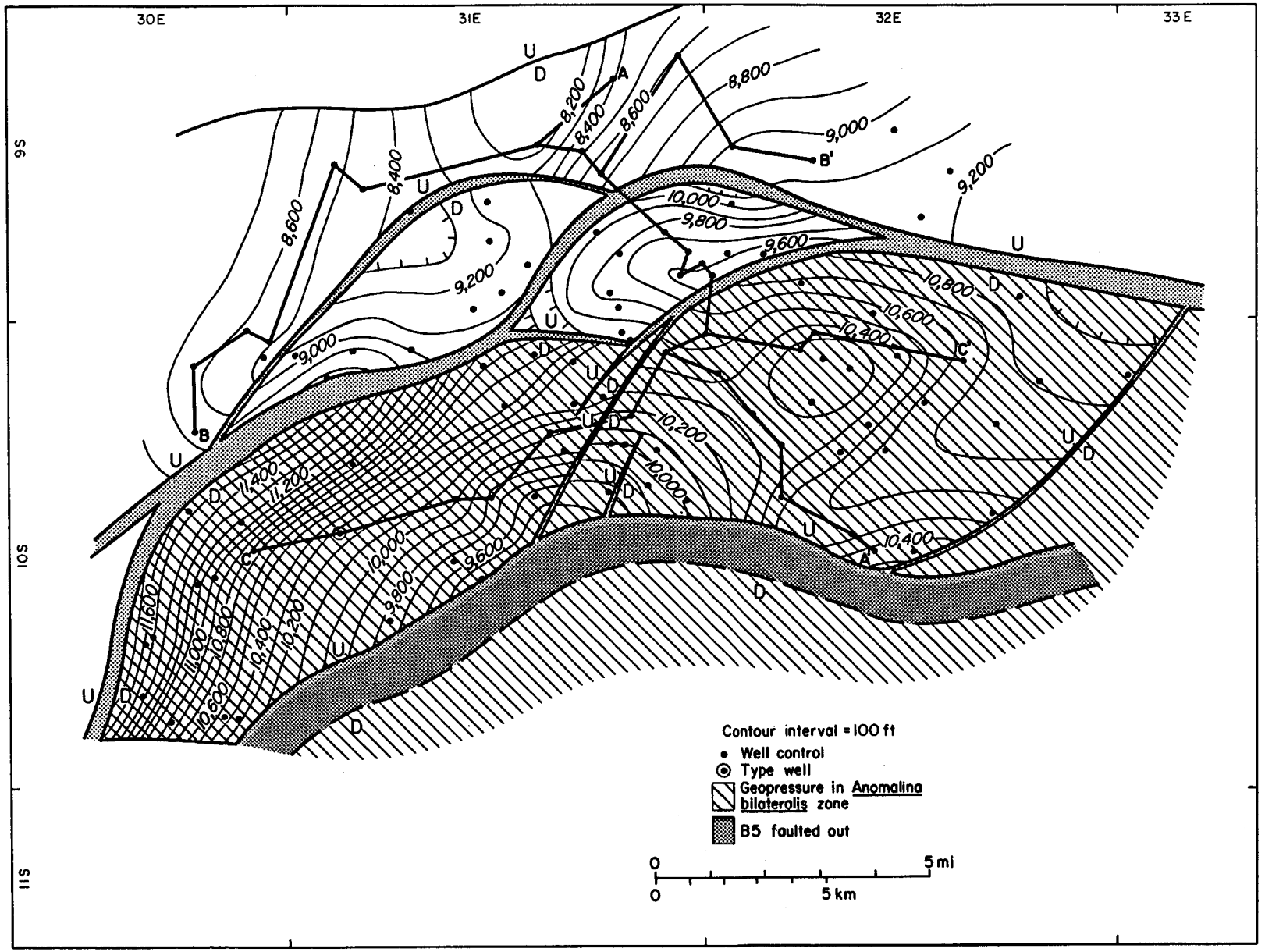

Figure 30. Structure map on B5 marker (lower Frio Formation), Blessing area. Fault patterns are similar to those in figure 29, but rollover is much greater at this stratigraphic level. Sections AA', BB', and CC' appear in figure 24.

Structural evolution (fig. 31) was characterized by a steady decline in growth-fault activity and late basinward tilting. During earliest Frio time (interval 6), the main updip growth fault underwent large-scale movement; growth ratios ranged from 4:1 to 10:1, and there was substantial rotation into the fault. This movement of the updip growth fault continued through unit 5 time and into unit 4 (middle Frio time). The downdip fault probably began to move during interval 6 time as well, but the data are inadequate to define this stage. In late-Frio to post-Frio time (units 1 through 3), fault activity was relatively minor, growth ratios being generally less than 1.2:1.

The Blessing fault block underwent major rotation and rapid subsidence near the updip growth fault from the time of unit 6 through unit 4. This movement resulted in predominantly landward dips in these units and in sealing of the sands in these units by pre-Frio slope shales to the north and northwest (figs. 27 and 28).

PLEASANT BAYOU AREA

The Pleasant Bayou study was based on logs of approximately 150 wells and 130 mi (80 km) of seismic data (fig. 32). Velocity surveys from five wells in the area provided velocity control for time-to-depth conversion. Cores from the Pleasant Bayou No. 1 were logged in detail (Morton and others, 1983); cores from other wells have also been examined (Tyler and Han, 1982).

Stratigraphy

Pleasant Bayou stratigraphy is similar to that of the nearby Blessing area. Geopressured sandstone aquifers occur within the *Anomalina bilateralis* zone of the lower Frio Formation, which represents the maximum pre-Miocene progradation of sandy facies in this area (table 6; fig. 33). Of the correlation markers used in this report, T2, T4, and T5 were also used in earlier reports on the Pleasant Bayou area (Bebout and others, 1978; Flanigan, 1981), whereas TA and T3' are new. The only serious difficulties in correlation were encountered with the sub-T2 markers across the South Chocolate Bayou fault zone (fig. 32), where growth faults are closely spaced and cause a great expansion of section (fig. 33). A tenuous lithologic marker was picked at the apparent base of the sandy Frio section for use in isopach mapping of interval 6 (figs. 34 and 35).

Interval Velocities

As in the other areas, velocity distribution in the Pleasant Bayou area (fig. 36) is controlled primarily by stratigraphy. In the Miocene section, interval velocities increase fairly steadily with depth, reaching a maximum near the base of the Miocene. High interval velocities in the lower Miocene section may be caused in part by "hard streaks," or zones of high log resistivity (Flanigan, 1981). The very high velocity interval in the geothermal test well at the base of the Miocene is probably due to an inconsistency between adjacent shots in picking the first breaks; the calculated interval velocity of 17,000 ft/sec is unreasonably high for a porous clastic lithology.

The top of the Anahuac Formation is marked by a sharp velocity inversion; all the velocity surveys show the Anahuac to be a low-velocity zone. Within the Frio section, interval velocities again increase fairly steadily, except in one well that penetrated a major growth fault and continued to considerable depth through pre-Frio shale. The low-velocity zone encountered in the deepest part of this well is not representative of the Frio. Most of the other data do not indicate that a significant velocity inversion occurs consistently with the top of geopressure. We therefore infer that a simple general relationship between interval velocities and formation pressures does not exist. Our observation casts doubt on the validity of using inversions observed on velocity analyses to predict the top of geopressure before drilling begins. This relationship is known to work in some areas of offshore Louisiana, but it does not appear to be universally applicable.

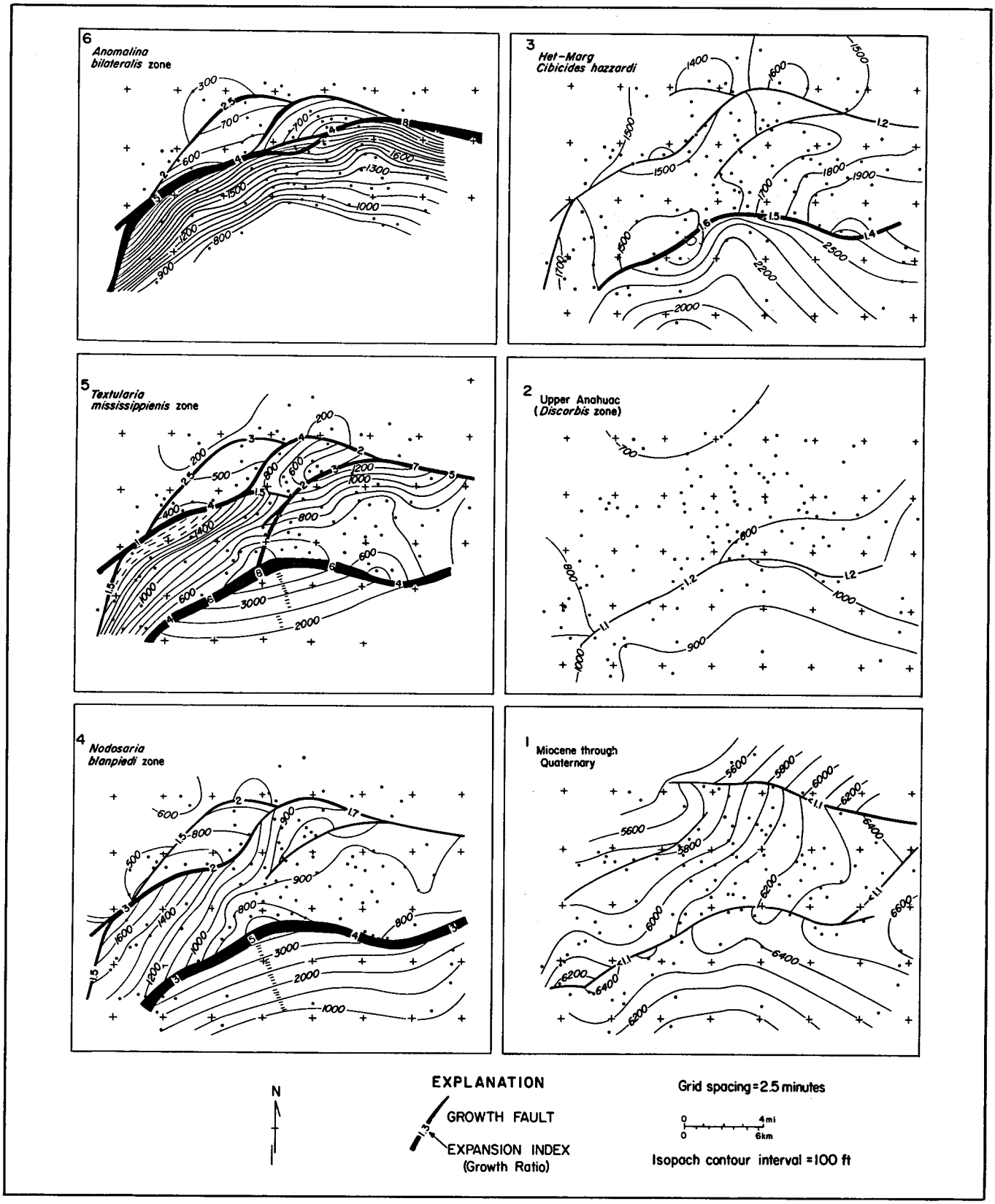

Figure 31. Sequential isopach maps illustrating structural evolution of the Blessing area. Distortion of the grid is caused by palinspastic restoration. As in the Cuero area, the major change with time is a steady decrease of expansion indices, indicating a weakening of the regional extensional regime. Areas of low subsidence rate in the oldest units (5 and 6) may represent residual shale masses, possibly having nonpiercement uplift. Regional basinward tilting was primarily post-Anahuac.

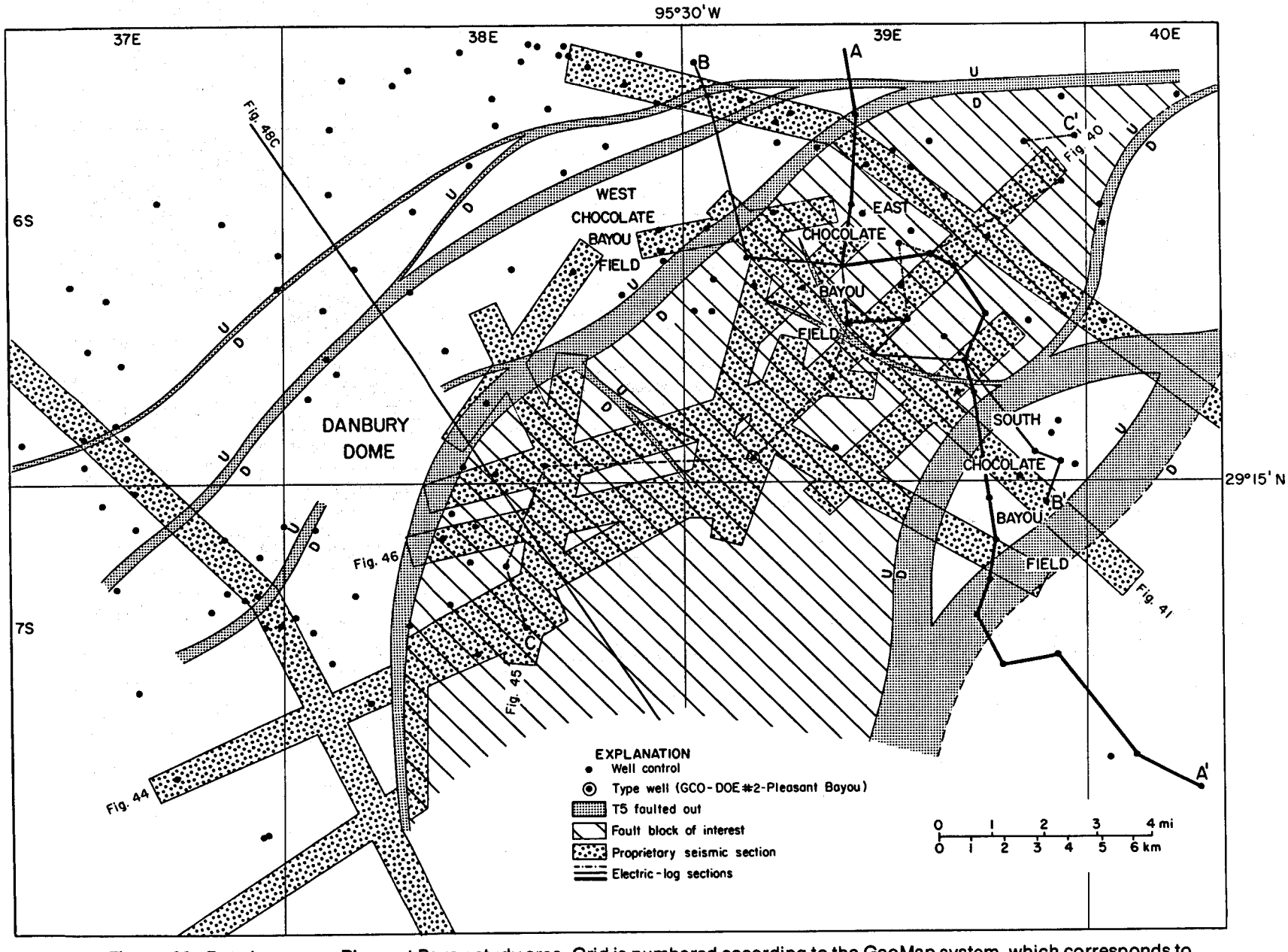

Figure 32. Data base map, Pleasant Bayou study area. Grid is numbered according to the GeoMap system, which corresponds to USGS 7.5-minute quadrangle. Exact locations of seismic sections are not shown because of proprietary restrictions.

Table 6. Characteristics of informal stratigraphic units in the Pleasant Bayou area.

Unit numbers for isopach maps and structural sections	Log-correlation marker	Benthic foraminiferal zone	Stratigraphic unit	Lithology	Relative velocity	Seismic signature	Overall transgressive/regressive character
1			Undifferentiated Miocene and younger	High sandstone; some "hard streaks" (high-carbonate beds) in lower part of section	High; approximately linear increase with depth	Variable amplitude and low continuity high in section, grading down into high amplitude and high continuity	Regressive
	TA						
2		*Discorbis* and *Het.-Marg.*	Anahuac	Shale (poorly indurated)	Low	Virtually transparent (coherent reflectors may be multiples)	Transgressive
	T2						
3		*Cibicides hazzardi*	Upper Frio	Interbedded sandstone and shale; sandstone percentage generally decreases upsection	High; general increase with depth. No apparent relationship with geopressure distribution	Moderate amplitude and continuity. On many sections, obscured by multiples from Miocene section	Transgressive (stacked regressive cycles)
	T3						
4		*Nodosaria blanpiedi*	Middle Frio				
	T4						
5		*Textularia mississippiensis*	Lower Frio				
	T5						
6		*Anomalina bilateralis*					Regressive
7		*Textularia warreni*	Vicksburg	Shale	Low	Low amplitude; often obscured by multiples	

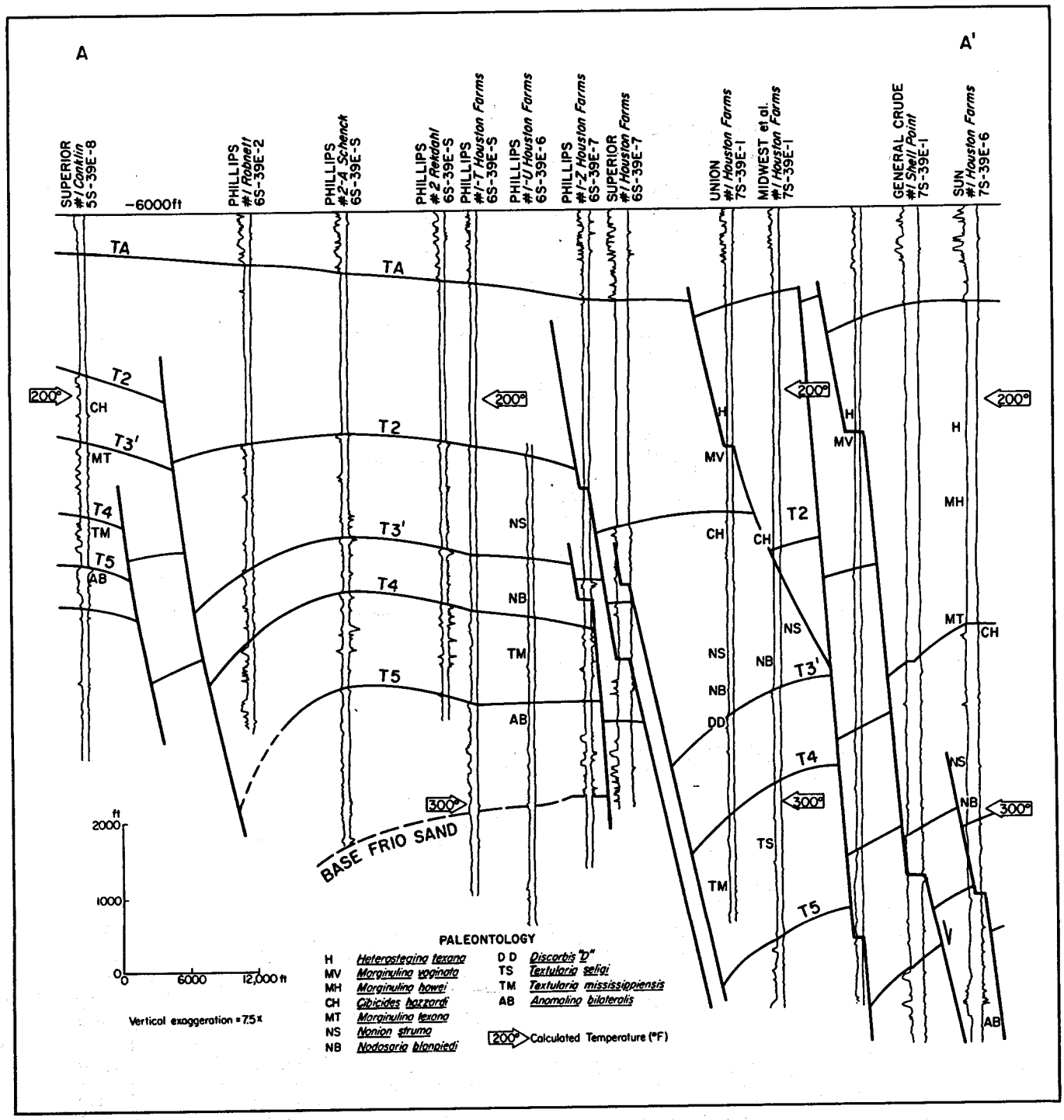

Figure 33. Structural dip section across Chocolate Bayou field illustrating electric-log character of the correlation markers and informal stratigraphic units in the Pleasant Bayou study area (table 4). Location is shown in figure 32.

Two factors may invalidate the pressure-interval velocity relationship. First, there may be controls on shale consolidation other than present fluid pressure. In the Pleasant Bayou test well, the consolidation state of clays increases steadily from the Anahuac, to the normally pressured Frio, to the overpressured Frio (K. L. Milliken, personal communication, 1982). This downward increase in shale consolidation is consistent with

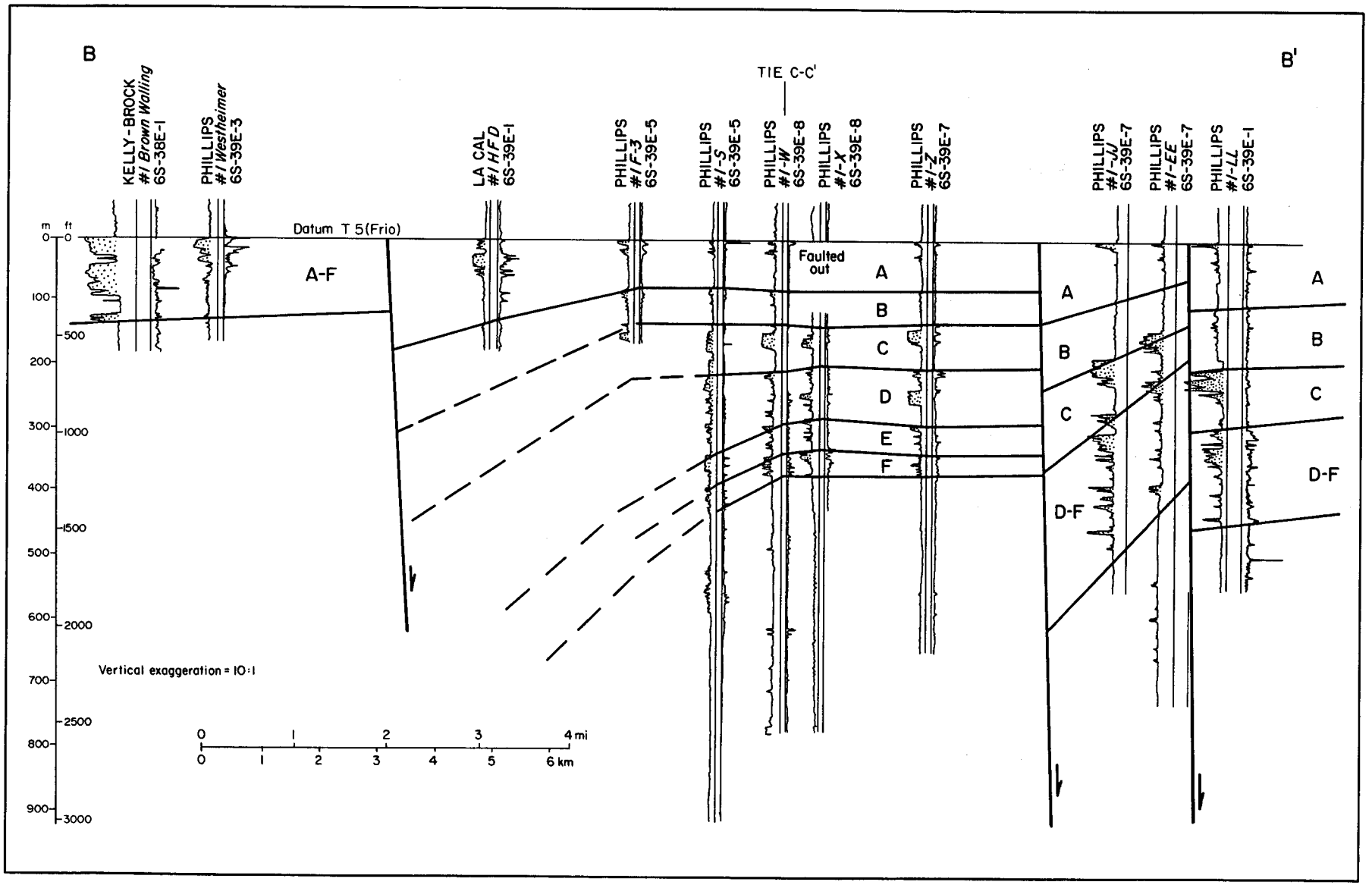

Figure 34. Stratigraphic dip section of the lower Frio *Anomalina bilateralis* zone across Chocolate Bayou field. Location is shown in figure 32. As in the Blessing area, vertical sequence, sandstone geometry, and differentiation of cycles are strongly affected by subsidence rate.

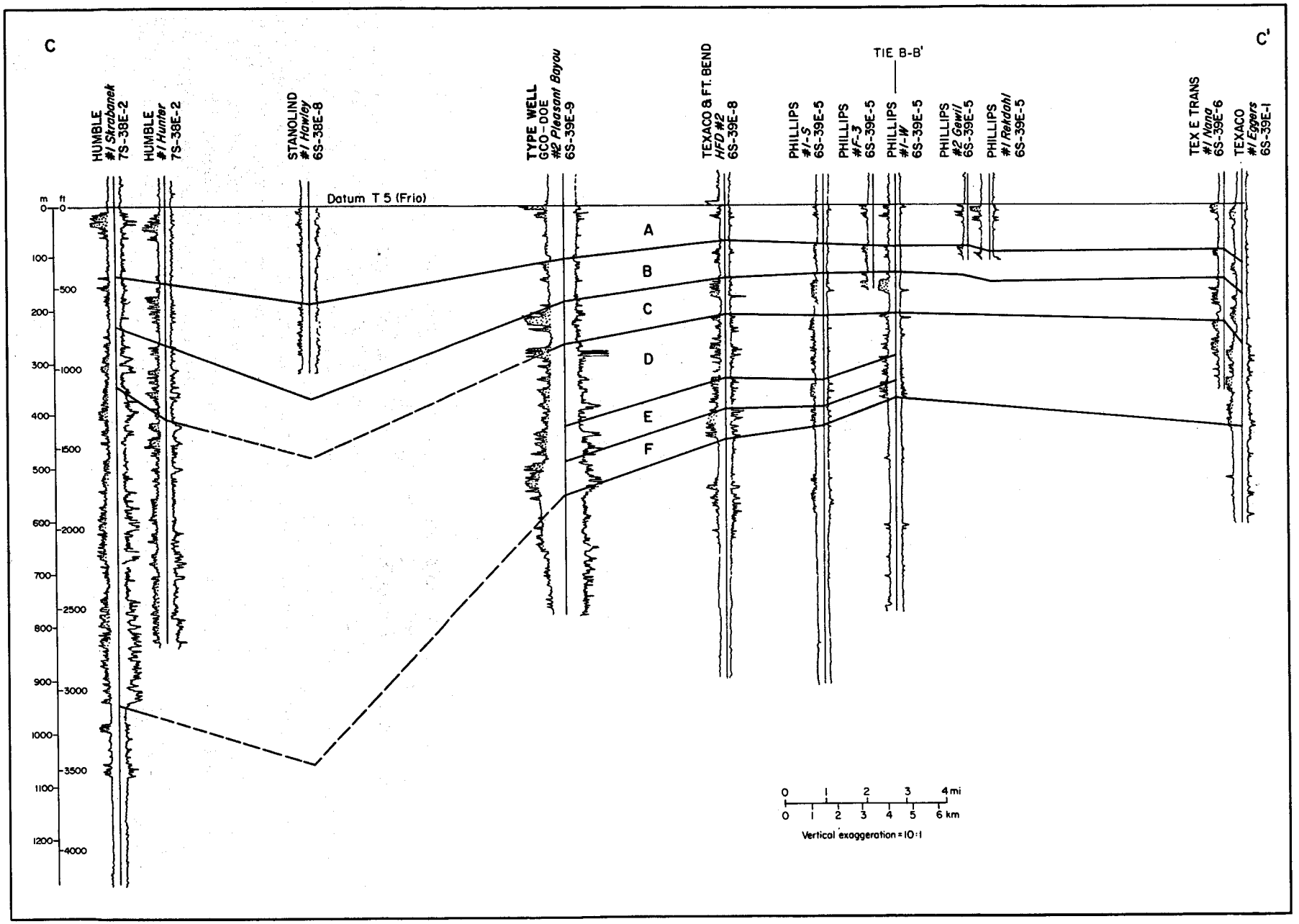

Figure 35. Stratigraphic strike section of the lower Frio *Anomalina bilateralis* zone in the East Chocolate Bayou fault block, including the Pleasant Bayou No. 2 geothermal well. Location is shown in figure 32.

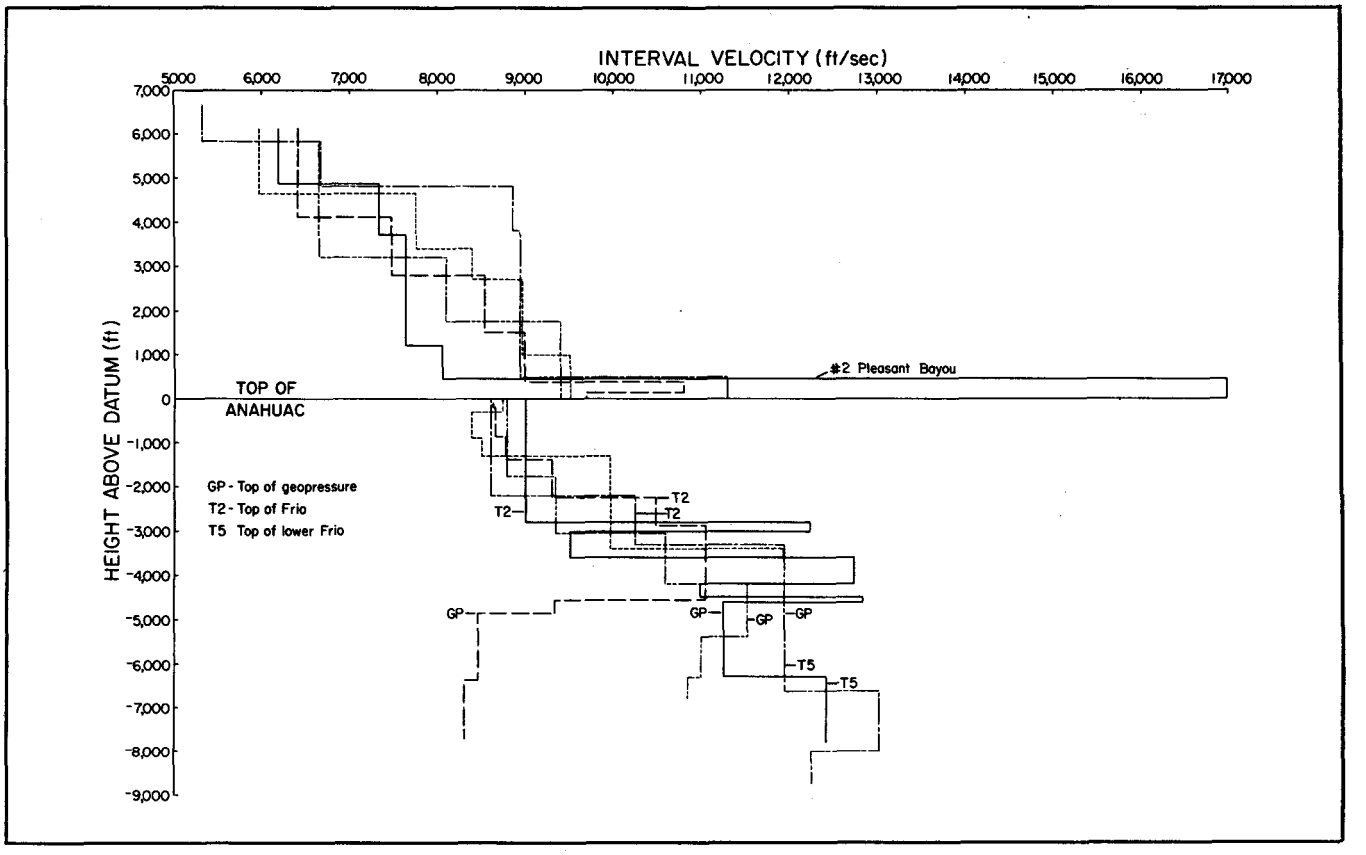

Figure 36. Interval velocities based on velocity surveys of five wells in the Pleasant Bayou study area. Datum is velocity inversion at the top of Anahuac. High-velocity zone just above Anahuac in the Pleasant Bayou well is probably an artifact of the data. Strong velocity inversion approximately 4,500 ft below the top of Anahuac in one well is caused by crossing a major fault into underconsolidated pre-Frio (Vicksburg, Jackson, and possibly Claiborne) shale, probably of deep-water origin. Otherwise, no clear relationship exists between geopressure and interval velocities.

interval velocities. Second, a high percentage of well-cemented sandstones in the geopressured zone could cancel any effect of low shale velocities, and no inversion of interval velocities would be apparent. This effect is expected to be particularly significant in geothermal prospect areas, where a high sandstone percentage in the geopressured zone is a prerequisite of exploration or well-site selection.

Lower Frio Sandstone Facies

Four sandstone facies were recognized in the *Anomalina bilateralis* zone (table 7). These facies may represent different depositional environments, but some of the differences in log character are probably attributable to large differences in subsidence rates, as in the Blessing area. Spatial relationships among these facies are shown by two stratigraphic sections (figs. 34 and 35) and by maps of log patterns for individual sandstones (figs. 37 through 39).

For reservoir evaluation, three kinds of facies variability that can be deduced from log patterns are considered significant: maximum thickness of an individual sandstone, vertical profile, and lateral continuity. Upward-fining sandstones, which are generally thought to represent distributary-channel facies, tend to be thicker than upward-coarsening sandstones, although this relationship is not as well defined here as in the Cuero study area. Sedimentary structures in core from the Pleasant Bayou No. 1 well corroborate a distributary-channel interpretation of the 'C' sandstone (fig. 38).

Aquifer permeabilities are generally high, commonly greater than 1 darcy in the 'A' and

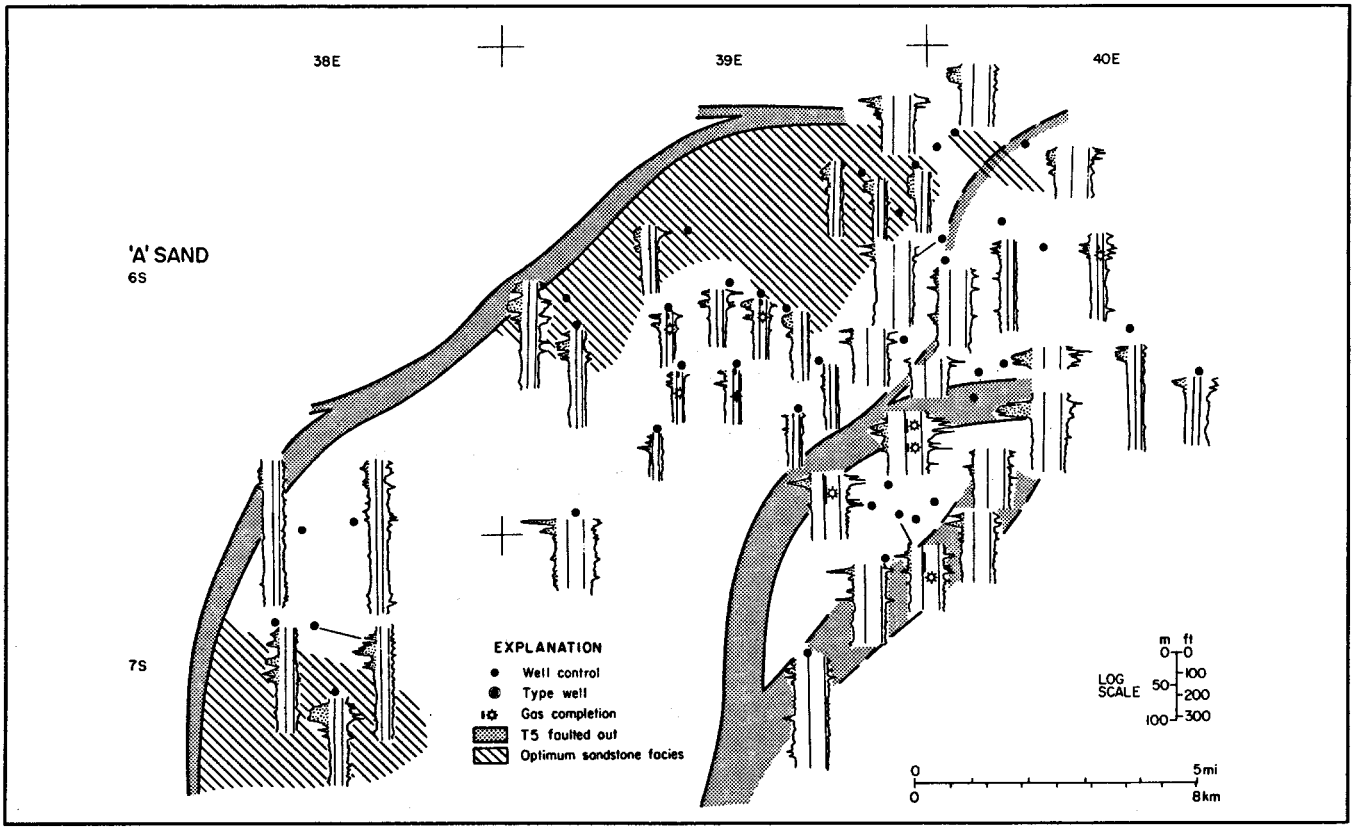

Figure 37. Geographic distribution of electric-log patterns of the geopressured 'A' sand, lower Frio Formation, East and South Chocolate Bayou fault blocks. 'A' sand is identified in figures 34 and 35.

'C' sandstones of the Chocolate Bayou area; however, no obvious relationship exists between log pattern and maximum permeability. Nonetheless, we regard the thicker upward-fining or blocky sandstones as representing the best geothermal reservoir facies. Extensive areas of optimum sandstone development (figs. 37 through 39), in combination with consistently high permeabilities, make the Pleasant Bayou area an excellent geothermal prospect.

Structure

Pleasant Bayou lies within the salt-structure province of the Houston Embayment. Salt tectonics have superimposed a pattern of domes and withdrawal basins (fig. 40) on the regional growth-fault structures (fig. 41), resulting in a complicated, multiphase structural style (figs. 42 and 43). Well logs provided the primary basis for structural mapping, except in the salt-withdrawal basin between Danbury Dome and the Chocolate

Table 7. Electric-log analysis of facies in the *Anomalina bilateralis* zone, lower Frio, Pleasant Bayou area.

Environmental interpretation	Log characteristics	Geographic distribution
Fluvial/deltaic plain and channels	High sandstone; blocky patterns; laterally discontinuous; total section thin	Updip of main growth fault
Distributary channel and channel-mouth bar	Blocky to upward-fining pattern. Thick sandstones with few shale breaks. Laterally continuous with delta-front facies	Downdip of main growth fault; patchy distribution
Delta front	Thin to thick, upward-coarsening sandstones. Laterally continuous	Widely distributed downdip of main growth fault
Delta front in rapid-expansion zone (very high subsidence rate)	Many thin sands interbedded with shale; difficult to correlate; very thick section	Near main growth fault on downthrown side

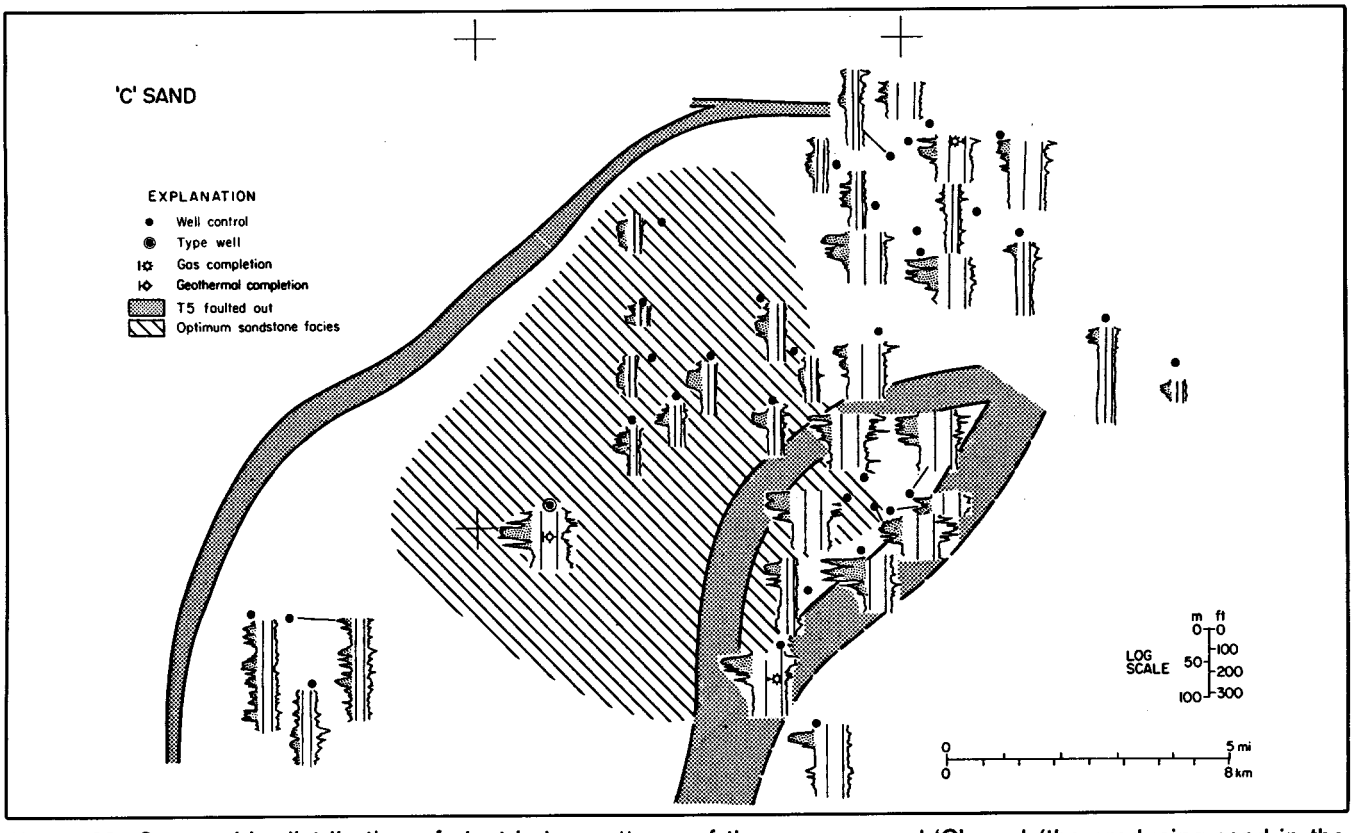

Figure 38. Geographic distribution of electric-log patterns of the geopressured 'C' sand (the producing sand in the Pleasant Bayou geothermal well), lower Frio Formation, East and South Chocolate Bayou fault blocks. This is one of the most extensive thick geopressured sandstones studied in the Texas Gulf Coast. 'C' sand is identified in figures 34 and 35.

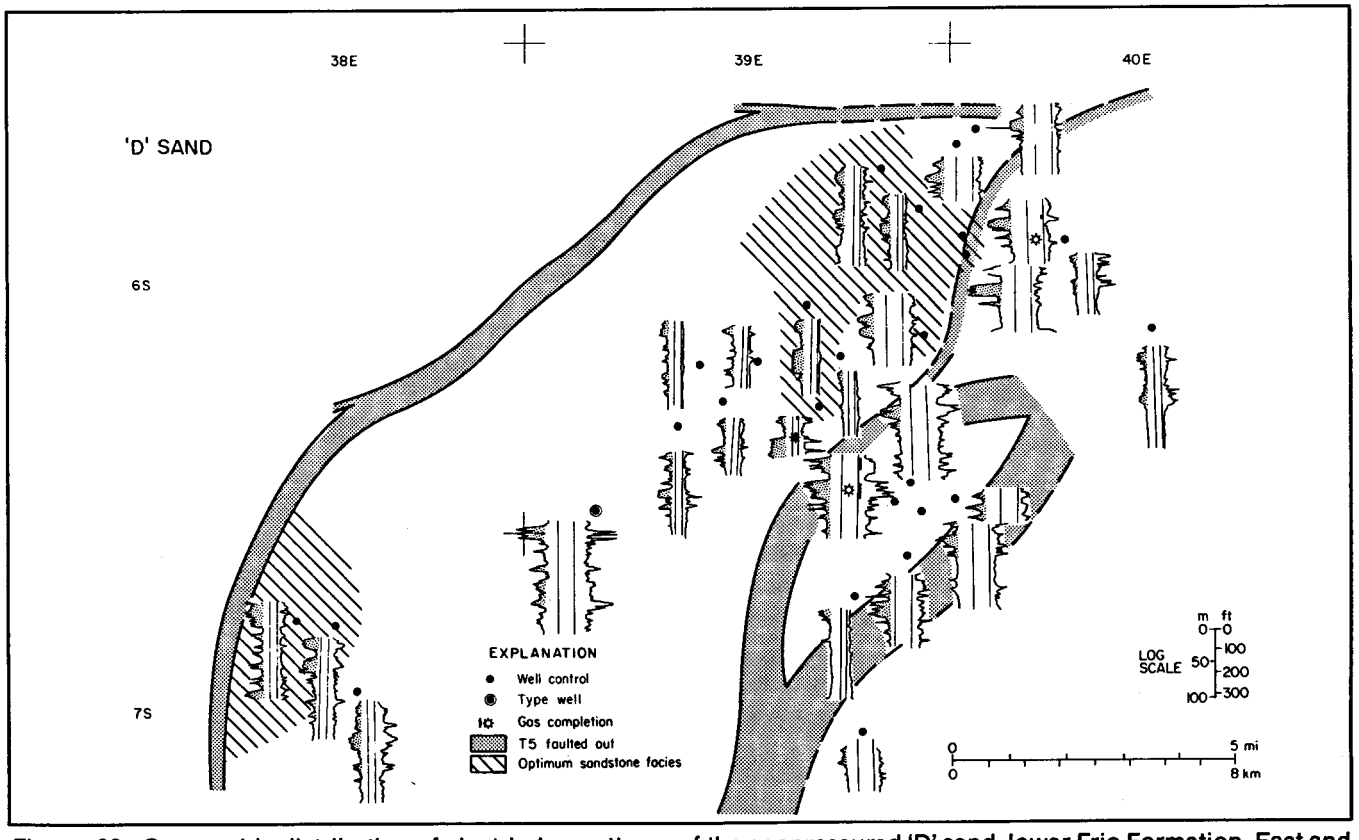

Figure 39. Geographic distribution of electric-log patterns of the geopressured 'D' sand, lower Frio Formation, East and South Chocolate Bayou fault blocks. 'D' sand is identified in figures 34 and 35.

Bayou field, where well control is sparse and structure maps were constructed using seismic data. The resulting structure map (fig. 43) on the zone of interest (T5) differs markedly from earlier maps of this area (Bebout and others, 1978; Flanigan, 1981).

The Pleasant Bayou structural style at depth has many elements in common with that of the Blessing area (fig. 30), which was not strongly affected by salt tectonics. Deep faults are predominantly down-to-the-basin, sinuous or arcuate in plan view, and have highly variable spacing; some have substantial rollover. In the Pleasant Bayou area, three sets of down-to-the-basin faults cut the lower Frio Formation (fig. 43): (1) A single, deep, listric fault of large displacement (figs. 41, 45, and 46) separates the East and West Chocolate Bayou fields and cuts through the Danbury Dome field (fig. 43). This fault is difficult to map properly except by use of sequential isopach maps; its displacement decreases and probably dies out to the southwest. (2) North of this fault are faults with closer spacing and less displacement and expansion of the Frio section (fig. 44). (3) In the South Chocolate Bayou field is a set of closely spaced faults of substantial displacement (figs. 41, 42, and 43).

In addition to these major down-to-the-basin faults, small faults cut obliquely across the East Chocolate Bayou fault block. The small fault in the East Chocolate Bayou field (fig. 44) is inferred from both well and seismic data (fig. 40); those faults near the type well are based strictly on seismic data (fig. 46). The origin of these faults is not well understood, but they probably resulted from minor distortions of the large fault block during movement along its bounding faults.

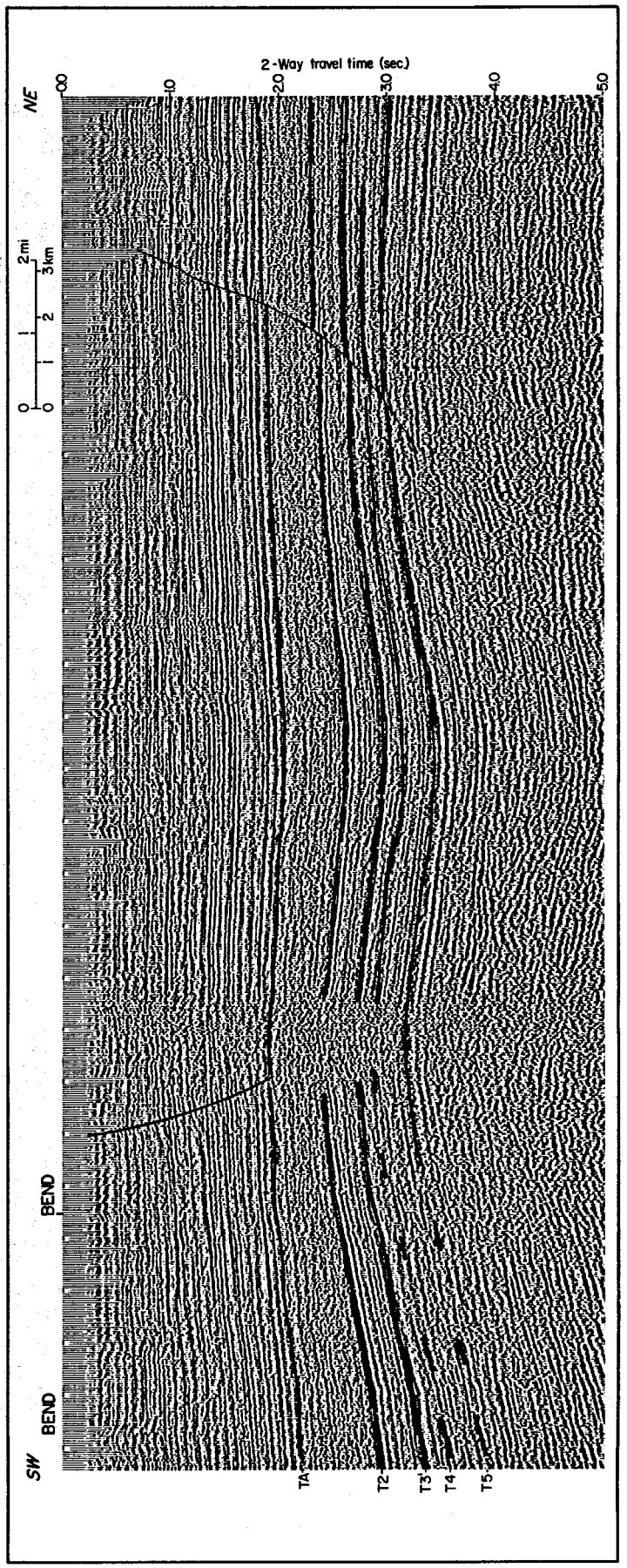

Figure 40. Six-fold seismic strike section (unmigrated), East Chocolate Bayou fault block. Location is shown in figure 32. Stratigraphic position of correlation markers is shown in table 1. One cross-fault (right side of section) is easily identified; otherwise, structural continuity is very good. Salt withdrawal occurred mostly in post-Frio time.

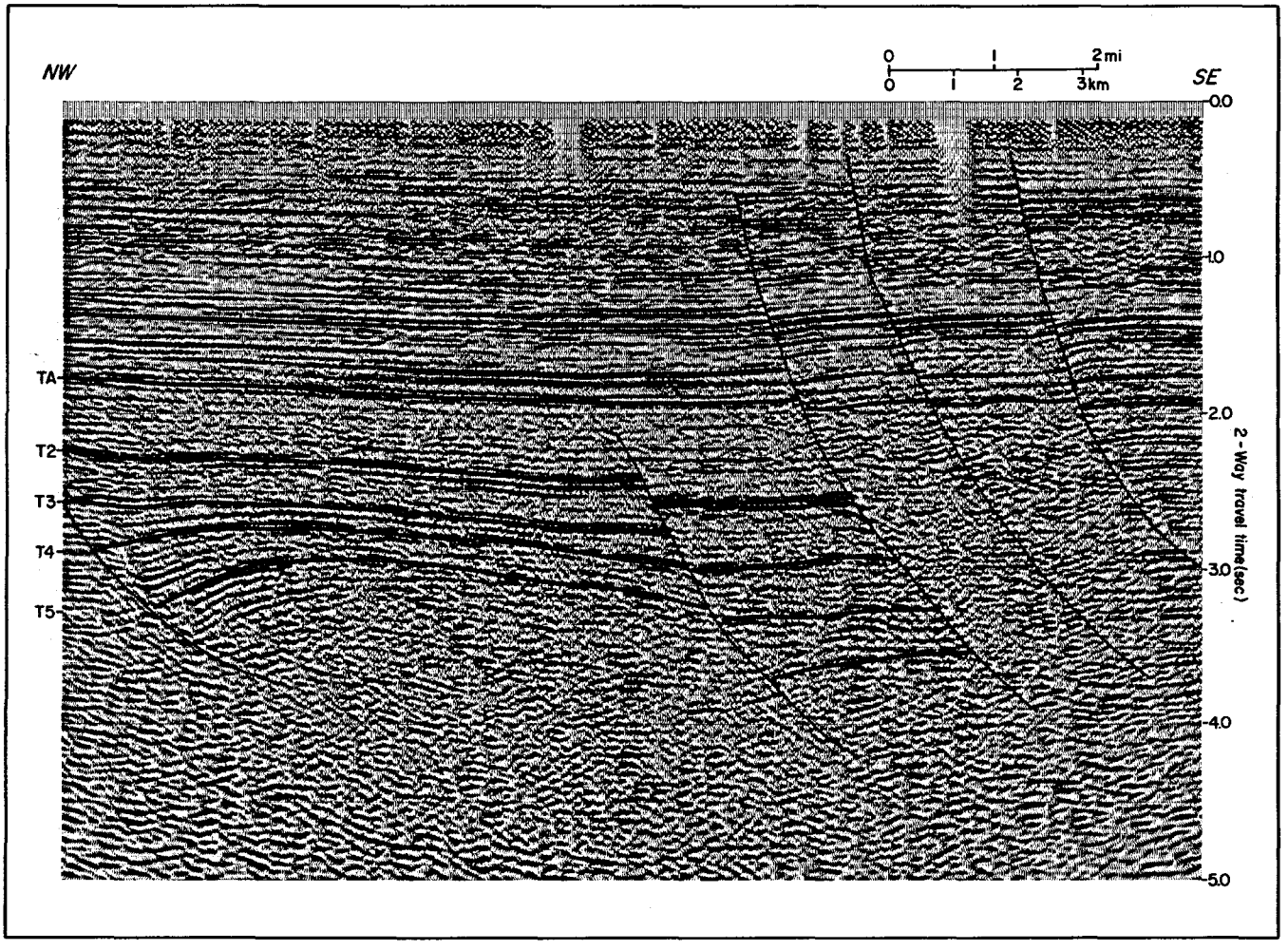

Figure 41. Twelve-fold seismic dip section (migrated) crossing East and South Chocolate Bayou fields. Location is shown in figure 32. Stratigraphic position of correlation markers is shown in table 1. Décollement appears shallower and rollover greater in the updip growth fault than in the downdip (South Chocolate Bayou) growth faults. Note the apparent absence of salt tectonics, perhaps caused by early (pre-Frio) salt withdrawal from this area.

Salt mobilization caused by the deposition of clastic sediments over salt led to the growth of Danbury Dome and an extensive salt-withdrawal syncline to the east and south. Arching of the strata over the growing dome resulted in the formation of radial faults (figs. 43 and 47) that are largely unrelated to the down-to-the-basin growth faults and that do not cut the lower Frio Formation (figs. 44, 45, and 46).

Sequential isopach maps (fig. 47) allow recognition of three stages of structural evolution: (1) During early Frio time (intervals 5 and 6), a major down-to-the-basin growth fault formed. Expansion ratios were as high as 6, and substantial rollover anticlines developed. This fault isolated downdip sandstones by placing them against older (Vicksburg?) slope shales, thus creating the seal necessary for formation of geopressure. The South Chocolate Bayou fault system was less active during this time. (2) During later Frio time (intervals 3 and 4), movement along the main reservoir-bounding fault declined substantially, while the South Chocolate Bayou fault system became very active. This basinward shift in the locus of major fault growth was probably caused by basinward progradation of the shelf margin and thus of the extensional regime. (3) In post-Frio time (intervals 1 and 2), structural growth was dominated

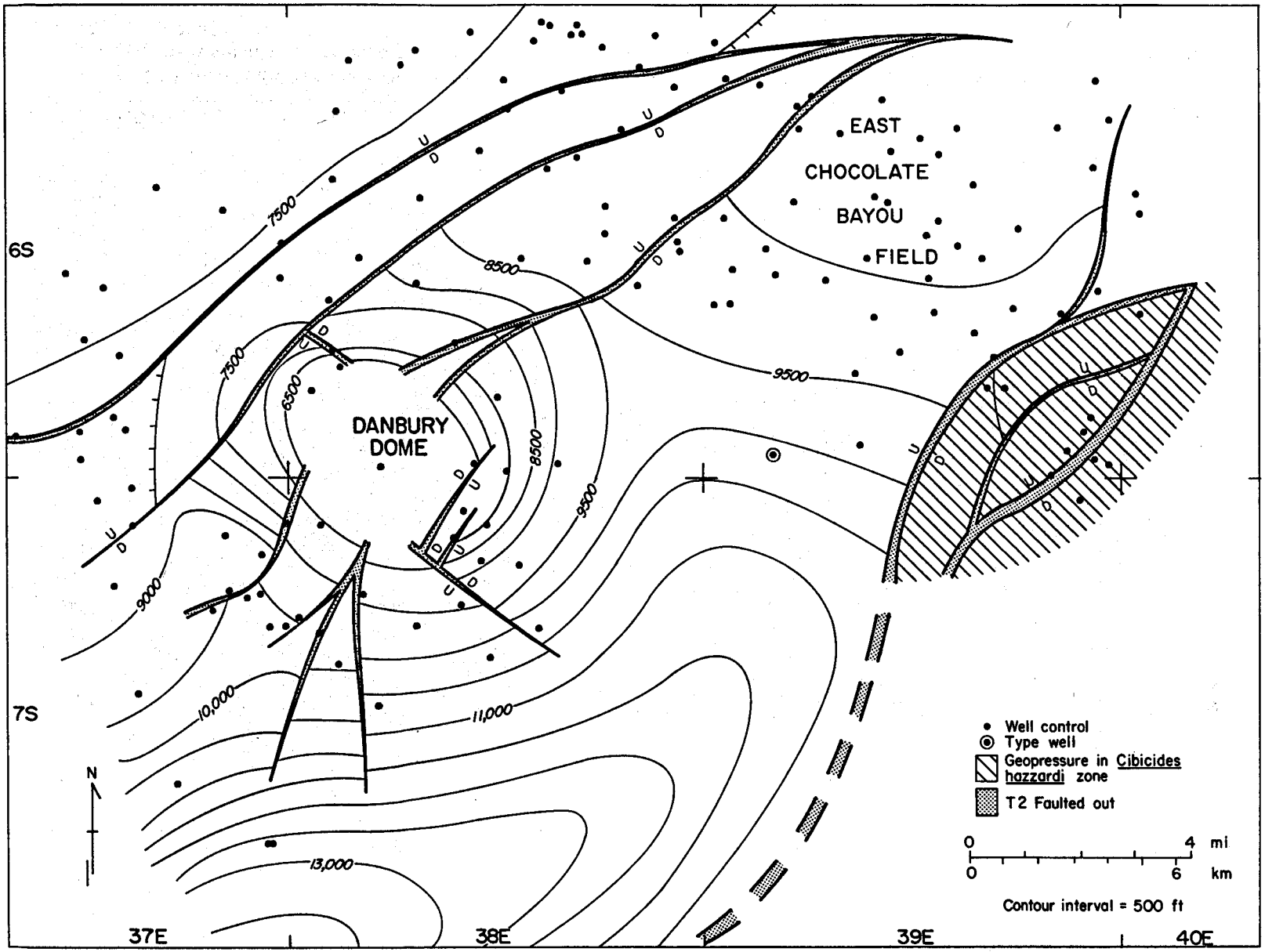

Figure 42. Structure on T2 horizon (top of *Cibicides hazzardi* zone), upper Frio Formation, Pleasant Bayou area. Structural relief is substantial, primarily because of post-Anahuac shale tectonics; displacement on down-to-the-basin growth faults is relatively small. Radial faults around Danbury Dome are complex and are shown schematically; structure near the dome has not been examined in detail.

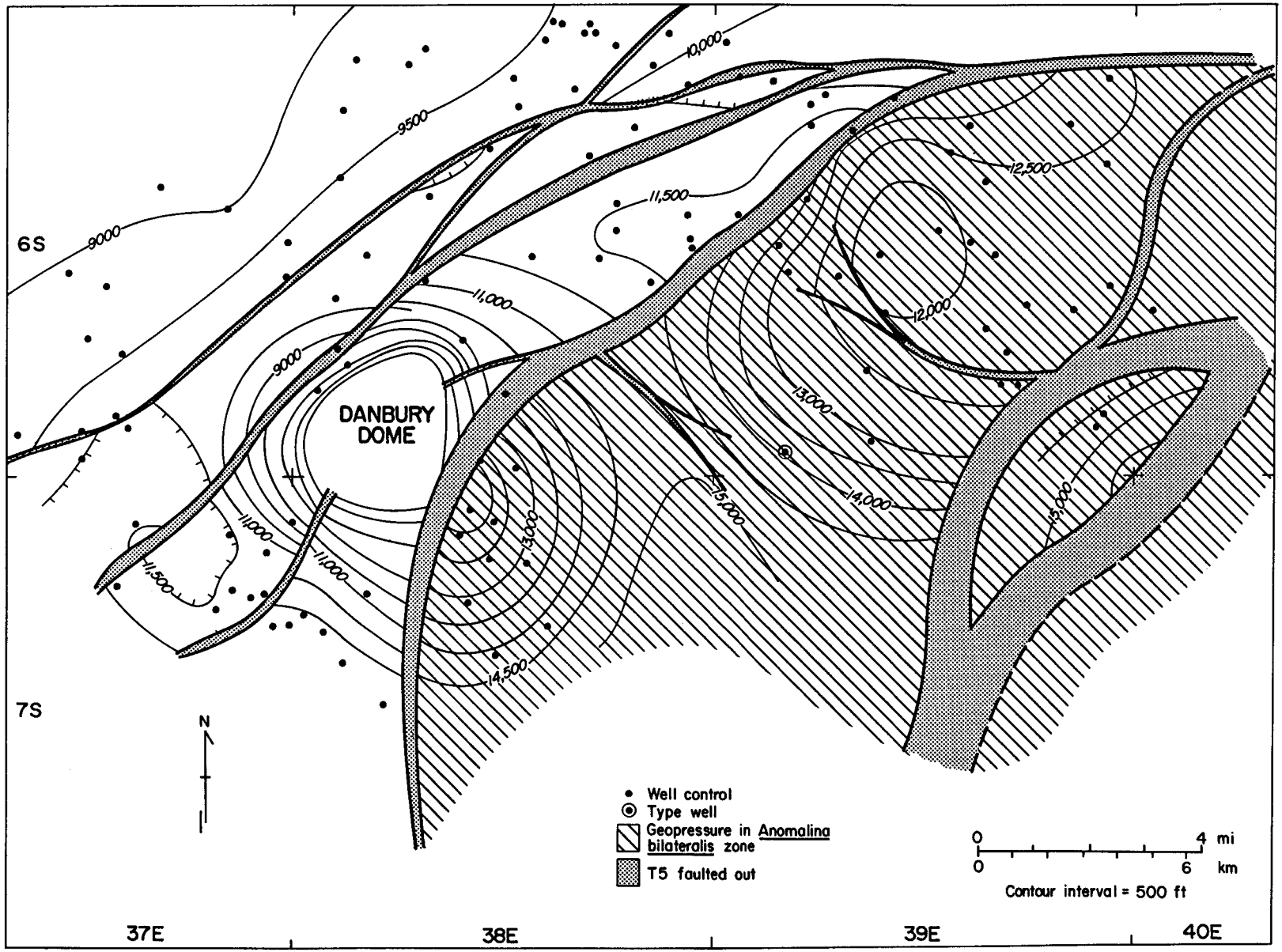

Figure 43. Structure on T5 horizon (top of *Anomalina bilateralis* zone), lower Frio Formation. Displacement on down-to-the-basin growth faults is much greater than that shown in figure 42, and rollover is substantial. Radial faults around Danbury Dome do not reach this horizon.

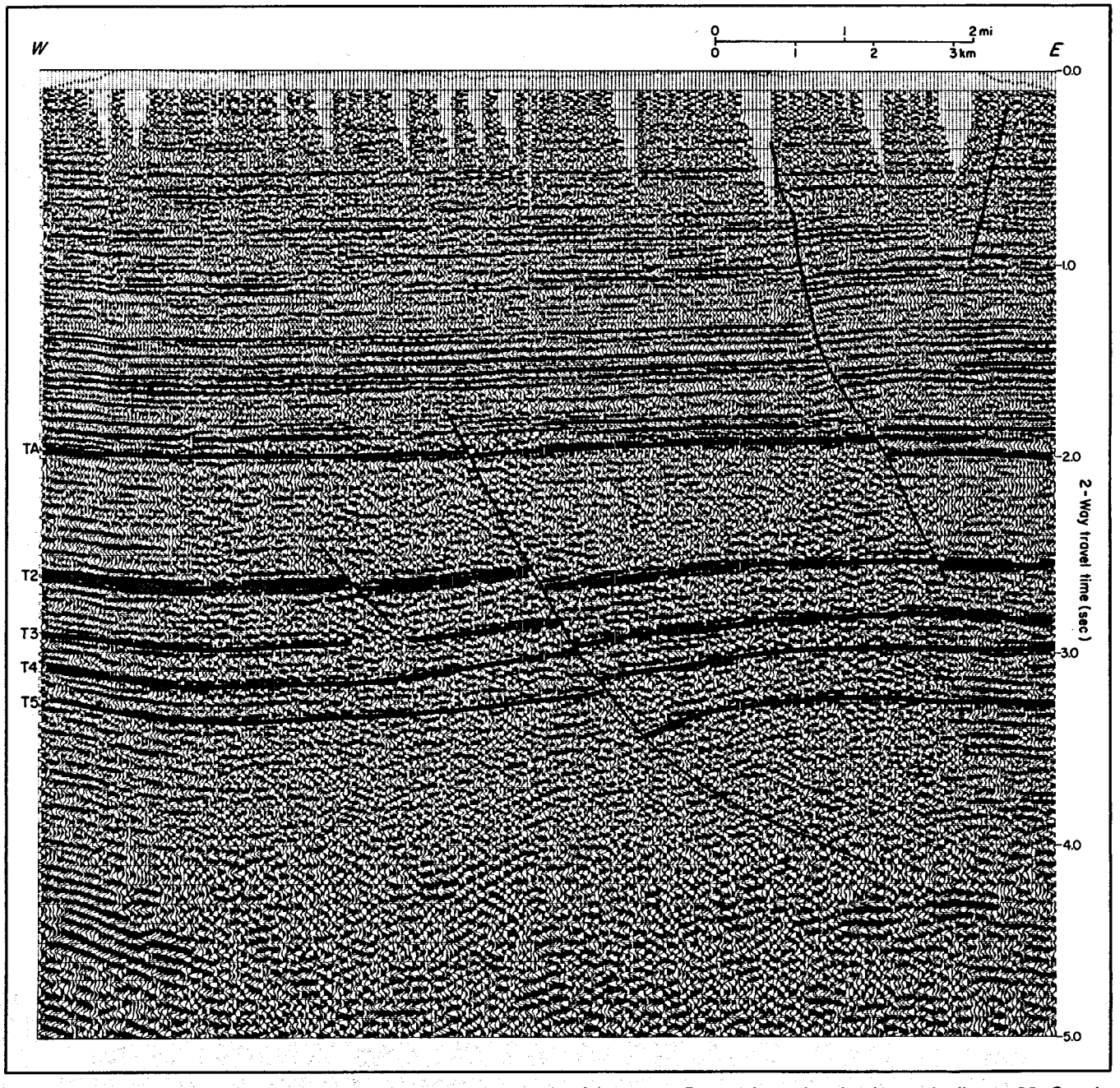

Figure 44. Twelve-fold seismic section (unmigrated) south of Danbury Dome. Location is shown in figure 32. Stratigraphic position of correlation markers is shown in table 1. Section illustrates two types of faults: (1) at depth, a regional, down-to-the-basin, listric normal growth fault, which dies out up-section, and (2) shallower, local radial faults associated with Danbury Dome, which die out down-section.

by deep-seated salt intrusion and related radial faults. Some of the down-to-the-basin faults continued to move, but at a greatly diminished rate.

Chocolate Bayou field apparently did not undergo either salt withdrawal or uplift during the time interval shown in the isopach maps (fig. 47). A likely explanation of this stability is that the area of Chocolate Bayou field underwent salt withdrawal during its pre-Frio history, while still in a continental-slope environment. Such salt-withdrawal basins are common on the Modern slope of the northwestern Gulf of Mexico (Lehner, 1969).

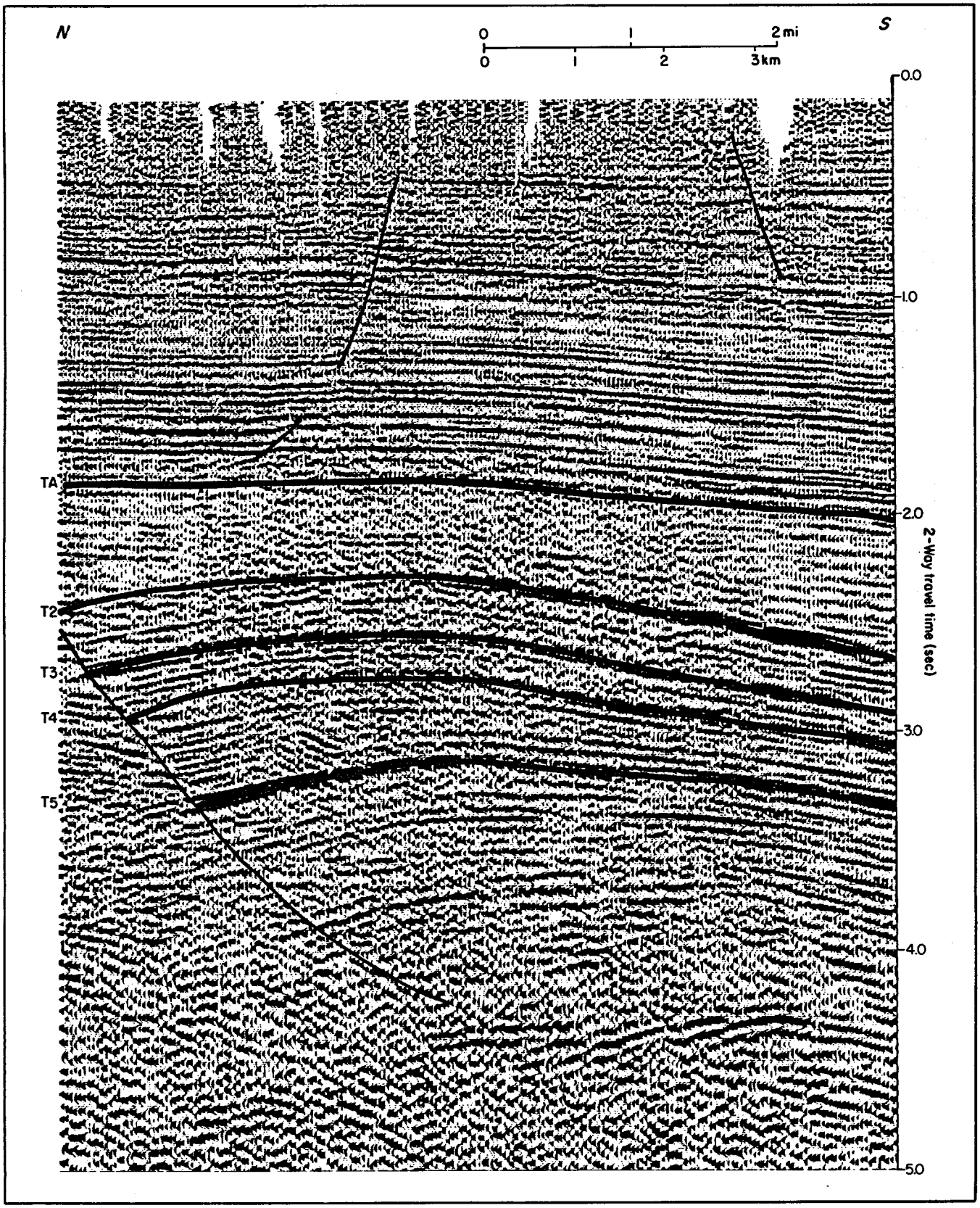

Figure 45. Twelve-fold seismic section (unmigrated) east of Danbury Dome. Location is shown in figure 32. Stratigraphic position of correlation markers is shown in table 1. Section also illustrates contrast between deeper regional growth fault and shallower radial faults.

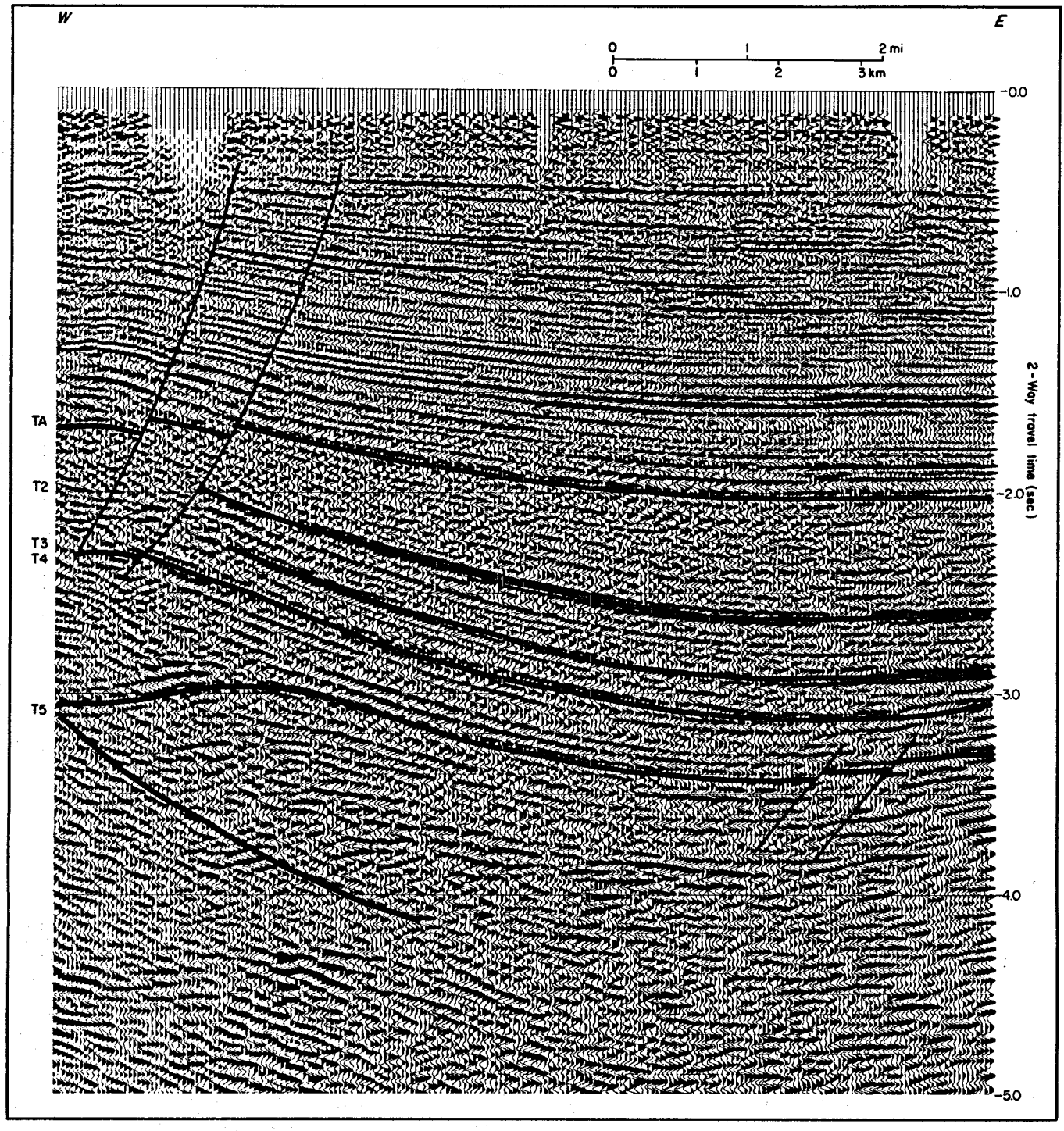

Figure 46. Twelve-fold seismic section (migrated) east of Danbury Dome. Location is shown in figure 32. Stratigraphic position of correlation markers is shown in table 1. Deep cross-faults on this section were inferred by tying reflectors around loops; these faults are not readily apparent on a single section.

Thus, Chocolate Bayou field may be analogous to "turtle structures" in the East Texas Basin and the North Sea, where broad structural closure is ultimately created in areas of initial salt withdrawal. In the Chocolate Bayou field, rollover associated with growth faulting accentuated the structural closure.

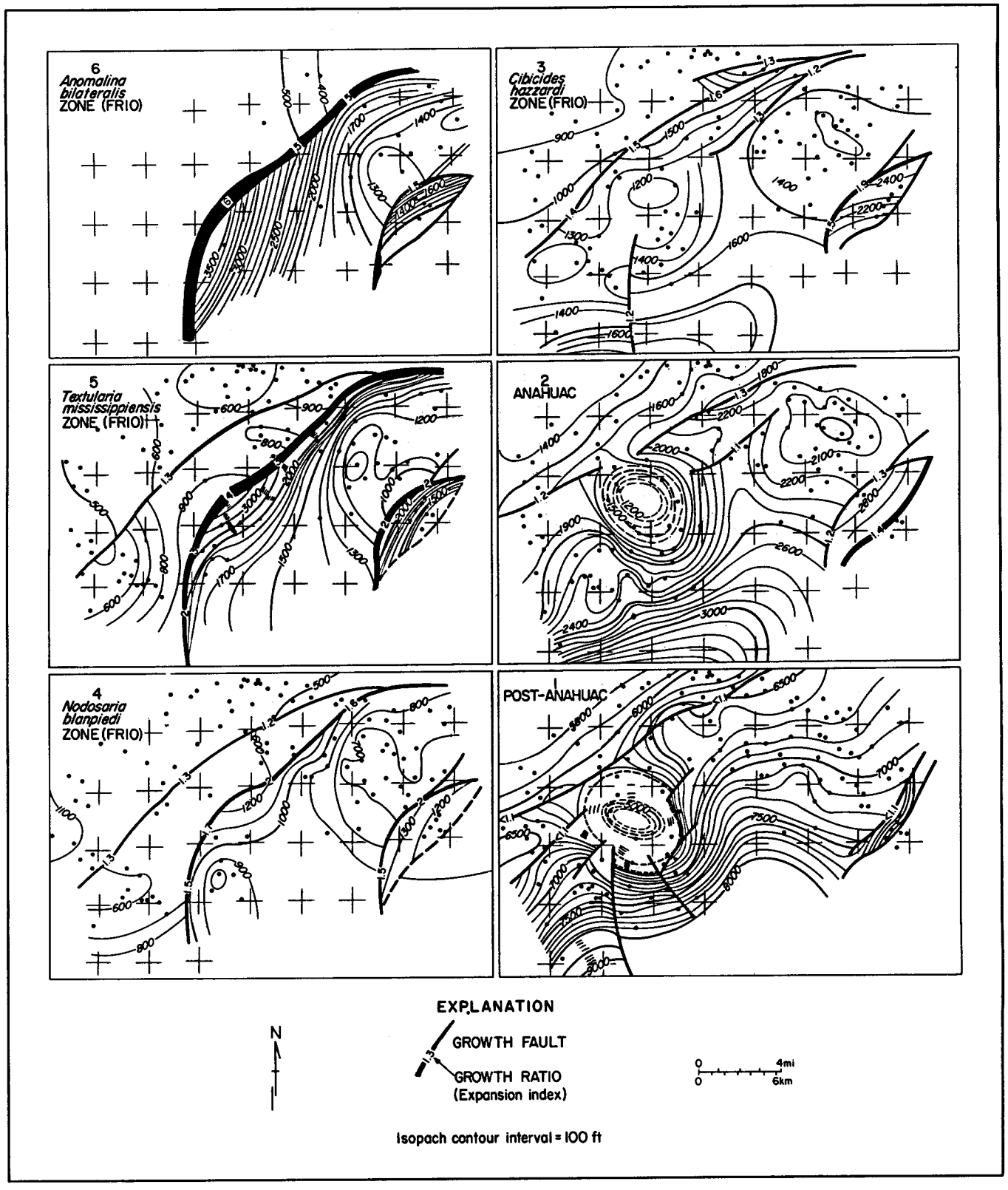

Figure 47. Sequential isopach maps of the Pleasant Bayou area illustrating structural evolution during Frio and post-Frio time. Distortion of the grid is caused by palinspastic restoration. During early Frio time, structural development was dominated by strong regional extension, as evidenced by down-to-the-basin growth faults with large expansion indices; salt tectonics are not evident. During post-Frio time, regional extension was weak, and structural growth was dominated by local salt withdrawal and uplift, the latter associated with radial faults.

COMPARISON OF THE GEOTHERMAL ENERGY POTENTIAL OF THE THREE AREAS

Among the three areas in Texas chosen for intensive evaluation, the most striking differences are in structural style (fig. 48) and sandstone distribution (fig. 49). In the Cuero and Blessing areas, the dominant structures are down-to-the-basin normal faults with maximum displacement at depth and subdued expression in the shallow section. These two areas differ substantially in fault spacing and structural relief, probably attributable to differences in mobility of the substrate, extension rate of the shelf margin, and depth of décollement. In contrast, structure in the Pleasant Bayou area is the result of two independent mechanisms superimposed to produce a complex, high-relief structure. Growth faulting and salt mobilization operated to produce the Chocolate Bayou anticline, Danbury Dome, and the intervening salt-withdrawal basin.

The two Frio fault blocks (Pleasant Bayou and Blessing) are both larger and structurally more suitable for water production than the Wilcox fault block (fig. 49). In the Pleasant Bayou area, the thickest sandstones with blocky SP patterns occur in an area that is nearly equidimensional and includes about 25 mi^2 of the large fault block. At Blessing, the axes of optimum sand distribution parallel the strike of the fault block and are centrally located within it. In contrast, the optimum reservoir facies of the Cuero area are much more limited in areal extent than those of the Frio sandstones (fig. 49). This results from the relatively narrow, dip-oriented sandstone trends perpendicular to the long axis of the fault block. This not only limits the potential reservoir volume but also severely constrains the location of test wells.

In spite of the higher geothermal gradient of the Wilcox as a whole (Bebout and others, 1982), potential geothermal aquifers in the Cuero area have lower temperatures than those in the Pleasant Bayou area because of the former's shallower depths. Cuero aquifer temperatures, however, are slightly higher than temperatures in the Blessing area (table 8). The Cuero and Blessing areas have similar pressures, but these are substantially lower than in the deeper Pleasant Bayou area (table 8).

In general, the stratigraphic and structural relationships that result in geopressure are similar in all three areas. All the geopressured reservoirs are characterized by rapid, syndepositional regional extension,

Table 8. Reservoir parameters for three geothermal areas in the Texas Gulf Coast.

	Pleasant Bayou	Blessing	Cuero
Maximum fault-block width (mi)	5	4	2
Fault-block area (mi^2)	50	36	12
Depth range of reservoir sandstones in type well (ft)	14,000 - 15,200	10,650 - 11,300	10,800 - 11,100
Area of optimum reservoir sandstones (mi^2)	A - 15 C - 25 D - 16	B - 10 C - 9	B - 2.3 C - 1.5 D - 0.4
Aggregate reservoir thickness in type well (ft)	400	170	200
Permeability range of reservoir sandstones in type well (md)	0.01 - 515	0.01 - 56	0.01 - 250
Average formation pressure (psi)	11,000	8,500	8,250
Average corrected formation temperature (°F)	300	245	285

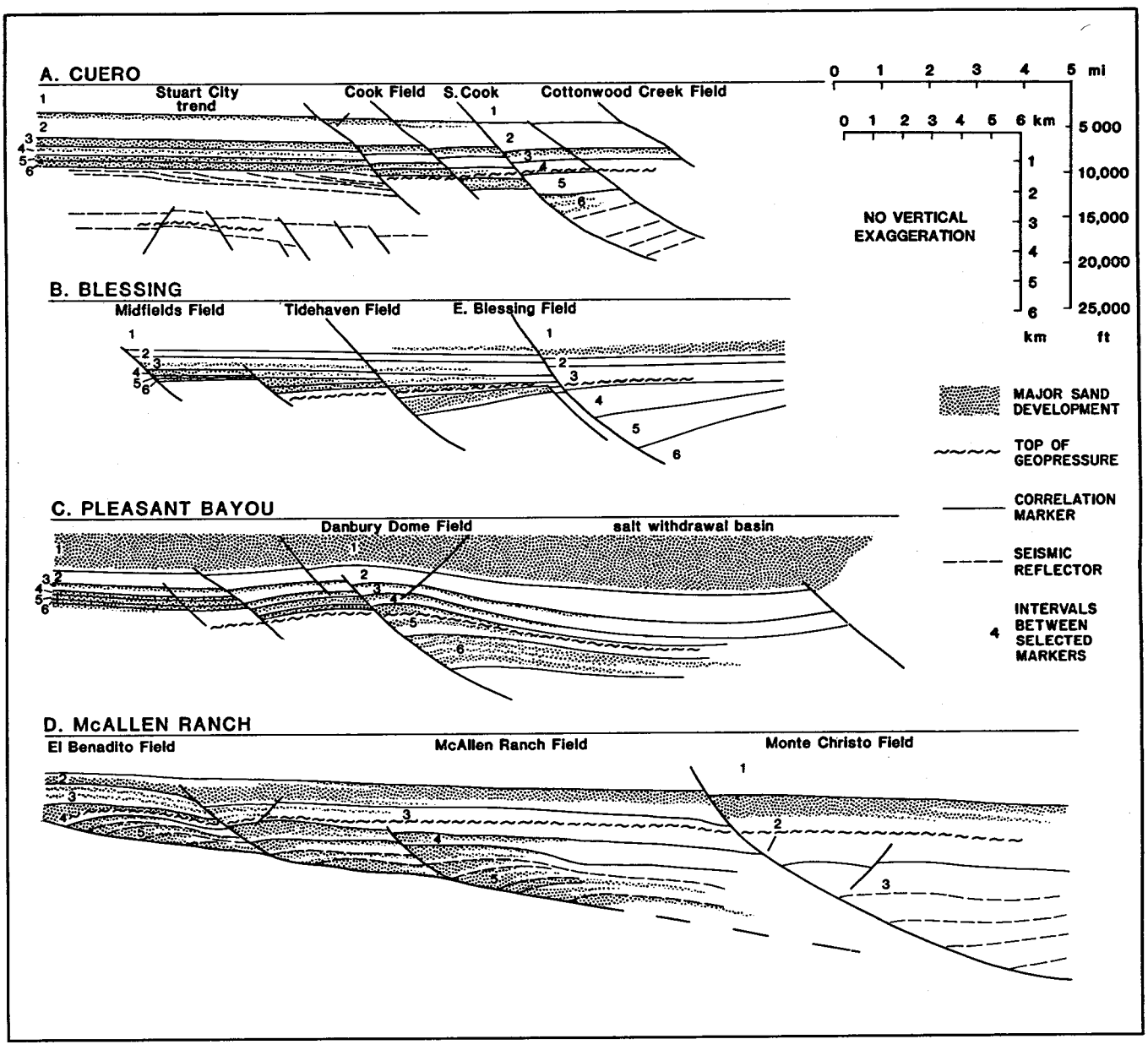

Figure 48. Dip sections of the three study areas, without vertical exaggeration, illustrating contrast of structural styles. Downdip part of the Pleasant Bayou section is shown schematically because of lack of data, and is inferred from isopach maps (fig. 47). Vicksburg section is based on a seismic section and log data from Han (1982); it is included here to show structures dominated by shallow décollement for purposes of comparison. Locations of these sections are shown in figures 4, 7, 22, and 32.

manifested by listric normal faults of large displacement. Shallow-water deltaic sandstones were faulted against older shales that were presumably deposited in a deeper-water environment. In this way the growth fault sealed the reservoir on the landward side.

Another common characteristic of these study areas is a significant transgression following the maximum regression that created the main geopressured aquifer. This transgression apparently affects the hydraulic isolation of the main geopressured aquifer on the basinward side. Without the subsequent transgression, that aquifer might be upfaulted on the basinward side against younger sandstones of high continuity and permeability, thus draining the aquifer and preventing the accumulation of geopressure.

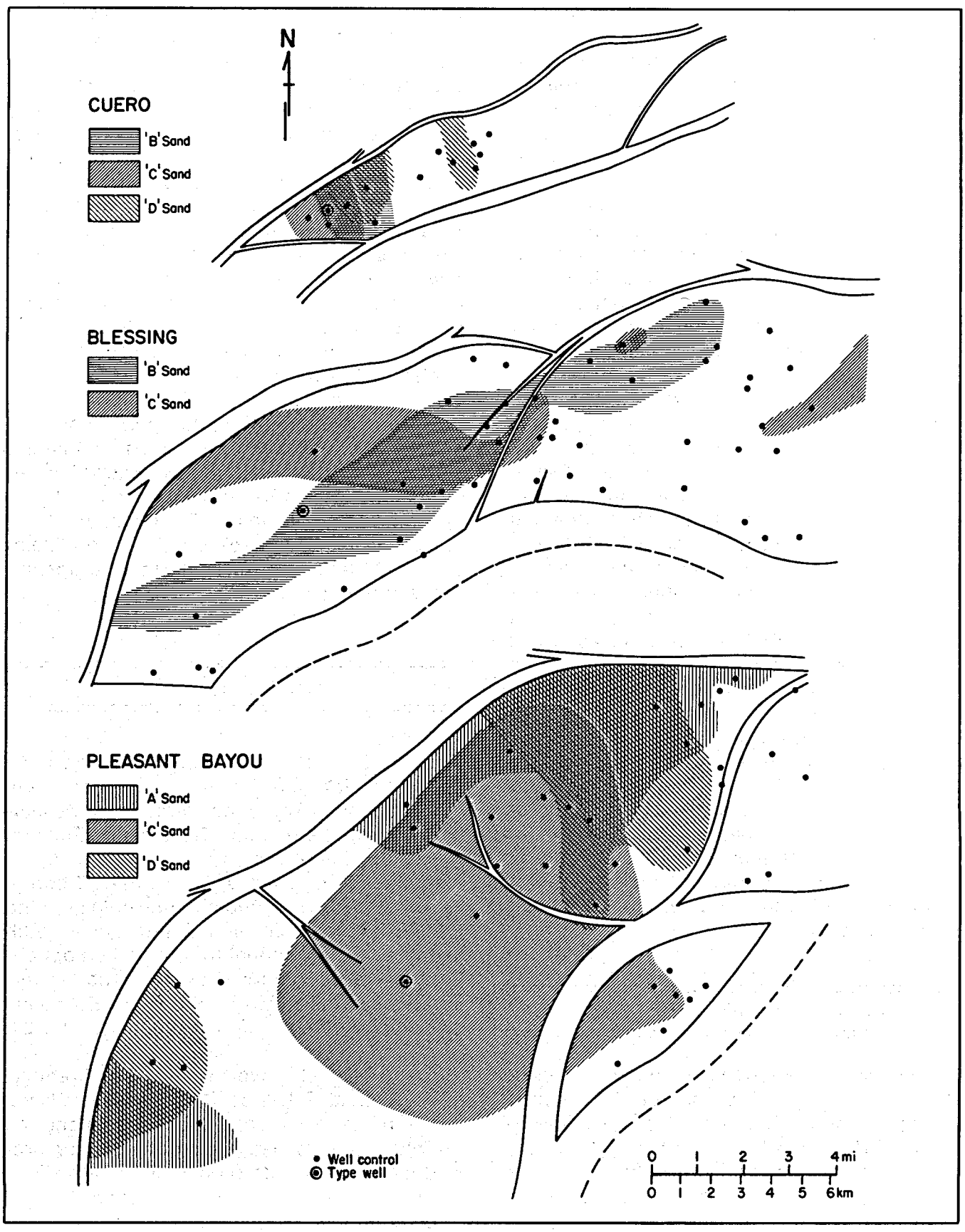

Figure 49. Distribution of optimum geopressured sandstone facies in the three study areas, based on figures 15, 26, 37, 38, and 39. Pleasant Bayou is superior in permeability, sandstone continuity, and structural continuity.

Finally, sandstone composition and diagenesis must be conducive to retention of porosity and permeability to permit efficient production from the reservoir. All the areas in this study are outside of the volcanogenic sandstone province of South Texas, characterized by low permeabilities in deep geopressured aquifers.

Generalizations about favorable structural style or setting are more difficult to make. Obviously, large fault blocks without subordinate small faults are ideal. It is also important that the growth fault that created the geopressure seal remained active far enough landward of the contemporaneous shelf edge to seal off a large area of shallow-water, proximal deltaic sandstones. The Pleasant Bayou area appears to be exceptionally favorable in this respect. Unanticipated structural complexities at depth, particularly small faults, may reduce the quality of an otherwise favorable geothermal area. Antithetic faults, caused by the flexure of bedding planes associated with rollover, may interrupt reservoir continuity near the crests of large structures. The number and density of parallel down-to-the-basin faults may increase with depth. Sediments within large fault blocks may undergo minor deformation during early structural movement, resulting in small but potentially reservoir-limiting cross-faults. Another important consideration is that deep structure is difficult to predict by downward extrapolation of shallow structures, particularly in areas of salt tectonics. Abundant deep well control and an extensive seismic grid are essential for predicting reservoir continuity in geopressured aquifers.

ACKNOWLEDGMENTS

This work was funded by the U.S. Department of Energy, Division of Geothermal Energy, under Contract Nos. DE-AS05-76ET28461 and DE-AC08-79ET27111. Geological maps and interpretations in the Blessing area were initially prepared by Scott Hamlin and Bonnie Weise as part of a study for the Gas Research Institute. We greatly benefited from discussions of seismic studies with Milo Backus, who designed the seismic data collection plan for the Cuero area and provided advice on data processing and interpretation. Mobil Exploration Company, Teledyne Exploration, Amoco Production Company, and The Coastal Corporation are thanked for permission to publish selected seismic lines. We are particularly grateful to personnel at the Bureau of Economic Geology who assisted in preparing this report. The manuscript was typed by Margaret Chastain and typeset by Phyllis Hopkins under the direction of Lucille C. Harrell; illustrations were drafted by John T. Ames, Thomas M. Byrd, Micheline R. Davis, Byron P. Holbert, Jeffrey Horowitz, and Jamie McClelland under the direction of Dan F. Scranton and Richard L. Dillon. The publication was edited by Amanda R. Masterson, designed by Micheline R. Davis, and assembled by Micheline R. Davis and Margaret L. Evans. L. F. Brown, Jr., W. E. Galloway, M. P. A. Jackson, A. G. Goldstein, and D. G. Bebout reviewed the manuscript and made many useful suggestions.

REFERENCES

Asquith, D. O., 1970, Depositional topography and major marine environments, Late Cretaceous, Wyoming: American Association of Petroleum Geologists Bulletin, v. 54, p. 1184-1224.

Bebout, D. G., Loucks, R. G., and Gregory, A. R., 1978, Frio sandstone reservoirs in the deep subsurface along the Texas Gulf Coast: their potential for production of geopressured geothermal energy: The University of Texas at Austin, Bureau of Economic Geology Report of Investigations No. 91, 92 p.

Bebout, D. G., Weise, B. R., Gregory, A. R., and Edwards, M. B., 1982, Wilcox reservoirs in the deep subsurface along the Texas Gulf Coast: their potential for production of geopressured geothermal energy: The University of Texas at Austin, Bureau of Economic Geology Report of Investigations No. 117, 125 p.

Berg, R. R., 1981, Deep-water reservoir sandstones of the Texas Gulf Coast: Gulf Coast Association of Geological Societies Transactions, v. 31, p. 31-39.

Bruce, C. H., 1973, Pressured shale and related sediment deformation: mechanism for development of regional contemporaneous faults: American Association of Petroleum Geologists Bulletin, v. 57, p. 878-886.

Cloos, E., 1968, Experimental analysis of Gulf Coast fracture patterns: American Association of Petroleum Geologists Bulletin, v. 52, p. 420-444.

Crans, W., and Mandl, G., 1981, On the theory of growth faulting: part II: genesis of the "unit": Journal of Petroleum Geology, v. 3, p. 455-476.

Crans, W., Mandl, G., and Haremboure, J., 1980, On the theory of growth faulting: a geomechanical delta model based on gravity sliding: Journal of Petroleum Geology, v. 2, p. 265-307.

Dobrin, M. B., 1976, Introduction to geophysical prospecting: New York, McGraw-Hill, 630 p.

Fisher, W. L., Brown, L. F., Jr., Scott, A. J., and McGowen, J. H., 1969, Delta systems in the exploration for oil and gas: a research colloquium: The University of Texas at Austin, Bureau of Economic Geology, 78 p.

Fisher, W. L., and McGowen, J. H., 1967, Depositional systems in the Wilcox Group of Texas and their relationship to occurrence of oil and gas: Gulf Coast Association of Geological Societies Transactions, v. 17, p. 105-125.

Flanigan, T. E., 1981, Abnormal formation pressures: recognition, distribution, and implications for geophysical prospecting, Brazoria County, Texas: Gulf Coast Association of Geological Societies Transactions, v. 31, p. 97-103.

Fowler, W. A., 1970, Pressures, hydrocarbon accumulation, and salinities—Chocolate Bayou field, Brazoria County, Texas: Journal of Petroleum Technology, v. 22, p. 411-423.

Galloway, W. E., Hobday, D. K., and Magara, K., 1982, Frio Formation of the Texas Gulf Coast Basin—depositional systems, structural framework, and hydrocarbon origin, migration, distribution, and exploration potential: The University of Texas at Austin, Bureau of Economic Geology Report of Investigations No. 122, 78 p.

Han, J. H., 1981, Genetic stratigraphy and associated growth structures of the Vicksburg Formation, South Texas: The University of Texas at Austin, Ph.D. dissertation, 162 p.

Harkins, K. L., and Baugher, J. W., 1969, Geological significance of abnormal formation pressures: Journal of Petroleum Technology, v. 21, p. 961-966.

Lehner, P., 1969, Salt tectonics and Pleistocene stratigraphy on continental slope of northern Gulf of Mexico: American Association of Petroleum Geologists Bulletin, v. 53, p. 2431-2479.

Loucks, R. G., Dodge, M. M., and Galloway, W. E., 1981, Sandstone consolidation analysis to delineate areas of high-quality reservoirs suitable for production of geopressured geothermal energy along the Texas Gulf Coast: The University of Texas at Austin, Bureau of Economic Geology Report of Investigations No. 111, 41 p.

Morton, R. A., Ewing, T. E., and Tyler, N., 1983, Continuity and internal properties of Gulf Coast sandstones and their implications for geopressured fluid production: The University of Texas at Austin, Bureau of Economic Geology Report of Investigations No. 132, 70 p.

Rettger, R. E., 1935, Experiments in soft-rock deformation: American Association of Petroleum Geologists Bulletin, v. 19, p. 271-292.

Thorsen, C. E., 1964, Age of growth faulting in southeast Louisiana: Gulf Coast Association of Geological Societies Transactions, v. 13, p. 103-110.

Tyler, N., and Han, J. H., 1982, Elements of high constructive deltaic sedimentation, lower Frio Formation, Brazoria County, Texas: Gulf Coast Association of Geological Societies Transactions, v. 32, p. 527-540.

Weise, B. R., Edwards, M. B., Gregory, A. R., Hamlin, H. S., Jirik, L. A., and Morton, R. A., 1981, Geological studies of geopressured and hydropressured zones in Texas: test-well site selection: The University of Texas at Austin, Bureau of Economic Geology,

Report to the Gas Research Institute, Contract No. 5011-321-0125, 308 p.

Winker, C. D., 1982, Cenozoic shelf margins, northwestern Gulf of Mexico: Gulf Coast Association of Geological Societies Transactions, v. 32, p. 427-448.

Winker, C. D., and Edwards, M. B., 1983, Unstable progradational clastic shelf margins, *in* Stanley, D. O., and Moore, G. T., eds., The shelfbreak: critical interface on continental margins: Society of Economic Paleontologists and Mineralogists Special Publication 33, p. 139-157.

Wrighton, Fred, 1981, An economic overview of geopressured solution gas: Louisiana State University, Proceedings, Fifth Conference on Geopressured Geothermal Energy, p. 45-48.